Dissertation
submitted to the
Combined Faculties for the Natural Sciences and for Mathematics
of the Ruperto-Carola University of Heidelberg, Germany
for the degree of
Doctor of Natural Sciences

presented by

Master of Science: Wannan Tang
Born in: Xi'an, China
Oral-examination……..…..…..

New biological tools for genetic manipulation of the mouse brain

Referees: Prof. Dr. Peter H. Seeburg

Dr. Rolf Sprengel

Erklärung gemäß § 7 (3) b) und c) der Promotionsordnung:

Ich erkläre hiermit, daß ich die vorgelegte Dissertation selbst verfaßt und mich dabei keiner anderen als der von mir ausdrücklich bezeichneten Quellen und Hilfen bedient habe. Desweiteren erkläre ich hiermit, daß ich an keiner anderen Stelle ein Prüfungsverfahren beantragt bzw. Die Dissertation in dieser oder anderer Form bereits anderweitig als Prüfungsarbeit verwendet oder einer anderen Fakultät als Dissertation vorgelegt habe.

Heidelberg, 31. March 2009 Wannan Tang

For My Parents

Acknowledgements

This study was performed in the laboratory of Prof. Peter H. Seeburg in Max Planck Institute for Medical Research Heidelberg. And it was supported by the Max-Planck-Gesellschaft and University of Heidelberg. I thank my thesis committee members, and I would like to express my deep and sincere gratitude to all those who gave me the possibility to complete this thesis.

Dr. Rolf Sprengel for his personal scientific supervision, supports, stimulating suggestions, encouragements, kindness and most of all, for his patience, which helped me all the time of my study and my writing of this thesis;

Prof. Peter H. Seeburg for offering me the opportunity to work in his lab, giving me important guidance and important supports throughout my study;

Dr. Maz Hasan, Dr. Martin Schwarz, Dr. Simone Astori, Dr. Güter Giese, Dr. Simone Freese, Dr. Paolo Mele, Dr. Yair Pilpel, Tobias Breuninger and Margarita Pfeffer for all their help, supports, interests and valuable hints.

Dr. Uli Krueth for teaching me at the very beginning the basic lab knowledge when I was still fresh, answering me many usual and unusual questions, offering me a lot of nice plasmid constructs and primers.

Annette Herold for her useful protocols, nice buffers, strong technical supports and warm friendship.

My lab members: Dr. Verena Marx, Dr. Verena Bosch, Dr. André Mihaljevic, Dr. Peixin Zhu, Jiss John, Dr. Melanie Bausen, Jan Herb, Cornelia Strobel, Pouya Balaghy-Mobin, Yiwei Chen, Ann-Marie Michalski, Godwin Dogbevia, Dario Arcos-Díaz, Dr. Liliana Layer and Dr. Simone Giese for providing a stimulating and fun environment in which to learn and grow.

Sabine Günewald, Simone Hundemer, Martina Lang, Liya Pan, Hans Gaugler, Horst Grosskurth for all their technical supports.

My special thanks to Chinese Christian Fellowship Heidelberg and all my friends for their invisible supports and sharing all my thoughts.

Lastly, and most importantly, I thank my parents. They bore me, raised me, taught me, support me, and love me. To them I dedicate this thesis.

Summary

The site-specific gene expression in the mouse brain is the most crucial issue for genetic studies of brain networks. In our studies, we used different fluorescent proteins (FPs) for monitoring brain anatomy, while for the functional analysis, proteins such as Cre recombinase and the tetracycline-controlled transactivator (tTA) were investigated. From the technical point of view, we attempted both mouse transgenic technology and recombinant adeno-associated virus (rAAV) gene delivery *in vivo* for transferring functional proteins into specific cell types of the mouse brain.

First we analyzed the cell-type specificity of a bacterial artificial chromosome (BAC) transgene. We selected an enhanced green fluorescent protein (EGFP) recombined BAC (from Genesat project) which was supposed to have mitral/tufted cell specific expression in the olfactory bulb. By pronuclear injection of the BAC, different founders were obtained. Out of 41 potential founders, one was mitral cell specific, and two were specific for mitral and tufted cells.

Regarding the limitations of cost and time using the mouse transgenic technology, we switched as an alternative approach to the rAAV gene delivery system. For visualizing cells that express the virus-delivered proteins, we applied two strategies: one with tTA/rtTA and its bi-directional responder Ptetbi to express Cre recombinase together with an FP in the specific brain regions. This provided a strong expression level of both Cre and FPs in cultured neurons and in neurons in the brain. For the second strategy, we applied a slightly modified T2A self-cleaving peptide bridge for the quantitative expression of Cre recombinase or tTA/rtTA together with FPs, respectively. By applying the T2A peptide approach, two proteins can be almost equally expressed with one rAAV construct. This opens a new avenue for gene function analysis in the central nervous system.

Next we analyzed whether rAAV can be used for the cell-type-specific expression. We selected glia cells, since in the transgenic field, specific promoters are described for

proteolipidprotein (PLP) and glial fibrillary acidic protein (GFAP). As second cell population we analyzed promoters for local interneurons, the glutamate decarboxylase 67 (GAD67) and the cholecystokinin (CCK). We investigated a complementation approach which splits Cre recombinase into two parts (N-Cre and C-Cre), each driven by a different promoter. The Cre recombinase is active when N-Cre and C-Cre are expressed in the same cell. With this genetic complementation approach, the infected Cre positive cells could be defined as PLP and GFAP or GAD67 and CCK double positive cells, respectively. Thus, the cell-type-specific expression is achieved via rAAV delivery, and the double positive cells for two different promoters are illustrated with the Cre complementation approach.

BAC transgenic technology, rAAV gene *in vivo* delivery, tTA/rtTA inducible gene activation, 2A peptide cleavage approach and the Cre complementation system, all these newly developed biological tools can be taken advantage of different aspects for different experimental purposes. Moreover, they open a convenient avenue for site-specific and cell-type-specific gene expression in manipulating brain circuits.

Zusammenfassung

Eine lokal kontrollierte Genexpression bei Mäusen ist einer der wichtigsten Forschungsansätze in genetischen Studien zur Gehirnfunktion. In unseren Studien analysierten wir verschiedene fluoreszierende Proteine (FPs), die Cre Rekombinase und den durch Tetrazyklin regulierten Transaktivator (tTA), die mittels transgener Maustechnologie oder rekombinantem Adeno-assoziierten Viren (rAAV) System in das Mausgehirn eingebracht wurden.

Zunächst wurde die zelltypische Besonderheit eines Transgens analysiert, das verstärkte grün fluoreszierenes Protein (EGFP), das spezifisch im Mausgenom in Mitral-/Tuftzellen des *Bulbus olfactorius* exprimieren sollte. Durch pronukleare Injektion des baterial artificial Chromosomes (BAC) wurden verschiedene Gründertiere erzeugt. Von 41 potentiellen Gründern zeigte einer eine spezifische Expression in Mitralzellen und zwei in Mitralzellen und Tuftzellen.

Zwecks einer Reduzierung von Kosten und Zeit, die bei der transgenen Maustechnologie anfallen, veränderten wir unsere Vorgehensweise und verwendeten das rAAV Gentransfer System. Um Zellen, welche die viral übertragenen Proteine exprimieren, zu visualisieren, wurden zwei Strategien angewendet: Zum einen wurden tTA/rtTA mit ihrem bi-direktionalen Responder Ptetbi übertragen, so dass Cre Rekombinase zusammen mit einem FP in der spezifischen Gehirnregion exprimiert wird. Dadurch wurde ein sehr vielversprechendes Expressionslevel von Cre und FPs in kultivierten Neuronen und in den injizierten Regionen erreicht. Für die zweite Strategie wurde eine leicht modifizierte T2A selbstschneidende Peptidbrücke verwendet, um die quantitative Expression der Cre Rekombinase oder auch von tTA/rtTA zusammen mit den FPs zu erreichen. Durch die Anwedung des T2A Peptid Ansatzes können zwei Proteine annähernd equimolar durch einen rAAV Genetransfer Vektor exprimiert werden. Dies eröffnet neue Möglichkeiten der Genfunktionsanalyse im zentralen Nervensystem.

In einem nächsten Schritt untersuchten wir, ob rAAVs für eine zelltypspezifische Expression angewendet werden können. Wir wählten Gliazellen, da in der transgenen Technologie spezifische Promotoren für das Proteolipidprotein (PLP) und das saure Gliafaserprotein (GFAP) beschrieben sind. Als zweite Zellpopulation analysierten wir die Promotoren für lokale Interneuronen, Glutamat Decarboxylase 67 (GAD67) und Cholecystokinin (CCK). Wir untersuchten einen Komplementierungsansatz, welcher die Cre Rekombinase in zwei Teile (N-Cre and C-Cre) auftrennt, wobei dieser Vorgang unter der Kontrolle von zwei verschiedenen Promotoren abläuft. Durch die Verwendung dieses Ansatzes wurde gezeigt, dass die Cre Rekombinase nur exprimiert wird, wenn beide Promotoren zur selben Zeit in der selben Zelle aktiv sind. Mit dem genetischen Komplementierungsansatz können die infizierten Cre positiven Zellen als PLP und GFAP oder GAD67 und CCK doppelt positive Zellen definiert werden. So wird die Zelltyp spezifische Expression durch rAAV Übertragung erreicht und die doppelt positiven Zellen für zwei verschiedene Promotoren durch den Cre Komplementierungsansatz dargestellt.

Mit all diesen neu entwickelten biologischen Werkzeugen, transgene BAC Technologie, *in vivo* rAAV Genübertragung, tTA/rtTA induzierbare Genaktivierung, der 2A Peptid Ansatz und das Cre Komplementierungssystem, kann ein Vorteil für verschiedene Aspekte und experimentelle Zwecke erzielt werden. Darüber hinaus eröffnen sie eine gute Möglichkeit der ortsspezifischen und zelltypspezifischen Genexpression, indem sie die Gehirnschaltkreise manipulieren.

1. Introduction

The amazing complexity of mammalian brain represents the composition of billions of neurons, including thousands of cell types, connected into circuits by trillions of synapes. The essential goal of neuroscience today is no longer the investigation of single neurons, but comprehending the principles of organizing these complex circuits and thereby to explain how they process information and guide the behavior.

The large number of cells existing in our brain consist actually of a large variety of heterogeneous neuron/cell populations. At a microscopic level, in the olfactory system for example, different neuronal populations respond preferentially by the olfactory sensory inputs (Mombaerts *et al*., 1996; Wachowiak *et al*., 2004; Shipley and Ennis, 1996). At a larger scale, cortex and hippocampus appear to be organized in spatially segregated areas associated with different functions (Andersen *et al*., 2007). To distinguish the function of different brain regions and diverse neuron/cell types, the most commonly used method for their characterizations is to look for genes expressed specifically in different locations or types of neurons/cells, for instance glutamate decarboxylase 67 (GAD67) for local interneurons and glial fibrillary acidic protein (GFAP) for glial cell expression. For further *in vivo* studies, transgenic mice were generated, in which the promoters for these site-specific or cell-type-specific genes drive the expression of either a fluorescent protein for visualization of cells that express the functional protein, such as Cre recombinase. In our study, we attempted from different aspects with several newly developed biological tools to achieve site-specific and cell-type-specific gene expression in the mouse brain, and therefore, offer new options for experimental design of genetically based studies in neuroscience.

1.1 Bacterial artificial chromosome (BAC) transgenic mouse model

Transgenic technology via microinjection of DNA into the pronuclei of fertilized oocytes is a commonly used method for gene transfer into the mouse genome (Gordon *et al*., 1980; Gordon and Ruddle, 1981). Not only small size plasmid DNA (Nagga *et al*., 2002; Pinkert and Polites, 1994), but also bigger size DNA fragment, such as bacterial artificial chromosome (BAC, Nielsen *et al*., 1997, Yang *et al*., 1997), can be

used for the generation of transgenic mice. Mice transgenic technology combined with bacterial artificial chromosome (BAC) recombineering (recombination-mediated genetic engineering, Copland *et al*., 2001) is a very powerful tool for the highly efficient tissue-specific expression in the mouse brain, since a single BAC contains the intact gene of interest and all its regulatory components for gene expression. The native genomic surrounding sequence can later protect the transgene from being influenced by other local genes that may come in next proximity during random genomic insertion. At the beginning of our study, we chose an EGFP recombined BAC which appears to limit its gene (*gap junction α9*) expression only in mitral cells in the mouse olfactory bulb.

1.2 Mitral and tufted cells

Mitral/tufted cells are the projection neurons in the mouse olfactory system, which receive input information via their dendrites from the olfactory sensory neurons (OSN) and process the information through their axons to the olfactory cortex (Buck and Axel, 1991; Zhang and Firestein, 2002; Zhao *et al*., 1998; Satou, 1990; Shipley and Ennis, 1996). Cell bodies of mitral cells are lined in the thin mitral cell layer (MCL), whereas those of tufted cells are distributed in the external plexiform layer (EPL) and glomerular layer (GL) (**Figure 1.1a**). In addition, the two types of neurons differ in the size of cell body and the terminal tuft of primary dendrite within the glomeruli, projection pattern of their secondary dendrites, laminar distribution of axon-collaterals within the OB, and the pattern of axonal projection to the olfactory cortex (**Figure 1.1b**) (Haberly and Price, 1977; Mori *et al*., 1983; Orona *et al*., 1984; Pinching and Powell, 1971; Schoenfeld and Macrides, 1984; Schoenfeld *et al*., 1985; Scott *et al*., 1980; Skeen and Hall, 1977).

Since mitral and tufted cells are the projection neurons of the olfactory bulb, and transmit the olfactory information from the periphery to the central nervous system (Shepherd *et al*., 2004), genetically marking mitral/tufted cells and manipulating their properties is crucial for the further understanding of olfactory circuits. We attempted to apply the BAC transgenic model to specifically outline this cell population in mouse olfactory bulb.

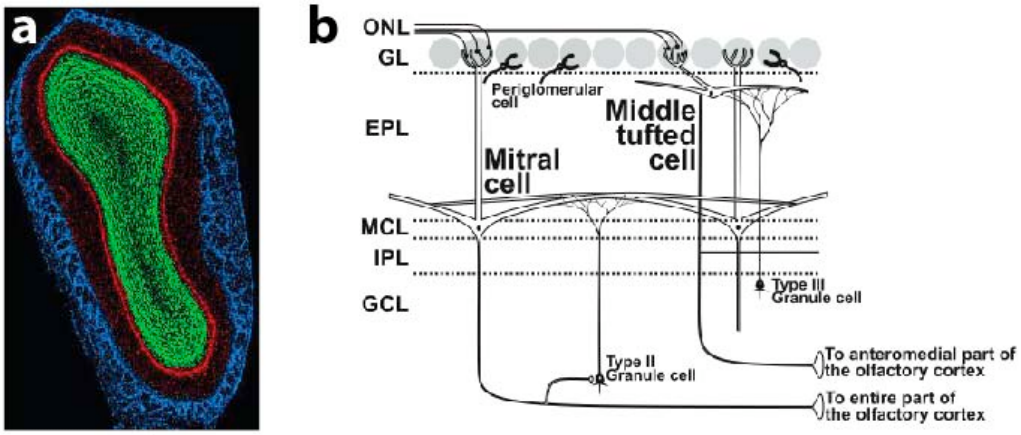

Figure 1.1 Organization of mouse main olfactory bulb. (a) Coronal image of mouse main olfactory bulb. Blue: Glomerular layer; Red: External Plexiform and Mitral cell layer; Green: Internal Plexiform and Granule cell layer. Scale: ventral to dorsal, is approximately 2mm. (From http://en.wikipedia.org/wiki/Olfactory_bulb) (b) Scheme of illustrating the morphological difference between mitral cells and middle tufted cells. Mitral cells have a relatively large cell body in the mitral cell layer (MCL). They extend long secondary dendrites in the deeper half of the external plexiform layer (EPL) and form synapses with the dendrites of granule cells (type II). They project their axons to the entire part of the olfactory cortex. Middle tufted cells have a relatively small cell body and are scattered in the EPL. They extend relatively short secondary dendrites to the superficial half of the EPL and form with granule cells (type III). Tufted cells project their axons only to the anteromedial part of the olfactory cortex. ONL: olfactory nerve layer; GL: glomerular layer; IPL: internal plexiform layer; GCL: granule cell layer. (From Nagayama *et al*., 2004).

1.3 *Gap junction α9* (*Gjα9*) gene

To genetically marking mitral/tufted cells, *Gap junction α9* (*Gjα9*) gene was chosen as the candidate. Gap junctions are clusters of intercellular channels sitting on neighboring cells that permit passage of small molecules of up to 1,000 kDa, such as ions, second messengers and small metabolites. These intercellular membrane channels are also called connexons. Each connexon is composed of subunit proteins, called connexins (Cxs). These gap junctions are presented in almost all cell types of vertebrate organisms, and in the nervous system (Beyer *et al*., 1990; Willecke *et al*., 1991; Bruzzone and Ressot, 1997).

The *Gjα9* is also named as *Connexin 36* (*Cx36*), which belongs to the connexin family. It appears to be preferentially expressed in the adult and developing central nervous system (CNS) in neurons known to be electrically coupled (Condorelli *et al*., 1998), such as the inner and outer plexiform cell layers of the retina, the olfactory bulb, pineal gland, inferior olive, superficial layers of the neocortex, the purkinje cell layer of the cerebellum, pyramidal cells of the CA3/CA4 region of adult hippocampus, and motor neurons in the spinal cord (O'Brien *et al*., 1996; Söhl *et al*.,

1998; Condorelli *et al*., 1998; Al-Ubaidi *et al*., 2000; Guldenagel *et al*., 2000; Parenti *et al*., 2000; Rash *et al*., 2000; Rozental *et al*., 2000; Teubner *et al*., 2000; Feigenspan *et al*., 2001).

Due to the abundant expression in the mitral cells shown in *in situ* hybridization analysis of *Gjα9* in adult rat brain (**Figure 1.2**, Condorelli *et al*., 1998) and the indication from the *Gjα9* gene knockout mice that coupled AMPA response between mitral cell pairs were absent (Christie *et al*., 2005), we chose the BAC clones which contains the complete *Gjα9* gene sequence and the first exon of the gene was substituted with EGFP sequence for generating mitral cell specific expression mouse line via BAC transgenic mouse technology.

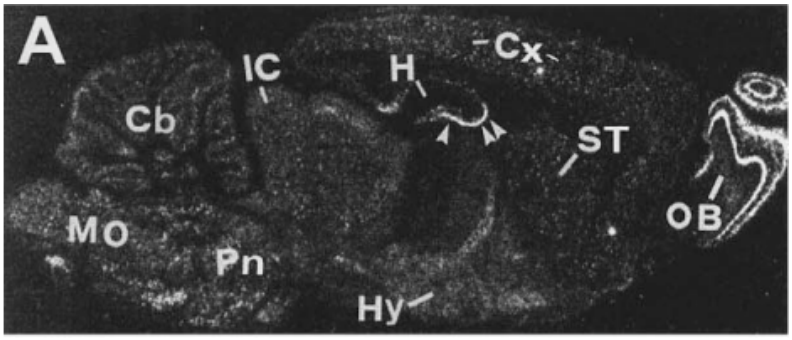

Figure 1.2 *In situ* hybridization analysis of *Gjα9* transcripts in rat brain. Tissue section was hybridized by ^{35}S labeled probes. Darkfield microphotographs of representative autoradiogram of sagittal whole brain section hybridized with an antisense probe. Arrows indicate the expression in hippocampus. Cb: cerebellum; Cx: cerebral cortex; H: hippocampus; Hy: hypotalamus; IC: inferior colliculus; Mo: medulla oblongata; OB: olfactory bulb; Pn: basilar pontine nuclei; ST: striatum. (From Condorelli *et al*., 1998).

1.4 Recombinant adeno-assoiated virus (rAAv) gene delivery

Regarding limitations of the mouse transgenic technology, and to investigate other alternative approaches, we switched to the rAAV gene delivery system, which is more flexible and timesaving in the achievement of the site-specific and cell-type-specific gene expression in the mouse brain.

1.4.1 Recombinant adeno-associated virus (rAAV) as gene delivery approach

Since the early 1980s, the successful cloning of adeno-associated virus (AAV) established the capability to express foreign genes within the recombinant AAV

(rAAV) vector in mammalian cells (Samulski *et al*., 1982; Laughlin *et al*., 1983), rAAV has become an attractive and promising delivery vector for gene therapy approach. The rAAVs are nonpathogenic, that all viral genes were removed, and the replication is dependent on co-infection with a helper plasmid (Muzyczka and Berns, 2001). The rAAV production and purification methods have also already very well established (Kaludov *et al*., 2002; Zolotukhin *et al*., 2002; Smith *et al*., 2003; Blouin *et al*., 2004; Davidoff *et al*., 2004). The fact that rAAV can target neurons in the nervous system, has made this vector a valuable system for the delivery of genes to the brain for functional studies of the nervous system. Therefore, the combination of cell-type selective promoters and local delivery of rAAV could provide a great chance for the brain tissue-specific labeling and the further manipulation of the brain circuits.

1.4.2 Genomic structure of rAAV

Adeno-associated virus (AAV) is a small non-enveloped virus that belongs to the parvovirus family (Blacklow, 1988; Berns *et al*., 1996). It was initially discovered as a contaminant in adenovirus preparations (Atchison *et al*., 1966; Hoggan *et al*., 1966). The AAV is a single-stranded DNA virus and is packaged as a plus or a minus strand. The viral genome is approximately 4.7 kilobase pairs (kb) in length, and is composed of two major open-reading frames encoding Rep (replication) and Cap (capsid) proteins. Four Rep proteins (Rep 78, Rep 68, Rep 52, and Rep 48) are generated from the 5' open-reading frame through the use of two different promoters and alternative splicing (Mendelson *et al*., 1986). The 3' open reading frame of wild-type AAV generates three capsid proteins (VP1, VP2, and VP3) through alternative splicing and alternative start codon usage (Trempe *et al*., 1988) (**Figure 1.3a**). The virion particle has icosahedral (20-faced) symmetry with a diameter of 26 nm and a molecular weight of 5.5 - 6.2 million Daltons (MDa) (Buller *et al*., 1978; Muzyczka, 1992; Berns, 1996; Linden *et al*., 2000).

In rAAV, the Rep and Cap genes are removed from the vector and replaced by a target transgene cassette or genes of interest (**Figure 1.3b**, promoter, cDNA of genes of interest and polyadenylation site).

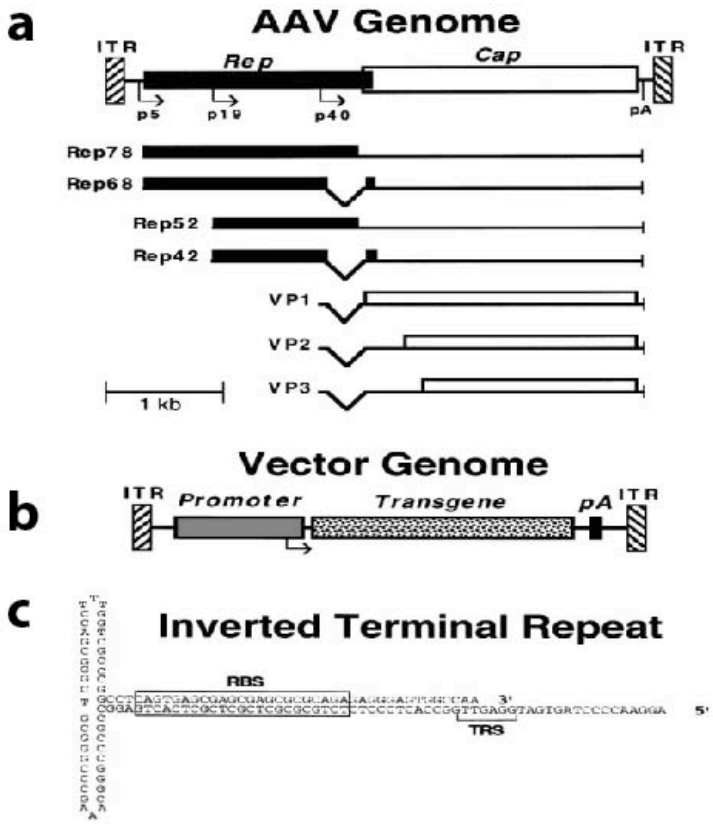

Figure 1.3 Structure of wild-type and vector AAV genomes. (a) Map of the wild-type AAV genome, including Rep (solid) and Cap (open) reading frames, promoters (p5, p19, and p40), polyadenylation site (pA), and inverted terminal repeats (ITR). The viral transcripts encoding the different Rep and Cap (VP1-3) proteins are shown below the genome. The smaller Rep proteins, VP2 and VP3, are translated from internal initiation sites. (b) Map of a typical AAV vector, showing replacement of the viral Rep and Cap genes with a transgene cassette (promoter, transgene cDNA, and polyadenylation site). (c) Secondary structure of the AAV ITR, with the locations of the Rep binding site (RBS) and terminal resolution site (TRS) indicated. (From Russell and Kay, 1999)

The two viral genes are flanked by the inverted terminal repeats (ITRs, 145 bp in length for AAV2, Lusby *et al*., 1980). These ITRs are self-complementary and GC-rich sequence (**Figure 1.3 c**). The stable T-shaped hairpin plays a very important role in the AAV genome and is the only necessary viral component in recombinant vector genomes. Included in the ITR are two motifs, a terminal resolution site (TRS) and a Rep binding site (RBS), which are necessary for replication and encapsidation of the viral genome.

1.4.3 Serotypes

To date, more than 110 primate's AAV capsid sequences have been identified (Gao *et al.,* 2005). Each of those that have unique serological profiles was named as a particular AAV serotype. And 12 primate's serotypes (AAV1 - 12) have been

described (Rutledge *et al*., 1998; Xiao *et al*., 1999; Samulski *et al*., 1983; Muramatsu *et al*., 1996; Chiorini *et al*., 1997; Chiorini *et al*., 1999; Gao *et al*., 2002; Gao *et al*., 2004; Mori *et al*., 2004; Schmidt *et al*., 2008). Because different AAV serotypes enter cells via distinct cell surface receptors (Summerford and Samulski, 1998; Qing *et al*., 1999; Summerford *et al*., 1999; Walters *et al*., 2001; Di Pasquale *et al*., 2003), it was hypothesized that different serotypes would target diverse tissue types. Numerous studies have evaluated and compared different serotypes regarding their transduction efficiency in tissues *in vivo*, such as different cell types and brain regions.

So far rAAV1, rAAV2, rAAV4, rAAV5, rAAV6, rAAV7 and rAAV8 have been tested in the nervous system (Alisky *et al*., 2000; Davidson *et al*., 2000; Yang *et al*., 2002; Passini *et al*., 2003; Vite *et al*., 2003; Burger *et al*., 2004; Taymans *et al*., 2007). The most commonly used vector has been based on AAV2. It has been successfully used to transduce adult mammalian brain, where mainly neurons are targeted (Davidson *et al*., 2000). However, rAAV1 and rAAV5 have demonstrated a higher distribution and number of neurons transduced than rAAV2 in the CNS, such as in striatum, hippocampus, globus pallidus, substantia nigra, spinal cord, and cerebellum (Alisky *et al*., 2000; Davidson *et al*., 2000; Wang *et al*., 2002; Burger *et al*., 2004; Paterna *et al*., 2004). Recent studies have shown greater infection efficiency with rAAV7 and rAAV8 than with rAAV2 in striatum, hippocampus, globus pallidus and substantia nigra in mouse brain (Taymans *et al*., 2007). In our study, to achieve high virus infection both *in vitro* and *in vivo*, we used a cross-packaging of rAAV1 and rAAV2.

1.4.4 Principle of the rAAV gene delivery system

Since rAAV is a replication defective virus, the production of the recombinant viral vector needs help from either a helper virus, such as adenovirus, or of some genes from the helper virus. The original protocol was using adenovirus (Hermonat and Muzyczka, 1984; Zhou and Muzyczka, 1998; Flotte and Carter, 1995) or herpes simplex virus (Conway *et al*., 1997) as helper virus. However, the adeno or herpes as helper virus in the rAAV production should be avoided for *in vivo* applications. To avoid contamination, the required helper genes E4, E2A, and VA from adenovirus were used to construct helper plasmids. These helper plasmids were termed pDG

plasmids (**Figure 1.4**). Not only E4, E2A, and VA from adenovirus, but also rep genes from AAV were inserted into these plasmids. The rep gene is from AAV2, while the cap gene originates from serotypes 1 - 6, thus 6 helper plasmids were cloned for 6 different serotypes (pDG1 – 6, Grimm *et al*., 1998; 2003).

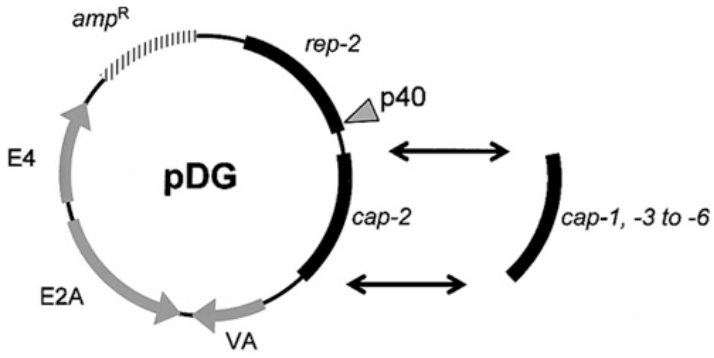

Figure 1.4 Map of pDG plasmid. Plasmid pDG carries all genes essential for packaging of AAV-2 vectors, i.e., AAV-2 *rep* and *cap* genes and VA, E2A, and E4 genes of adenovirus 5. Five novel helper constructs were derived from pDG by exchanging the AAV-2 *cap* gene with *cap* of AAV serotype 1, 3, 4, 5, or 6. (From Grimm *et al*., 2003).

1.4.5 The rAAV production

The cross-packaging of rAAV vector plasmid and different pDG helper plasmids was about 10 times more efficient than the traditional adenovirus-help method (Grimm *et al*., 1998; 2003). Figure 1.5 shows the general scheme of rAAV production.

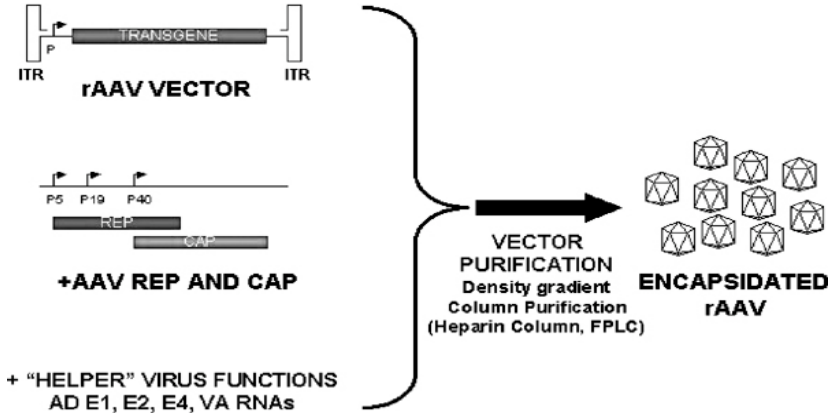

Figure 1.5 General Scheme of rAAV2 vector production. The rAAV vectors have been constructed by removal of endogenous viral genes, and insertion of an expression cassette(s) between flanking ITRs. The rAAVs are generally encapsidated by transfection of a plasmid containing the rAAV vector into cells with provision of AAV rep and cap (as either plasmids or by using cells expressing them) and 'helper' virus functions such as Adenovirus E1, E2, E4, and VA RNAs (either as a plasmid or by viral infection). The resulting vector is then purified using density gradient centrifugation ($CsCl_2$ or Iodixanol) and/or column purification. (From Sun *et al*., 2003).

1.4.6 Cellular entry and trafficking of rAAV

Understanding the rAAV cellular entry and trafficking is very important for improving the efficiency of rAAV-mediated gene delivery. The entry and trafficking can be divided into several steps (**Figure 1.6**). First, the viral particles attach to the cell surface by binding to the receptor. The most significant factor effecting viral binding is the abundance of AAV receptors. This stage can be most significantly influenced by the choice of rAAV serotype or type of capsid variant used to generate the recombinant virus. Second stage is receptor-mediated endocytosis of the virus. This step may be influenced by the AAV co-receptors on the surface of the target cells, which can trigger the endocytosis. Next stage involves rAAV movement to the nucleus, including vesicular trafficking, endosomal escape and nuclear transport. The final post nuclear step for rAAV trafficking is viral uncaging and genome conversion of the single-stranded rAAV genome to double-stranded DNA, which is capable of expressing transgenes (Douar *et al.*, 2001; Yan *et al.*, 2004; Xiao *et al.*, 2002; Hansen *et al.*, 2000).

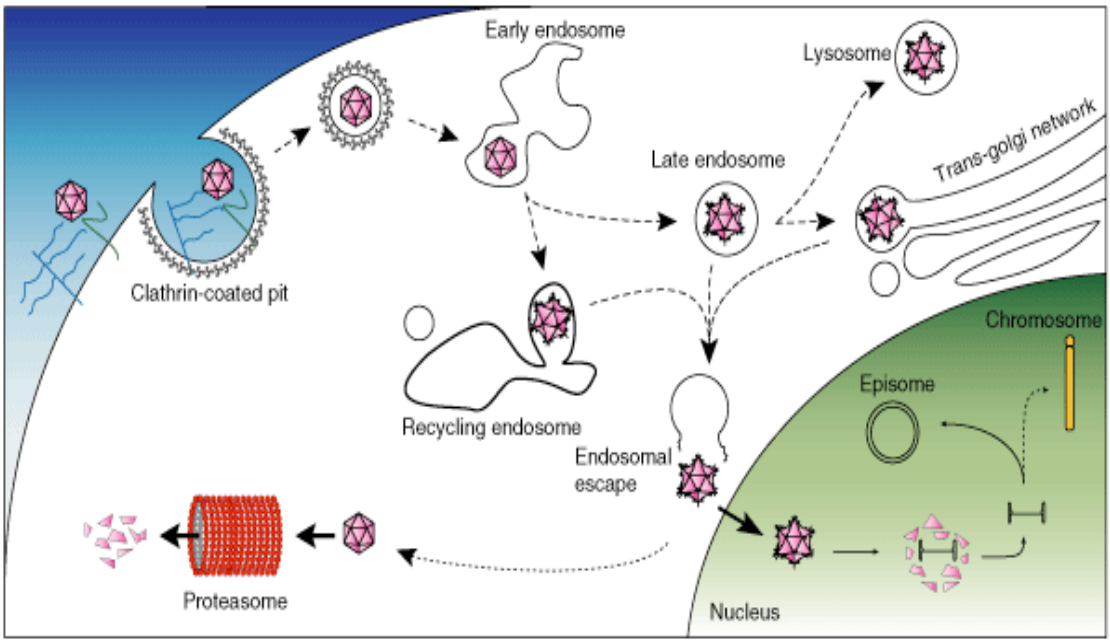

Figure 1.6 Cell entry and trafficking of recombinant adeno-associated virus (rAAV). Stages and events during AAV cell transduction. Transduction of target cells by AAV is initiated by viral binding of AAV to the cell-surface receptor and co-receptors, followed by internalization (endocytosis), trafficking to the nucleus, nuclear entry and uncoating, and nuclear gene expression. (From Schultz and Chamberlain, 2008).

1.5 Tetracycline-controlled transactivator (tTA) inducible gene expression

By applying rAAV gene delivery approach, the functional proteins, such as Cre recombinase, can be flexibly expressed at the desired brain regions. However, the *in vivo* visualization of delivered genes is still an unsolved issue. To fulfill this, a delivery method of two different proteins is required. At the beginning of the rAAV work, we took tetracycline-controlled transactivator (tTA) or reverse tTA (rtTA) inducible gene expression system which has been used to regulate gene expression in a number of species. It was first described by Gossen and Bujard (Gossen and Bujard, 1992) and is the best characterized and well studied regulated promoter system. The system is based on the *E.coli* tetracycline-resistance operon, a regulatory unit that detects minute concentration of tetracycline and mounts an appropriate resistance response. Since the elements are derived from a prokaryotic organism, there is no endogenous expression in mammalian cells (Gossen *et al*., 1993).

1.5.1 Principles of the Tet-controlled gene expression

1.5.1.1 Inducible Tet-system in prokaryotes

The tTA-system is based on regulatory elements of the Tn10- tetracycline-resistance operon from *E.coli* (Gossen and Bujard, 1992). In Gram-negative bacteria, tetracycline (Tet) can kill bacteria by blocking protein synthesis (Epe and Woolley, 1984). A gene called TetA mediates resistance to Tet (Yamaguchi *et al*., 1990). In the absence of Tet, TetA is not expressed since it is blocked by the tetracycline repressor (TetR), which binds in the TetR and TetA promoter regions to the operators, tetO1 and tetO2, respectively. This results in a transcriptional blockade of TetR and TetA, thereby down-regulating expression of TetR and TetA. In the presence of Tet, Tet binds to TetR, thereby reducing the affinity of TetR to the tetOs, which results in the loss of the transcriptional blockade.

1.5.1.2 Tet-controlled gene expression in Eukaryotes

The Tet regulation system from prokaryotes has been adapted for experimental gene regulation in eukaryotes by fusing TetR to the VP16 transcriptional activating domain

from herpes simplex virus VP16, thereby creating a synthetic tetracycline-regulated transcriptional activator protein (tTA) that can be used to regulate a gene that is under the control of a tetracycline-responsive promoter, so called Tet-inducible system (Gossen and Bujard, 1992). This system consists of two components, the Tet-controlled transactivator protein (tTA), and the Tet-regulated element (TRE). The tTA is a fusion protein of the TetR and the C-terminal VP16 protein. The TRE region consists of seven copies of tetOs and a minimal cytomegalovirus (CMV) promoter that contains the transcription start site with a TATA box (Ptet). The TetR-VP16 fusion protein binds to tetO sequences located in front of the minimal promoter via the TetR domain, while the C-terminal VP16 domain participates in the recruitment of the RNA polymerase II (Pol II) transcriptional initiation complex. In the absence of tetracycline, tTA binds to the Ptet and drives the expression of the downstream gene. The addition of tetracycline to the medium prevents tTA from binding the tetO sequence and the promoter is inactive (**Figure 1.7**).

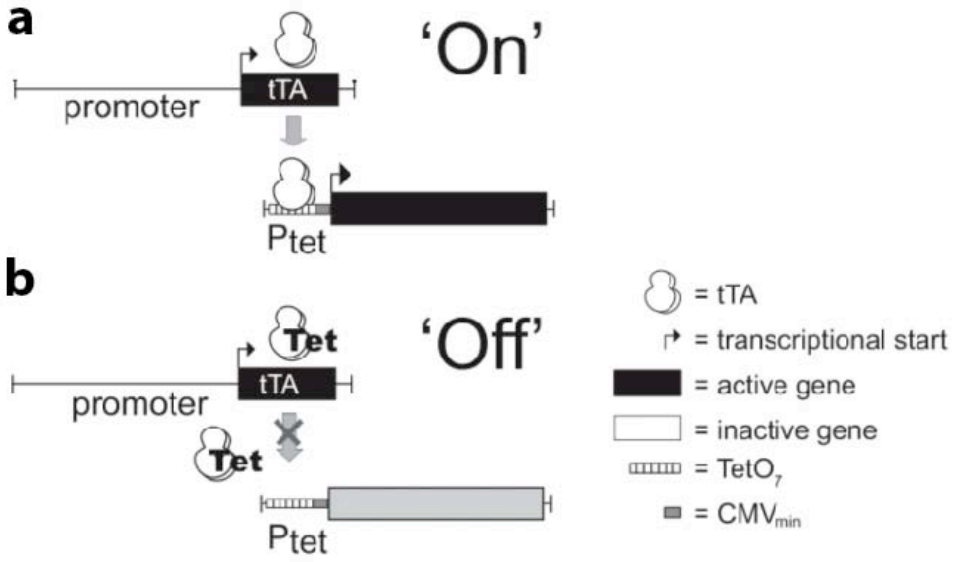

Figure 1.7 Principle of the Tet-Off-system. (a) When the constitutively expressed tTA binds to tetO7 (Ptet), tTA initiates transcription. (b) In the presence of Tet, tTA is unable to bind to Ptet and Ptet - controlled gene transcription is turned-off (Tet-Off). (From Sprengel and Hasan, 2007).

1.5.1.3 The reverse tTA (rtTA) system

A variation of this system uses a 'reverse' tetracycline transactivator (rtTA). This was achieved by exchanging the TetR of tTA by a TetR mutant with four point mutations (E71K, D95N, L101S and G102D) to generate the reverse tTA (rtTA). The rtTA only

binds tetO in the presence of tetracycline. In this case, a gene under Ptet-control is expressed in the presence of tetracycline, but not in its absence (Hecht *et al*. 1993; Gossen *et al*. 1995).

1.5.1.4 Improvement of the tTA system

Since the original tTA system was derived from prokaryotic system, the application of this system on mouse transgenics is relatively limited. It is difficult to generate transgenic mice expressing the tTA to direct efficiently a gene of interest in a region specific manner in brain (Kim, 2001; Jerecic *et al*., 1999). Replacement of the VP16 activation domain by three copies of a 12 amino acid minimal activation F-domain, improved its tolerance in mammalian cells (Baron *et al*., 1997; Kim, 2001). Additionally, a nuclear localization signal sequence located at the N-terminus of tTA and improved the binding efficiency of tTA on the Ptet responder in the nucleus (**Figure 1.8**).

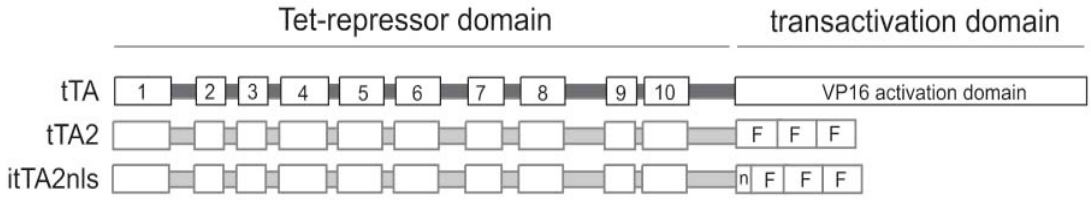

Figure 1.8 Schematics of tTA and improved tTA composites. The TetR-core region with 10 α-helices (1–10) contains sites for tetO-binding, Tet-binding and homodimerization. VP16 or minimal F-domains make up the transactivation domains. The position of the nuclear localization domain (n) is indicated. (From Sprengel and Hasan, 2007).

1.5.2 The Tet-inducible gene expression via rAAV delivery

The transgenic approaches (Sprengel and Hasan, 2007) for site- and cell-type specific expression is very time consuming and in many cases unsuccessful. As already mentioned above, rAAV mediated gene delivery is a fast and efficient method for the gene expression both *in vitro* and *in vivo*. It is also a very attractive method to deliver Tet-regulated genes into experimental animals. The two components (tTA activator and tetO responder) of the Tet-inducible system can be inserted into two separate rAAV vectors (McGee Sanftner *et al*., 2001; Zhu *et al*., 2007). The tTA activator expression can be driven by a cell-type-specific promoter to achieve cell type

specificity. In our study, tTA activator virus was driven by the Synapsin promoter to achieve neuron specificity and local injection of rAAV could mediate desired site-specific expression in the mouse brain.

1.5.3 The tTA/rtTA dependent Ptet-bi promoter

As described above, the TRE region on the tTA/rtTA responder vector has seven copies of tetOs and a minimal cytomegalovirus (CMV) promoter that contains the transcription start site with a TATA box. This vector is named 'Ptet' responder vector (**Figure 1.9**). Additional insertion of another CMV minimal promoter containing TATA box on the opposite side of tetO7 produced a bi-directional Tet promoter (Ptet-bi), which enables the expression of two genes with one responder vector. This offers us the possibility for expressing two genes (a functional protein and a fluorescent protein) within one construct and could be at the same time controlled by the tTA/rtTA inducible system.

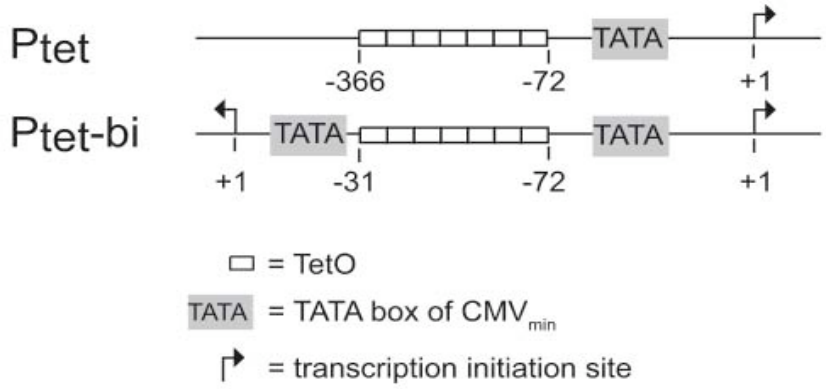

Figure 1.9 Scheme of Ptet and Ptet-bi promoters. The different promoter elements of the two tTA/rtTA-controlled promoters are depicted. Nucleotide positions relative to the transcriptional start sites (position +1) are indicated. (From Sprengel and Hasan, 2007)

To apply the tTA/rtTA inducible system together with the rAAV delivery approach, we tested the feasibility of this combination under both *in vitro* and *in vivo* conditions, and demonstrated the efficient dual gene expression in the brain. The rtTA Tet-on system also showed very robust gene activation upon the induction of Doxycycline, a Tetracycline derivative. Furthermore, with the strong gene activation, the anatomic brain circuits of infected brain regions were clearly visualized by fluorescent proteins, indicating the contribution of local individual neurons to the entire brain circuits.

1.6 The 2A peptide-mediated self-processing

Although the tTA/rtTA inducible system combined with rAAV gene delivery approach shows a very efficient gene expression level, the Ptet based bi-cistronic viral vectors have to be used with great care. The strengths of the left and right promoters were never quantified and the translation efficiencies and mRNA stabilities of two gene products can be very different. Conventionally, rAAV delivery of multiple genes within a single transcriptional unit was performed mainly using internal ribosomal entry sites (IRES) from picornavirus or by using Ptet based bi-cistronic viral vectors as metioned above (Zhu *et al*., 2007). The IRES is a nucleotide sequence that allows for translation initiation at any position of an mRNA sequence. However, in many examples translational initiation at IRES elements is too weak for efficient gene expression, and large sequence (~500 nucleotides) also results the limitation (Hennecke, *et al*., 2001).

An alternative and more promising approach involves the use of self-processing viral peptide bridges. So-called 2A or 2A-like peptide sequences separate different protein coding sequences in a single ORF transcription unit of *Picornaviridae* (Ryan *et al*., 1991). The 2A peptide sequences from different members of the picornavirus family share a highly conserved motif of only 18 amino acids, mediating the cleavage between the C-terminal glycine and the N-terminal proline of the downstream 2B sequence (Ryan *et al*., 1991). Initially, the 2A peptide was supposed to have an auto-proteolytic event (Ryan *et al*., 1991), therefore, it was termed as "self-cleaving peptide". Ultimately, a ribosomal-skip mechanism was proposed, and 2A and 2A-like sequences are referred to as cis-acting hydrolase elements (CHYSEL), rather than self-cleaving peptides (de Felipe *et al*., 2006). However, 2A or 2A-like peptide sequences do result a cellular expression of multiple, discrete proteins (in essentially equimolar quantities), derived from a single ORF (de Felipe *et al*., 2006).

Figure 1.10 Amino acid sequence of 2A peptide from *Thosea asigna* virus. The arrow indicates the cleavage site.

The 2A peptide-mediated cleavage has previously been shown to result in faithful co-expression of heterologous proteins in different cell lines (de Felipe *et al*., 2006) and in neurons (Furler *et al*., 2001). Surprisingly, the potential of this system has not been exploited in cellular and systems neuroscience. In particular, it has not been addressed whether 2A peptide-mediated co-expression of heterologous proteins is quantitative in neurons and expression levels of fluorescent reporters would be high enough for *in vivo* imaging applications. Another important point is to ensure that 2A peptide transcripts have no detrimental impact on neuronal viability and function.

To address these questions, we analyzed the efficiency of co-expression of various proteins in neurons *in vitro* and *in vivo*, using a peptide bridge from *Thosea asigna* virus (Donnelly *et al*., 2001). We demonstrate that this system has clear advantages because it achieves efficient and reliable functional co-expression of multiple proteins in neurons *in vivo*. We also show that viral co-expression of Cre recombinase (Sauer, 1993) or a tetracycline-controlled transactivator (tTA, Kistner *et al*., 1996) with fluorescent proteins (FPs) is compatible with *in vitro* and *in vivo* gene expression and imaging approaches and can be combined with inducible genetic mouse models to enable targeted manipulation of faithfully labeled neuronal subgroups.

1.7 Cre recombinase and Cre complementation system

After achieve the site-specific expression in the mouse brain by applying two different strategies, we next analyzed whether rAAV can be used for the cell-type specific expression of Cre recombinase *in vivo* via a Cre complementation system.

The bacteriophage P1 possesses a site-specific recombination system, the Cre/LoxP system. Expression of Cre recombinase results in recombination between pairs of 34-bp LoxP elements in direct orientation (Abremski and Hoess, 1984). Cre mediated deletion of floxed alleles is a powerful tool to study gene function in conditional knockout mouse models. The locally restricted and time induced expression of active Cre permits a precise analysis of gene function in subsets of cells. Particularly in neuroscience, Cre-mediated mutagenesis is full of importance, since most of the CNS specific genes are expressed in many different brain regions and in global gene knockout can thus lead to a complex phenotype.

Although the Cre/LoxP-system has been widely used to analyze the cell-type-specific function of a gene by conditional inactivation or conditional ectopic expression (Lewandoski, 2001; Bockamp *et al.*, 2008), in many cases a single marker gene or a single promoter activity is not sufficient to identify a certain cell type unequivocally (Luo *et al.*, 2008). For instance, local interneurons in the forebrain release the transmitter γ-aminobutyric acid (GABA) (Monyer and Markram, 2004; Markram *et al.*, 2004; Maccaferri and Lacaille, 2003) and therefore, express the enzyme glutamate decarboxylase (GAD). However, among all interneurons there are many subpopulations regarding expression of various combinations of different proteins or neuropeptides, such as calcium-buffering proteins (parvalbumin, calbindin) and cholecystokinin (CCK) (Pawelzik *et al.*, 2002; Somogyi *et al.*, 1984; Markram *et al.*, 2004). These markers are not only expressed in interneurons, but also some other neuron types. Therefore, genetically targeting of these marker-positive interneurons by driving Cre recombinase from a single promoter will almost certainly hit several distinct neuron types.

To overcome this limitation, a novel Cre complementation system was developed to introduce a second promoter controlling the range of recombination based on the complementation of Cre-protein fragments. This was achieved by constructing fusion proteins of a constitutive protein-protein interaction domain with either an N- or C-terminal Cre fragment (designated N-Cre and C-Cre, respectively, Jullien *et al.*, 2003; 2007). Each of these 'split-Cre' proteins is driven by a distinct promoter, and does not catalyze DNA-recombination alone. Expressed together in one cell they readily assemble into a functional enzyme *in vivo* (**Figure 1.11**).

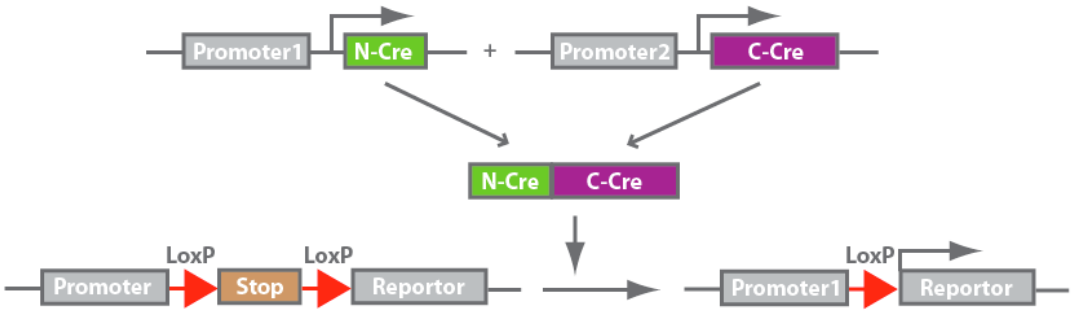

Figure 1.11 Principle of Cre complementation system. The expression of N-Cre and C-Cre are placed under the control of two different promoters (promoter 1 and 2, respectively). Only if both promoters are active, functional complementation takes place and LoxP (red triangles) – flanked sequences are recombined, thereby activating/inactivating reporter genes.

We combined this complementation system with the rAAV gene delivery approach, the infected Cre positive cells could be defined as double-promoter (promoter1 and promoter2) positive cells. Thus, the cell-type-specific expression can be achieved with the rAAV system and double positive cells for two different promoters are illustrated with the Cre complementation system.

In summary, with our study of site-specific and cell-type-specific gene expressions of visualized functional proteins, we could combine some new tools for different experimental goals which permits a new level of gene manipulation of the neuronal circuits in the brain of animals.

2. Results

2.1 Generation of transgenic mice expressing EGFP in mitral cell layer in mouse olfactory bulb

We first applied the BAC transgenic technology in the hope to achieve the specific expression of enhanced green fluorescent protein (EGFP) in mitral/tufted cells in mouse olfactory bulb. Bacterial artificial chromosome (BAC) modification was performed by the GENSAT project at the Rockefeller University. Using BAC recombinerring technique, a BAC containing mouse gap-junction-α9 gene (*Gjα9*) was modified by homologous recombination (Gong *et al*., 2002), yielding the replacement of the first exon of *Gjα9* by EGFP sequence. NotI linearized BAC DNA was then purified by sucrose gradient and injected into pronuclei of fertilized mouse oocytes at the Interfakultäre Biomedizinische Forschungseinrichtung (IBF) Heidelberg to generate several transgenic mouse lines.

By tail biopsy and genomic PCR, the existence of EGFP in founder animals was assessed. Twelve out of 41 potential founders were identified. To further characterize the expression pattern of these founders, they were bred with wild-type C57Bl/6 mice to obtain F1 generation. For unknown reasons some of those founders lacked transgene transmission or the ability to reproduce, only 8 provided F1 offspring. The F1 mice were analyzed by anti-GFP immunostaining of brain sections at postnatal day 42 (P42). All mice from F1 generation showed EGFP expression in olfactory bulb and other brain regions with different expression intensities and cell-type specificities. Three founder lines were selected, which showed very strong expression in the olfactory bulb.

The F1 offspring from founder 27 showed strong expression restricted to mitral cells in the olfactory bulb. Most mitral cells are labeled and as well as their axon projections. The lateral olfactory tract, which is composed of axon projections from mitral cells, could be detected in piriform cortex (**Figure 2.1 a**). The F1 mice from founder 30 had less labeled cells in the mitral cell layer, but showed expression in some other brain regions, such as hippocampus and cortex (**Figure 2.1 b**). The F1

mice from founder 32 showed strong labeling in both mitral and tufted cells in the olfactory bulb. The lateral olfactory tract was as well strongly immunolabeled (**Figure 2.1 c**).

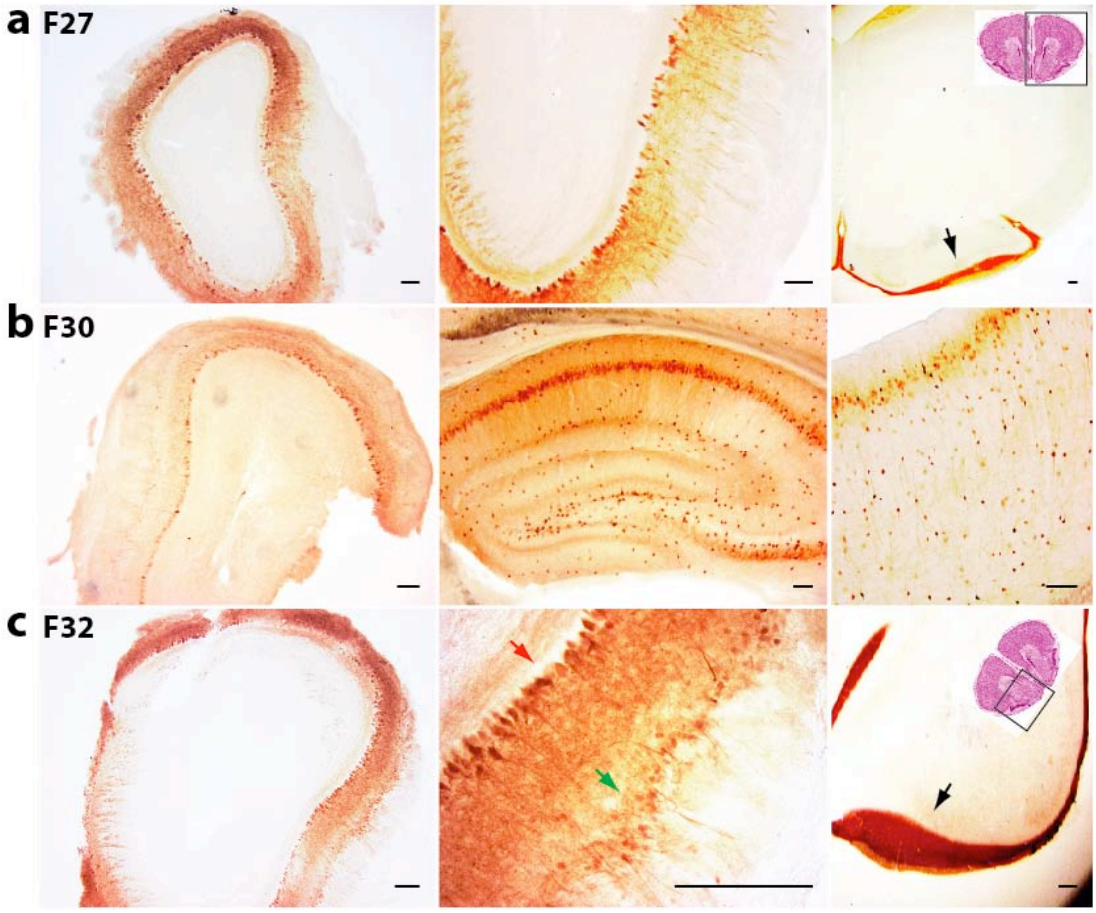

Figure 2.1 Founder analysis of *Gjα9* BAC transgene by DAB staining. (a) Founder line F27, only mitral cells were labeled in the olfactory bulb, the lateral olfactory tract was indicated by black arrow. (b) Founder line F30 shows the EGFP expression in mitral cells in the olfactory bulb, in hippocampus and somatosensory cortex (from left to right, respectively). (c) Founder line F32, both mitral (indicated by red arrow) and tufted (indicated by green arrow) cells are detected in the olfactory bulb, and lateral olfactory tract is indicated by black arrow. All sections are coronal sections, scale bar: 125 μm.

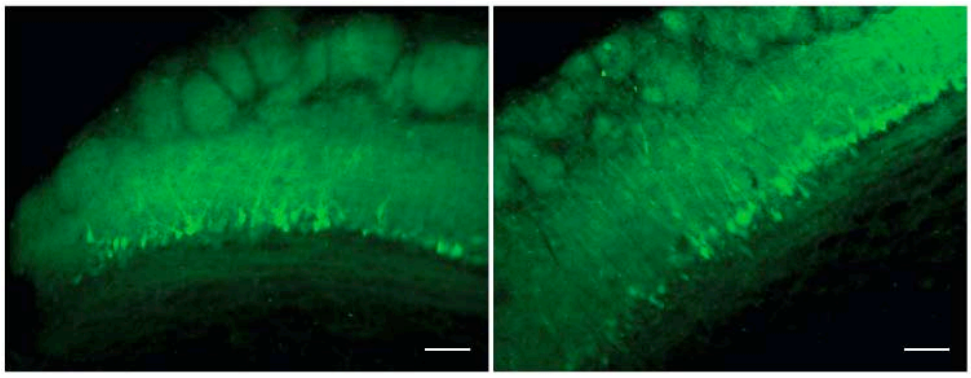

Figure 2.2 Native fluorescence in olfactory bulb from in-bred offspring of founder line F27. Mitral cells were clearly detected by EGFP fluorescence, in both cell bodies and dendrites. Scale bar: 50 μm.

Although the native fluorescence in the olfactory bulb from founder line F27 can be detected, the intensity of EGFP was not very high. Therefore, in-bred offspring was used to obtain higher fluorescent expression. Olfactory bulb sections from in-bred offspring were directly placed under the fluorescent microscope after perfusion and fixation. And as expected, EGFP fluorescence could be detected clearly in the cell bodies of mitral cells as well as in their dendrites (**Figure 2.2**). This finding would offer the possibility for mouse olfactory bulb *in vivo* imaging with two-photon microscopy.

2.2 Multiple gene expression via recombinant adeno-associated virus (rAAV) gene delivery

Bacterial artificial chromosome (BAC) modification and mouse transgenic technology as applied above is often used for tissue-specific labeling. However, this method is expensive and is time-consuming. Therefore, we changed to a virus mediated gene transfer as a short cut method for tissue-specific gene transduction and gene manipulation.

2.2.1 Tetracycline-controlled transactivator (tTA) inducible gene expression

Considering the visualization of cells with virus delivered proteins by fluorescent proteins, we applied an inducible gene expression system, the tetracycline-controlled transactivator (tTA) system, combined with rAAV gene delivery approach. With this system, two heterologous proteins can be expressed with one Ptet-bi vector. At the same time, the expression of the Ptet-bi controlled genes can be regulated by the tTA or rtTA.

2.2.1.1 Tetracycline-controlled transactivator (tTA) induced iCre and Venus expression in hippocampal neuron culture

Tetracycline-controlled transactivator (tTA) induced responder gene expression was introduced into the rAAV system as described before (Zhu *et al*., 2007). Both activator construct with tTA driven by the neuron specific Synapsin promoter and a responder Ptet-bi construct expressing the proteins, improved Cre recombinase (iCre),

and Venus fluorescence were cloned into the rAAV backbone as listed (**Figure 2.3 a**). First the cultured primary hippocampal neurons were co-infected with both rAAV-Syn-tTA and rAAV-Ptetbi-iCre-Venus viruses. Both unpurified viruses, 0.5 µl each, were added into each well of a 24-well plate, which had a cultured neuron density of about 50,000 cells/well. Ten days after the co-infection, strong Venus fluorescence was detected in almost all the neurons in the culture. And the cultured neurons were later immunostained with rabbit anti-Cre antibody, which was visualized with Cy3 coupled secondary antibody. The Venus fluorescence and Cy3 signal were co-localized in nearly 100% of the infected neurons. The iCre signal was detected mainly in nuclei, while Venus was distributed over the whole cell, including soma, dendrites and axons (**Figure 2.3 b**).

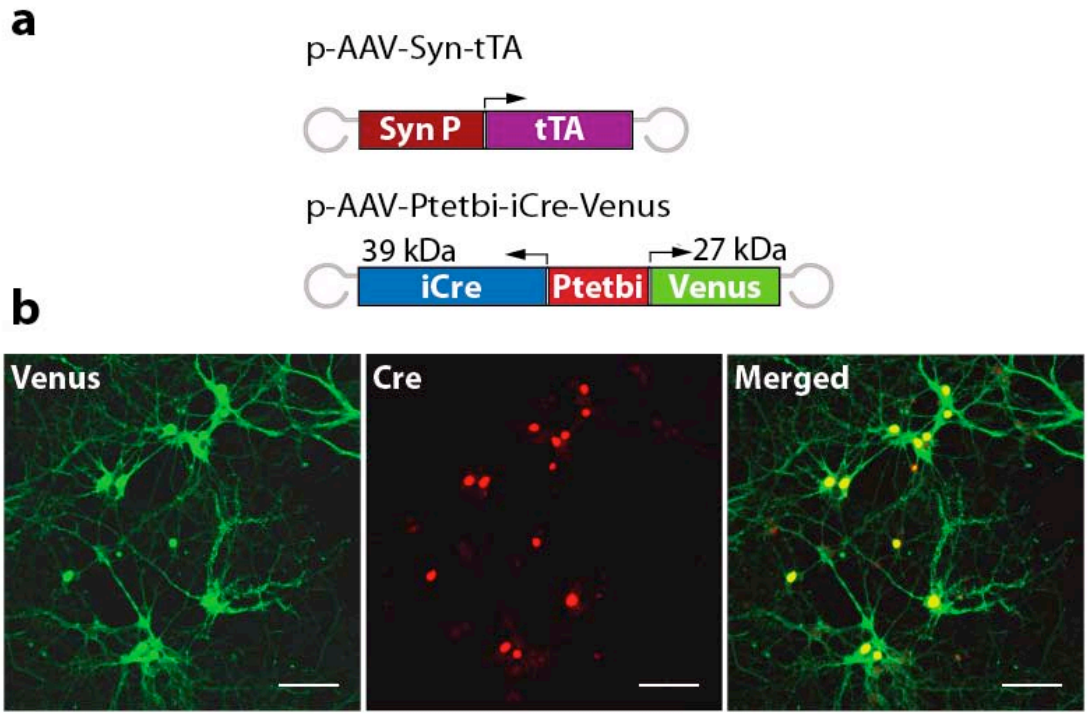

Figure 2.3 Co-infection of rAAV-Syn-tTA and rAAV-Ptetbi-iCre-Venus in primary hippocampal neuron culture. (a) Scheme of the tTA inducible system in the rAAV plasmid vector. (b) Fluorescence confocal microscopy image of co-infected culture neurons. Ten days after virus co-infection, cultured neurons were fixed and iCre signal was detected by a polyclonal primary antibody and Cy3 coupled secondary antibody, while the Venus fluorescence was directly imaged. Scale bar: 50 µm.

2.2.1.2 Tetracycline-controlled transactivator (tTA) inducted iCre and Venus expression in the mouse brain

For *in vivo* application, both activator virus rAAV-Syn-tTA and responder virus rAAV-Ptetbi-iCre-Venus were co-injected into cortex (**Figure 2.4 a**) and hippocampus (**Figure 2.4 b**) of wild-type mouse. Two weeks after virus infection, the

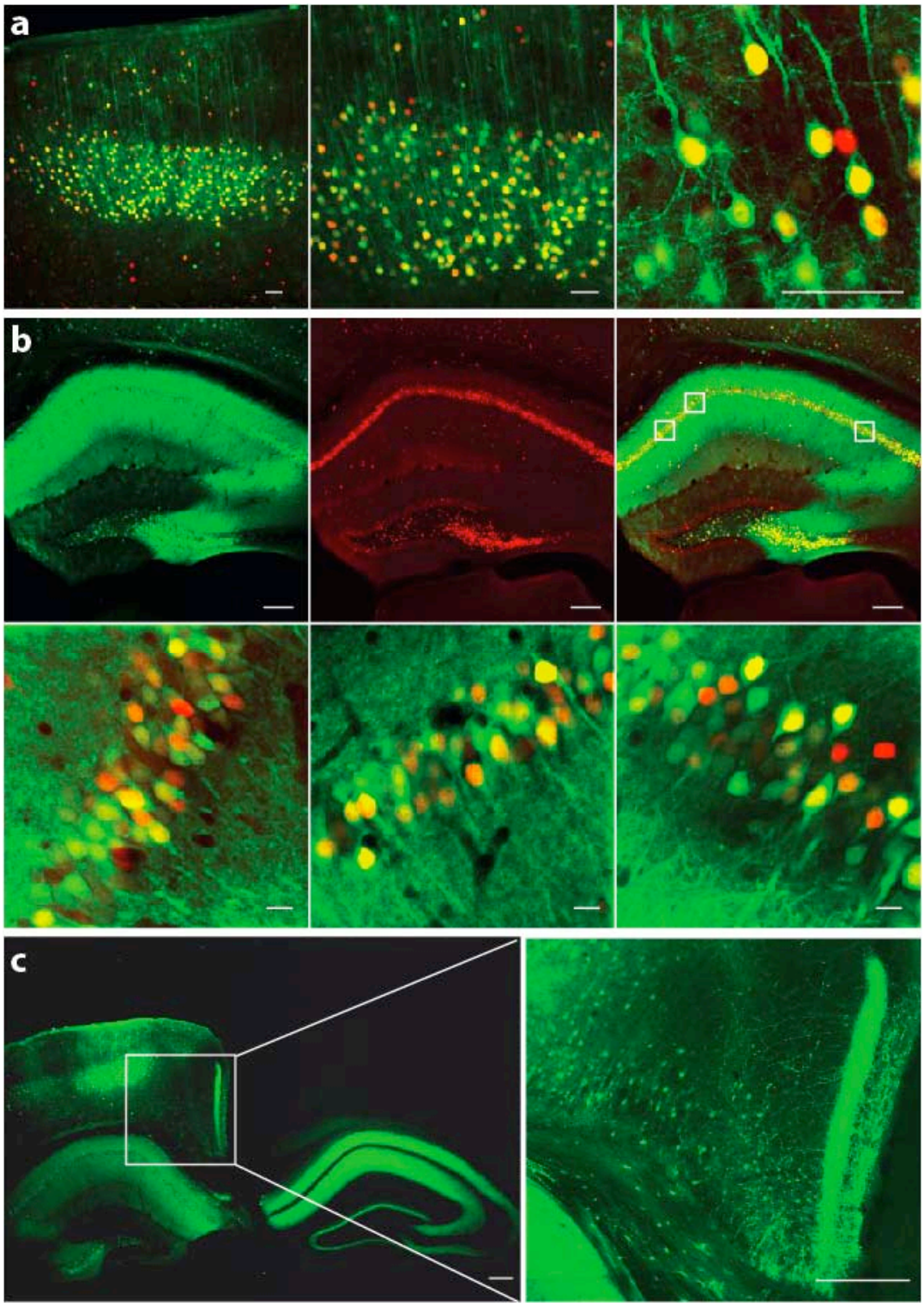

Figure 2.4 The tTA inducible gene activation system in mouse cortex and hippocampus by rAAV delivery. (a, b) Confocal images of brain sections from a wild-type mouse co-injected with rAAV-Syn-tTA and rAAV-Ptetbi-iCre-Venus in cortex and hippocampus. Venus was directly imaged and Cre was detected with a rabbit polyclonal antibody together with a Cy3 coupled secondary antibody. Nearly 100% of the Venus positive green cells were Cre positive, in cortex as well as in hippocampus (a) Images of infected cortical region with different magnifications. Scale bar: 50 μm (b) Overview image of infected hippocampus and detailed images as boxed. Scale bar: upper 200 μm; lower 10 μm (c) Cortical and hippocampal unilateral injection (left hemisphere), cortical projections (boxed region) and hippocampal contra lateral hemisphere projections were detected. Scale bar: 200 μm.

injected cortical region and the entire hippocampus were infected expressing strong Venus fluorescence. Immunostaining with rabbit anti-Cre antibody together with Cy3 coupled secondary antibody revealed that almost 100% of the infected neurons showed both Venus and Cy3 signals. This demonstrates that the rAAV gene delivery method combined with tTA inducible gene activation system can be applied successfully *in vivo* simultaneous delivery of of two heterologous proteins. However, there are few cells that are detected either only with green or with red fluorescence. Although the virus co-infection obtained very high expression level of both proteins, this finding pointed out the unequal expression of the bi-directional Ptet-bi promoter.

Surprisingly, by unilateral rAAV infection *in vivo*, we found labeled neuron projections not only in the injected hemisphere, but also in the contra lateral hemisphere in hippocampus (**Figure 2.4 c**). Since the mouse was injected only unilaterally, we could predict that the labeled projections in the contra lateral hemisphere can only originate from the injected hemisphere. Cortical projection could be also distinctly revealed at the injection hemisphere (**Figure 2.4 c**).

2.2.1.3 The tTA induced functional iCre in Cre-reporter Rosa26R mice

To testify the enzymatic activity of the expressed iCre *in vivo* via rAAV delivery, we co-injected rAAV-Syn-tTA and rAAV-Ptetbi-iCre-Venus into cortex and hippocampus of adult Cre-reporter Rosa26R mice (Soriano, 1999). Two weeks later, expression of the Cre-dependent lacZ reporter gene indicated successful delivery of functional iCre in the injected cortical region and dorsal hippocampus (**Figure 2.5**).

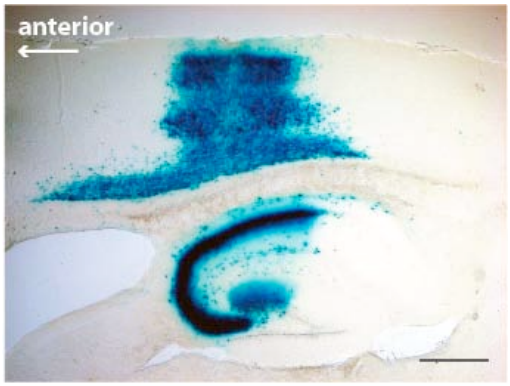

Figure 2.5 LacZ staining of a sagittal brain section from a Cre-reporter Rosa26R mouse co-injected with rAAV-Syn-tTA and rAAV-Ptetminibi-iCre-Venus. Positive lacZ staining indicated the functional iCre *in vivo*. The infected cortical region and dorsal hippocampal showed positive blue staining. Scale bar: 500 μm.

2.2.1.4 Reverse tTA (rtTA) induced iCre and tdTomato expression *in vivo*

To demonstrate the functionality of the reverse tTA (rtTA) *in vivo* via rAAV delivery approach, which is a complementary genetic module uniquely suited for strict and rapid gene activation by addition of Doxycycline (Dox) in cultured cells (Gossen and Bujard, 1992) and *in vivo* (Kistner *et al*., 1996), we used rAAV-Syn-rtTA and rAAV-Ptetbi-iCre-tdTomato for further *in vivo* test of the Dox regulated tdTomato expression. Viruses were co-injected unilaterally into 8 adult Cre-reporter Rosa26R mice. And 6 were treated with 800 mg/l of Dox via drinking water directly after injection (two for cortex injection, two for hippocampus injection, and two for both cortex and hippocampus injection). Two were left untreated. Two weeks after virus infection and Dox induction, robust native red tdTomato fluorescence was detected all over at the injection site (**Figure 2.6**). In contrast, the Dox untreated mice showed only very few fluorescent positive cells (data not shown), which was expected and could be explained by the leakiness of the Ptet-bi bi-directional promoters (Zhu *et al*., 2007). The robust native tdTomato fluorescence indicates the successful Dox induction in rtTA inducible gene activation system combined with rAAV gene delivery approach.

Due to the strong and stable tdTomato fluorescence, neuronal projections from the injection sites to the contra lateral hemisphere and other brain regions, which were shown previously by Venus fluorescence, were again clearly visible (**Figure 2.6**). In the brain of only cortically injected mice, the projections from infected neurons are observed symmetrically in the injection site and contra lateral cortical region, both sides of corpus callosum, thalamus, hypothalamus and striatum (**Figure 2.6a**). In the brain of only hippocampally injected mice, we found again symmetrically projected termini of infected neurons in injected hippocampus and contra lateral hippocampus, both sides of corpus callosum, thalamus, hypothalamus, striatum, and perifornical nucleus. Unilateral cortical projections were also observed in the injected hemisphere (**Figure 2.6b**). Except hippocampus and striatum, the signal of projections from infected neurons at the contral lateral side are very weak, and can only be visualized with high magnification imaging. We speculate that the number of contra lateral projections is lower or much lower than the ones in the injected hemisphere, but the existence of these projections proves that the extendibility of the functional activity

from a single neuron to the complete neural network. This observation reveals the potential possibility how does the individual neuron act in synchronizing neuronal activity of both hemispheres of the brain.

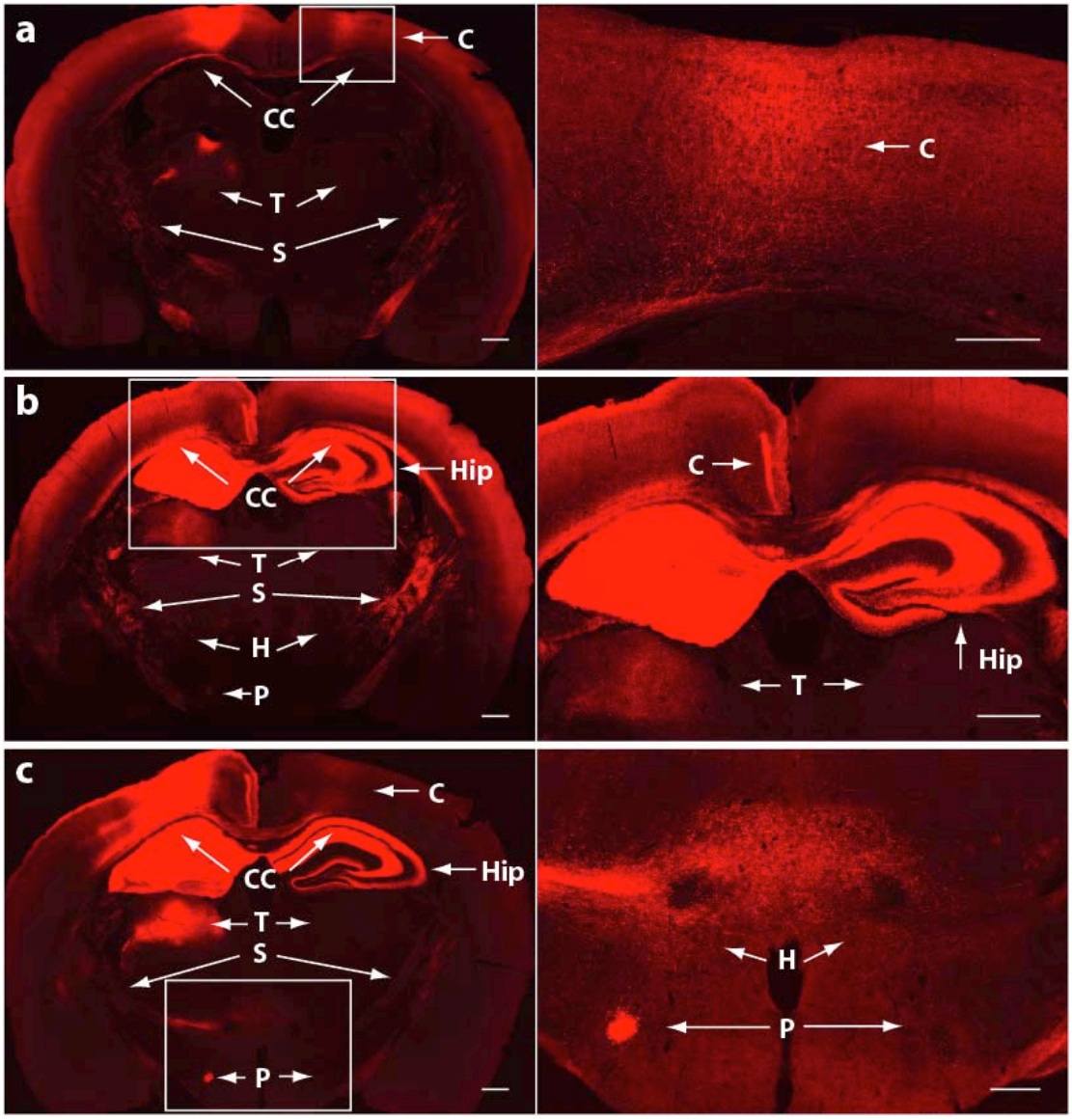

Figure 2.6 Neuronal projections of rAAV-Syn-rtTA and rAAV-Ptetminibi-iCre-tdTomato co-infected cells by unilateral injection. Two weeks after injection, mice were analyzed and images were taken directly by confocal microscopy. Boxed regions are shown in magnification on the right panel. (a) Cortical unilateral rAAV co-injection. Neuronal projections were found in contralateral cortex, in both sides of thalamus, hypothalamus, striatum, and corpus callosum of the brain. (b) Hippocampus unilateral rAAV co-injection. Projections were found in contra lateral hippocampus, both sides of thalamus, hypothalamus, striatum, corpus callosum and perifornical nucleus. (c) Unilateral co-injection of both cortex and hippocampus. Projections were found in all regions mentioned above. C, cortex; CC, corpus callosum; T, Thalamus; H, hypothalamus; Hip, hippocampus; S, striatum; P, perifornical nucleus. Scale bar: 500 μm.

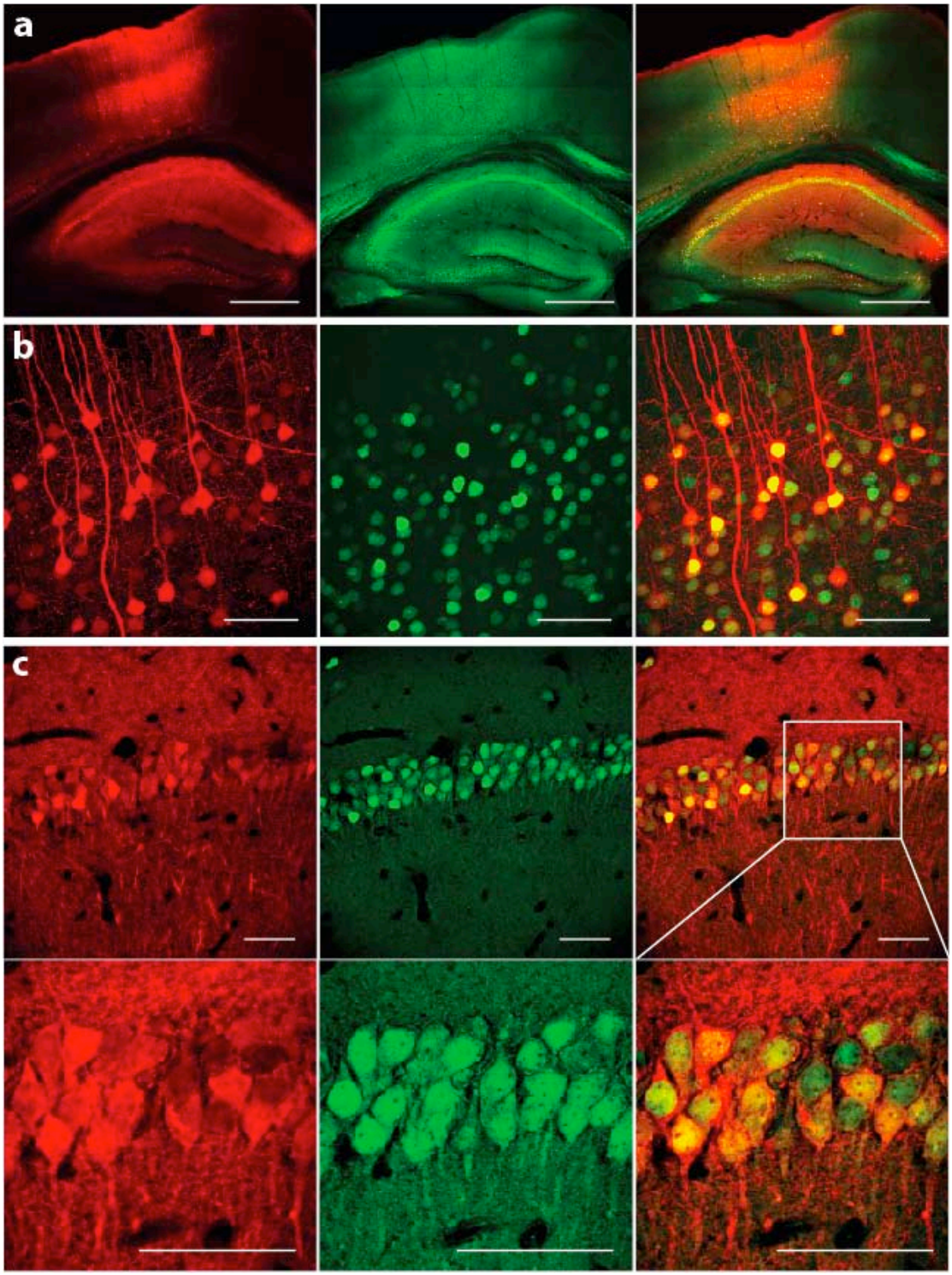

(to be continued)

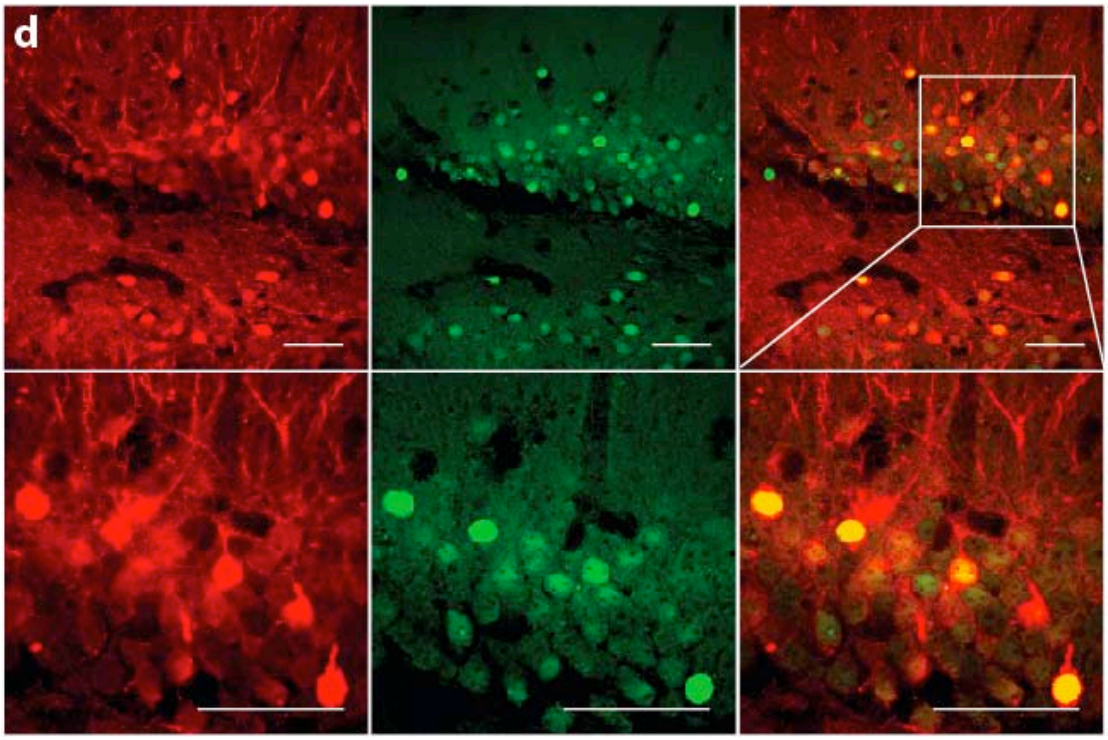

Figure 2.7 Co-expression of tdTomato and iCre in injected mouse brain. Two weeks after injection, brain sections were stained with a rabbit anti-Cre primary antibody and a FITC coupled secondary antibody. Infected neurons were strongly visualized by the native fluorescence of tdTomato, while iCre signal was illustrated in the nuclei in green. (a) Overview of infected brain regions, including cortex and hippocampus. tdTomato fluorescence was co-localized with FITC signal from iCre. Scale bar: 500 μm. (b) Z-project image of a confocal stack of an infected cortical region. Scale bar: 50 μm. (c, d) Images from infected hippocampal CA1 (c) and dentate gyrus (d) regions. Higher magnification images from the boxed regions are shown below. Scale bar: 50 μm.

To further demonstrate the bi-directionality of the Ptet-bi promoter in the rtTA inducible system, the existence of second delivered gene iCre was revealed by immunohistochemistry with a polyclonal rabbit anti-Cre primary antibody and a FITC coupled secondary antibody. The Cre positive green cells were detected nearly 100% co-localized with tdTomato positive cells (**Figure 2.7**). Due to the leakiness of the Ptet-bi promoters, few single positive cells were also observed (**Figure 2.7b)**. The enzymatic activity of iCre was proven by lacZ staining on brain sections showing positive blue signals in the injected regions (**Figure 2.8**), demonstrating the functionality of the delivered Cre recombinase. Therefore, in the presence of Dox, the full activation of both delivered genes indicates the ability of complete dual-gene expression via Dox induction and the bi-directionality of the Ptet-bi responder virus. Hence, the combination of Dox dependent rtTA inducible system and rAAV gene *in*

vivo delivery approach could offer great chance for inducible fast gene expression at specific brain regions.

Figure 2.8 LacZ staining of rAAV-Syn-rtTA and rAAV-Ptetminibi-iCre-tdTomato co-infected mouse brain sections. Blue staining indicates the enzymatic activity of rAAV delivered iCre at the different injection sites *in vivo*, including only cortical and only hippocampal injections and the injection at the both sites. Scale bar: 500 μm.

2.2.2 Efficient and quantitative expression of multiple heterologous proteins in mouse brain via 2A peptide approach

A method allowing for efficient and quantitative co-expression of multiple heterologous proteins in neurons *in vivo* would be highly valuable for many applications in neuroscience. As described above, the tTA/rtTA inducible gene activation system can be applied together with the rAAV gene delivery approach to achieve high expression of multiple genes at the desired brain regions *in vivo*. However, as we described above, in the bi-directional promoters, the expression levels of the two Ptet-bi controlled genes are unequal and not quantitative. Therefore, self-cleaving peptide bridges, so-called 2A or 2A-like peptide sequences from *Picornaviridae* virus family or insect virus *Thosea asigna* virus, are considered as an alternative and more promising approach for multiple gene expression.

In this set of experiments, we analyzed the efficiency of co-expression of various proteins in neurons *in vitro* and *in vivo* using a 2A peptide bridge from *Thosea asigna* virus when applied in rAAV delivered genes. We demonstrate that this system has clear advantages because it achieves efficient and reliable functional co-expression of multiple proteins in neurons at the desired specific brain regions *in vivo*. And can be combined with other inducible genetic mouse models to enable targeted manipulation of faithfully labeled neuronal subgroups. Furthermore, the 2A peptide approach can

be combined with tTA/rtTA inducible gene activation system to not only visualize the existence of tTA/rtTA, but also induce the responder gene expression both *in vitro and in vivo*.

2.2.2.1 Plasmid construction of rAAV iCre2A fusion

To introduce the 2A peptide into the rAAV system, 54 base-pair DNA sequence of the 2A peptide from *Thosea asigna* virus was assembled from oligonucleotides (**Figure 2.9 a**). Four plasmids were constructed using either the Kusabira Orange (KO, Karasawa *et al*., 2004) were linked in frame with the DNA sequence of iCre via the 2A peptide sequence (**Figure 2.9 b**).

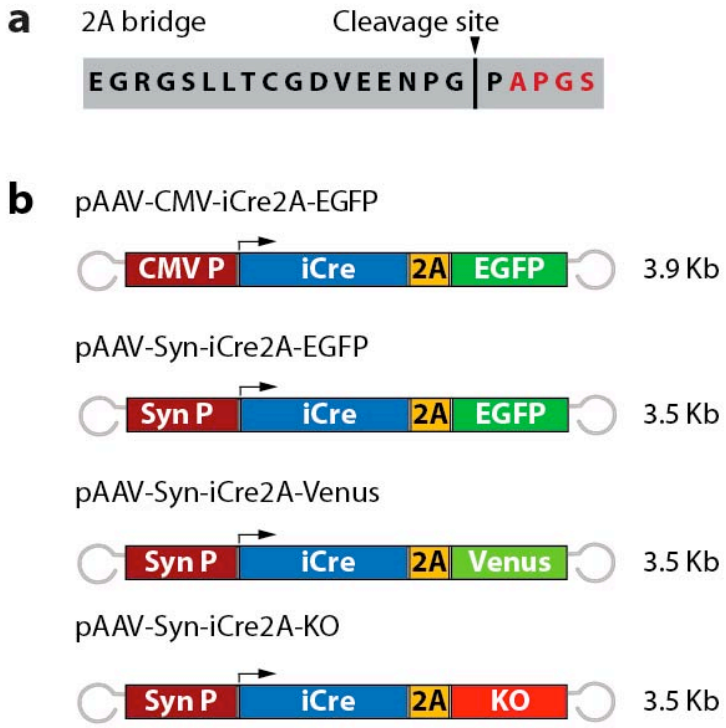

Figure 2.9 Plasmid constructs of iCre2A fusion in rAAV vector. (a) Amino acid residues of 2A peptide from *Thosea asigna* virus. The cleavage site is indicated with the arrow. Amino acid residues in red were added to keep the C-terminal environment constant between different constructs. Bottom: Diagram of rAAV vector constructs. (b) Diagram of rAAV vector constructs of iCre2A fusions with different fluorescent proteins (GFP, Venus or KO) and two different promoters (CMV or Synapsin promoter). Lengths of sequences between ITRs are noted.

2.2.2.2 Quantification of cleavage efficiency of 2A peptide in HEK293 cells

To test the cleavage efficiency of 2A peptide, first pAAV-CMV-iCre2A-EGFP was transfected into HEK293 cells **(Figure 2.10a)**. Three days after transfection, bright

EGFP fluorescence was observed in the culture with high tranfection efficiency (**Figure 2.10b**). Western blot analysis was performed with the transfected HEK293 cell lysates for both EGFP and iCre expression to verify the 2A-mediated cleavage. Both full-length protein iCre2A-EGFP and cleaved products, iCre2A and EGFP, were detected demonstrating the functional 2A peptide cleavage in HEK293 cells. The molecular weight (MW) of the released iCre2A was slightly bigger than that of "wild-type" iCre (39 kDa, co-transfection of pAAV-CMV-tTA and pAAV-Ptetbi-iCre-Venus) due to the short, remaining 2A tail of 17 aminoacid residues (40.8 kDa). About two-thirds of the full-length protein was cleaved according to the intensity of the bands (**Figure 2.10c**).

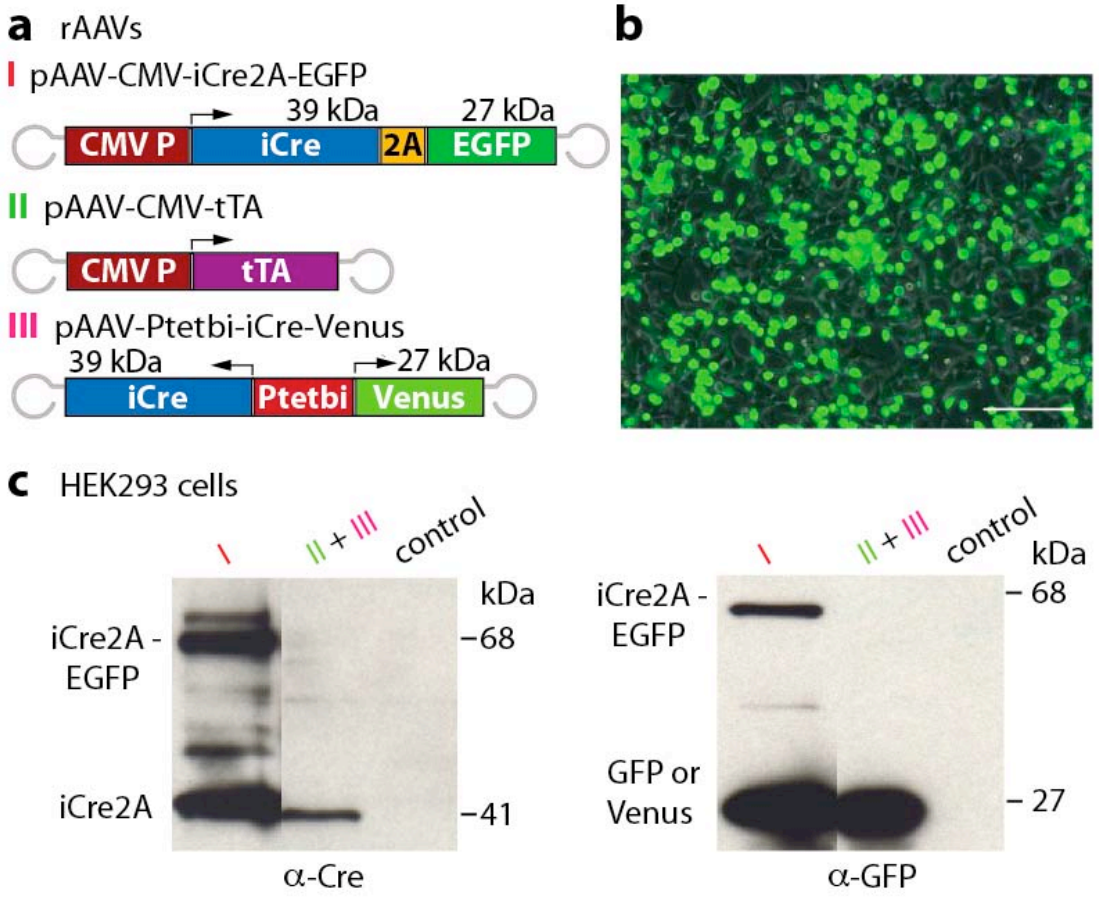

Figure 2.10 Constructs of 2A fusion were cleaved in HEK293 cells resulting in functional and reliable co-expression of heterologous proteins. (a) Diagram of transfected rAAV vecotor constructs. (b)Overlay of fluorescent image and phase image of HEK293 cells transfected with pAAV-CMV-iCre2A-EGFP. HEK293 cells were fixed 3 days after transfection and imaged directly by fluorescent microscopy. Scale bar: 100 μm. (c) 2A-mediated cleavage in HEK293 cells. Western blots of protein extracts from transfected HEK293 cells. The 40.8 kDa iCre2A fusion protein and the 27.3 kDa EGFP were detected, and to lesser extent, the 68.1 kDa precursor full-length protein. I: Cells transfected with rAAV-CMV-iCre2A-GFP. II+III: Cells co-transfected with rAAV-CMV-tTA and rAAV-Ptetbi-iCre-GFP. Control: Non-transfected cells.

2.2.2.3 Efficient 2A peptide cleavage and co-expression in primary neurons

For virus production, both pAAV-Syn-iCre2A-GFP and pAAV-Syn-iCre2A-Venus plasmid constructs were used to generate rAAVs. To examine 2A peptide cleavage and functional co-expression of proteins in neurons, we infected rat primary hippocampal neurons separately with both rAAVs (each 0.5 µl). Ten days after infection, strong green fluorescence was detected nearly in all cultured neurons and Venus showed brighter signal than EGFP (**Figure 2.11**). To demonstrate the co-expression of EGFP or Venus with iCre, a polyclonal antibody raised against Cre was used for the immunohistochemistry and EGFP or Venus fluorescence was directly imaged. The 2A-mediated cleavage was supported with the finding that the iCre signal was detected exclusively in the nucleus and Venus mainly in the cytosol. Even without enhancement, Venus expression was high enough to visualize fine cellular processes (**Figure 2.11**).

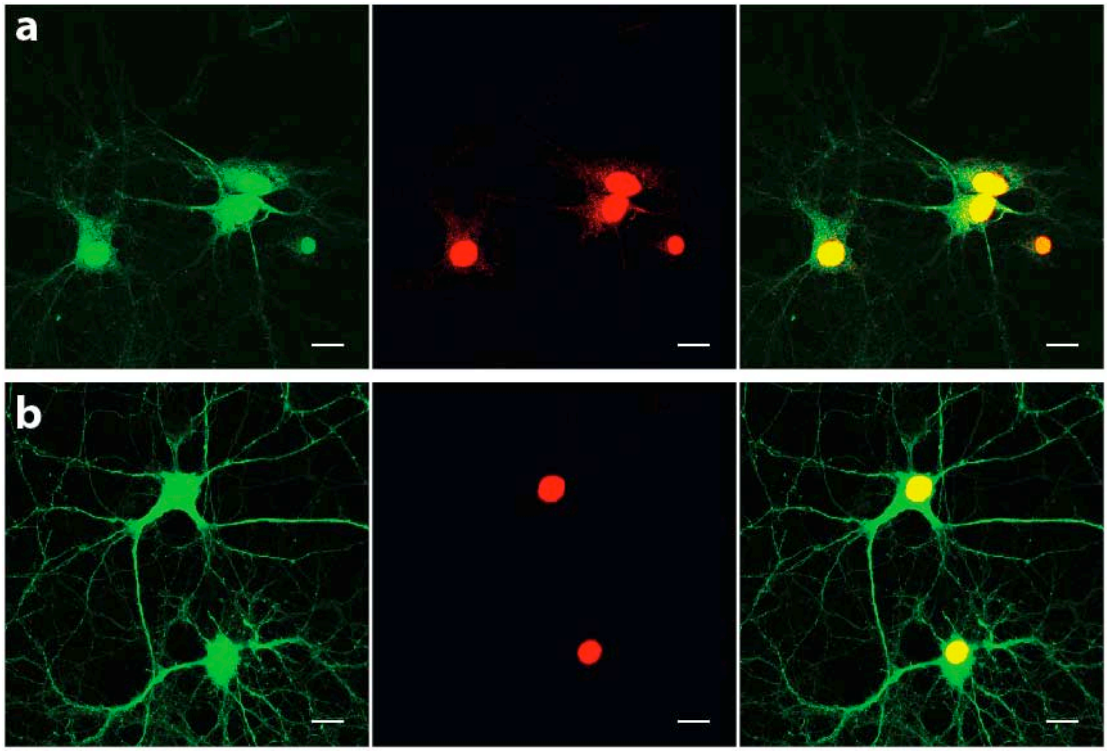

Figure 2.11 Co-expression of EGFP or Venus with iCre in rat primary hippocampal neuron cultures. Confocal images of primary hippocampal neurons infected with rAAV-Syn-iCre2A-EGFP (a) and rAAV-Syn-iCre2A-Venus (b). Neurons co-express cleaved and freely diffusible Venus (green) and nuclear restricted iCre (red, visualized with Cy3-coupled antibody), indicating that the 2A fusion construct was cleaved successfully *in situ*. Scale bars: 10 µm.

To quantitatively determine the efficiency of 2A peptide cleavage, neurons were harvested from the rAAV-infected primary hippocampal neuron culture. We found in Western blots of neuron lysates high levels of released iCre and Venus together with low levels of the full-length protein, indicating efficient 2A-mediated cleavage (**Figure 2.12b**). When compared to cleavage in HEK293 cells (**Figure 2.10c**), the balance between newly synthesized full-length iCre2A-Venus and the released iCre2A and Venus appeared much more in favor of cleaved products in neurons, indicating that the 2A strategy may be particularly suitable for co-expression in non-dividing cells such as neurons or in the brain.

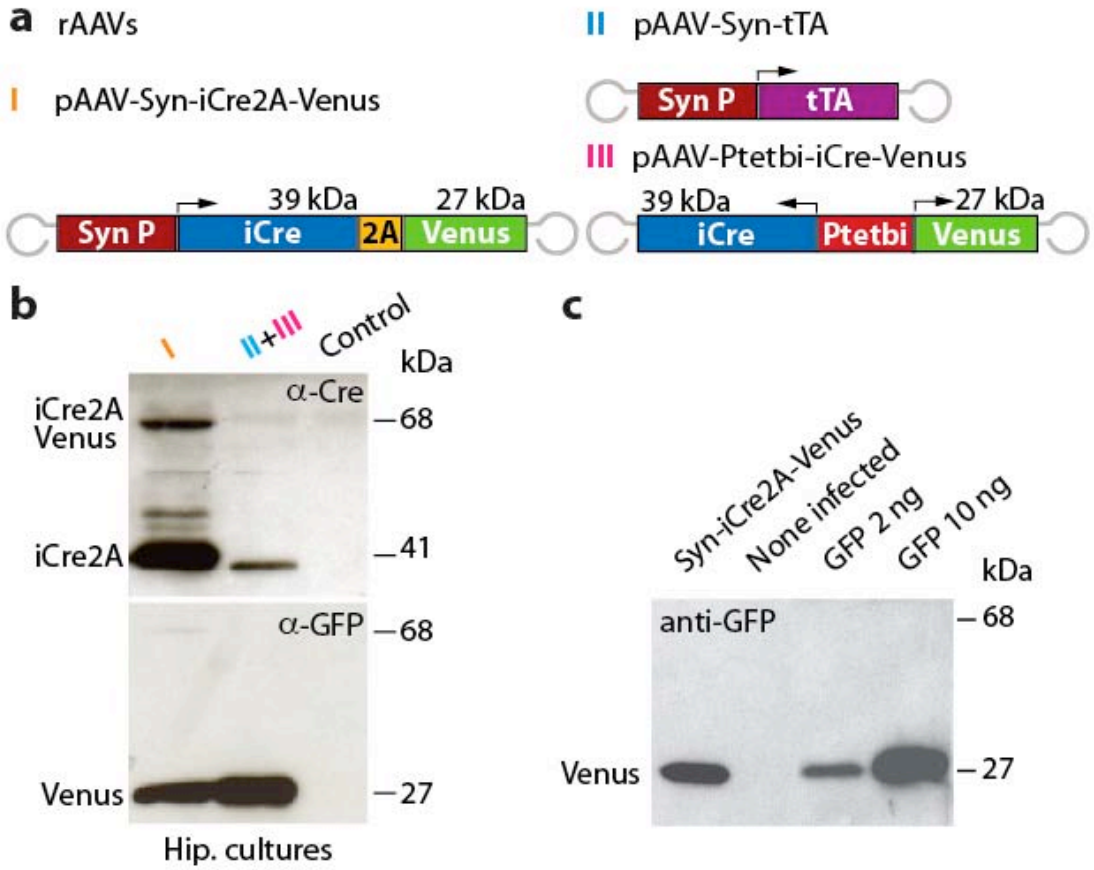

Figure 2.12 Western blot analysis of 2A-mediated cleavage in rAAV infected primary hippocampal neurons. (**a**) Diagram of rAAV vector constructs. (**b**) 2A-mediated cleavage in primary hippocampal neuron cultures. Western blots of protein extracts from rAAV-infected hippocampal neurons. The 40.8 kDa iCre2A fusion protein and the 27.3 kDa Venus were detected, and to a very small extent, the 68.1 kDa precursor full-length protein. I: neurons infected with rAAV-Syn-iCre2A-Venus. II+III: neurons co-infected with the activator virus rAAV-Syn-tTA and rAAV-Ptetbi-iCre-Venus. Control: Non-infected neurons. (c) Western blot analysis and quantification of hippocampal primary neuron culture infected with rAAV-Syn-iCre2A-Venus. Cell lysate (10 µg) was loaded together with none infected neuron lysate, 2ng and 10ng of purified GFP protein. Quantification was done by ImageJ, and in comparison to purified GFP, the amount of fluorescent signal from the infected neuron culture is equivalent to 5.99 ng (0.11 x 10^{-4} pmol/cell) of purified GFP protein.

To directly compare the 2A approach with the tTA induced co-expression of iCre and Venus, we used a bi-directional Ptet-bi promoter construct as described before (**Figure 2.3a, 2.12a**). When expressed from this bi-directional promoter, iCre levels were much lower than those obtained from the iCre2A-Venus fusion construct when normalized to the levels of Venus (**Figure 2.12b**). The immunosignal of Venus from 10 μg hippocampal neuron lysate can be quantified and equivalent to 5.99 ng (0.11 x 10^{-4} pmol/cell) of GFP protein, as estimated by comparison with purified GFP **(Figure 2.12c)**. Assuming that iCre and Venus are released in a one-to-one ratio from the iCre2A-Venus fusion construct, the amount of expressed iCre2A is in the same range (0.11 x 10^{-4} pmol/cell) for the iCre2A-Venus expressing cells. This amount of expressed iCre was about 6-fold higher with the 2A strategy than with the bi-directional promoter, demonstrating that expression levels at the left and the right site of the bi-directional promoter Ptet-bi are very different. In summary, the 2A peptide strategy is superior for quantitative co-expression in heterologous cells and in particular in neurons.

2.2.2.4 Enzymatic activity of released iCre2A fusion in CV1/lacZ indicator cells

Due to the 17 amino acid residues from 2A peptide in iCre2A fusion, the enzymatic activity of released iCre was comfirmed in CV1/lacZ indicator cells (Shimshek *et al*., 2002). In this assay, β-Gal is expressed when iCre enzymatic activity removes the floxed stop codon in CV1 cells. The iCre2A-Venus cassette was cloned into the pHD vector (Kellendonk *et al*., 1996). The plasmid pHD-iCre2A-Venus or pHD-iCre was cotransfected together with an expression plasmid coding for alkaline phosphatase (AP) p-HD-AP into CV1 cells. Three days after transfection, both X-Gal staining and fast red staining were performed with the fixed cells to visualize iCre and AP expression. The number of AP-positive cells was used for normalization of transfection efficiency. Compared with pHD-iCre transfected cells, pHD-iCre2A-Venus transfected cells showed similar ratio, indicating the enzymatic activity of the released iCre2A fusion was completely intact by assaying Cre-mediated activation of lacZ expression in the Cre reporter cell line CV1 (**Figure 2.13**).

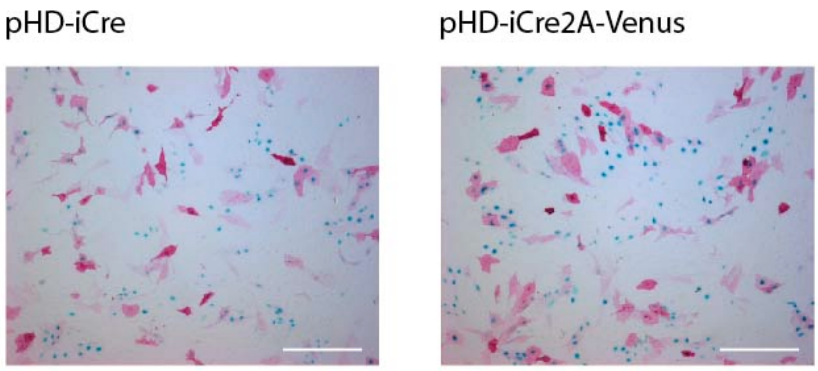

Figure 2.13 The released iCre after 2A cleavage is functional in cell culture. CV1/lacZ indicator cells were co-transfected with pHD-AP together with either pHD-iCre (positive control) or pHD-iCre2A-Venus. The ratio of blue (iCre recombination positive) to red (alkaline phosphatase positive) cell numbers represents efficiency of functional iCre. Values for pHD-iCre2A-Venus infected cells were normalized to the positive control and not significantly different (n = 10, P > 0.1). Scale bar: 100 μm.

2.2.2.5 Functional co-expression in intact brain and *in vivo* imaging

To examine 2A peptide-mediated cleavage in the intact brain *in vivo*, we injected rAAV-Syn-iCre2A-Venus into cortex and hippocampus of adult Cre-reporter Rosa26R mice (Soriano, 1999). Two weeks later, expression of the Cre-dependent lacZ reporter gene indicated successful delivery of functional iCre2A (**Fig. 2.14a**). At the injection sites, cytosolic Venus fluorescence and nuclear iCre staining were co-localized in the very same neurons, confirming the efficient proteolytic processing of iCre2A and Venus *in vivo* (**Fig. 2.14b, c**). In Western blots from infected brain areas, we detected exclusively the released iCre2A and Venus, but not the full-length iCre2A-Venus fusion protein (**Fig. 2.14d**).

Next, we examined whether in the living animal, the expression level of fluorescence would be sufficiently high to enable high resolution imaging of neurons and their processes in the intact brain. Indeed, three weeks after infection with rAAV-Syn-iCre2A-Venus, fluorescence was strong enough to allow for *in vivo* imaging of cortical neurons in anesthetized mice by two-photon microscopy. The labeled neurons and their processes, including spines, were readily visible in the superficial cortical layers (**Fig. 2.14e**).

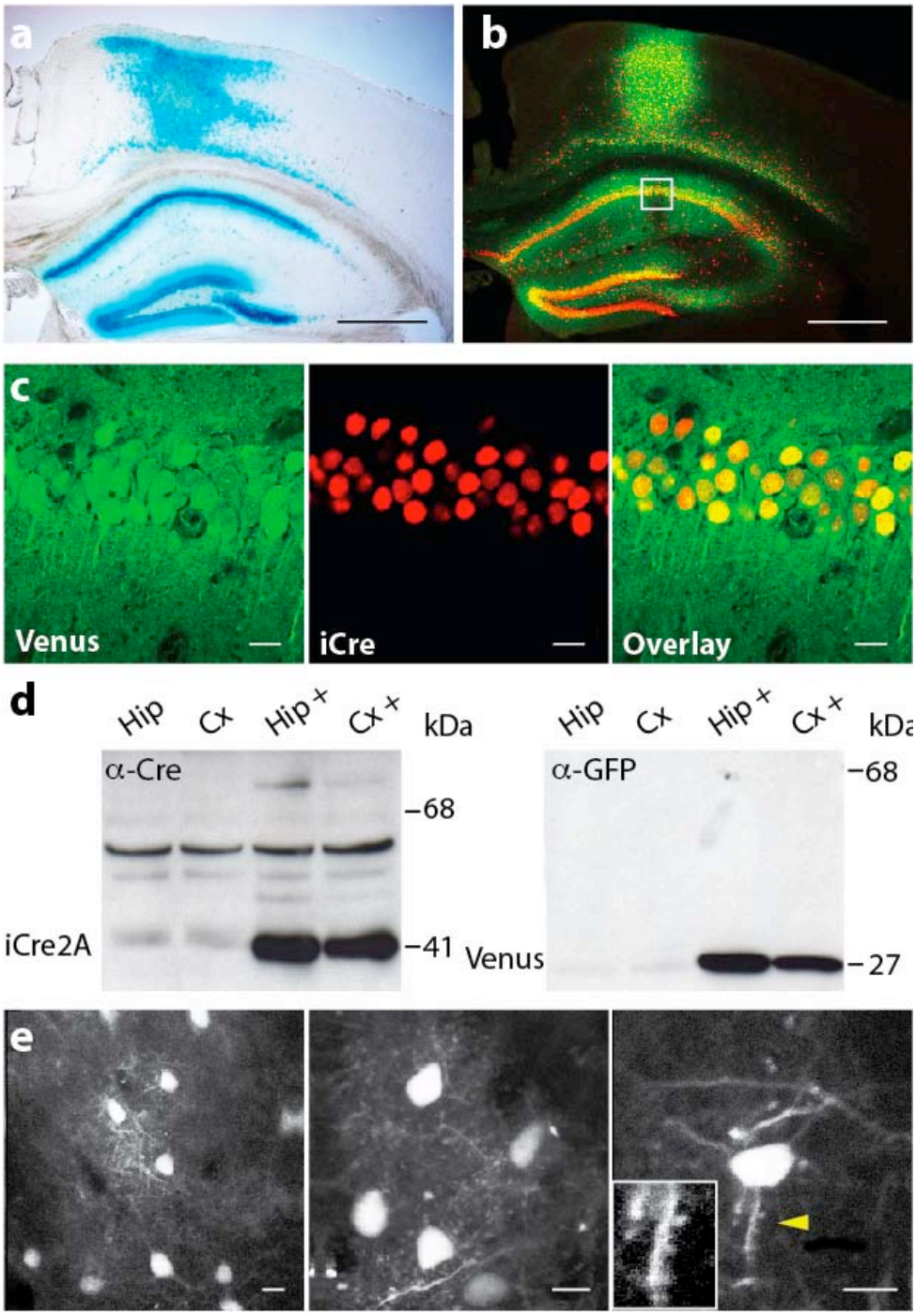

Figure 2.14 Functional and reliable co-expression using 2A peptide bridges *in vivo* and its application in life imaging. (**a**) LacZ staining of a brain section from a Rosa26R mouse injected with rAAV-Syn-iCre2A-Venus, indicating the released iCre2A protein was functional *in vivo*. Only infected brain regions showed positive blue signal. Scale bars: 500 μm (**b**) Confocal image of a brain section from a wild-type mouse injected with rAAV-Syn-iCre2A-Venus. Scale bars: 500 μm. (**c**) Higher magnification of the CA1 region. Co-expression of Venus (green) and iCre (red, visualized with Cy3-coupled antibody) was seen in virtually all infected neurons. Scale bars: 10 μm. (**d**) Western blots of extracts from infected brain regions demonstrate near complete 2A peptide cleavage *in vivo*. Tissues were dissected from brains of non-injected or rAAV-Syn-iCre2A-Venus injected wild-type mice. The 40.8 kDa iCre2A (left) and the 27.3 kDa Venus (right) were clearly detected, the 68.1 kDa full-length protein was hardly visible. Hip: Hippocampus; Cx: Cortex; + = infected with rAAVs. (**e**) *In vivo* two-photon images of rAAV-Syn-iCre2A-Venus infected neurons in somatosensory cortex of a wild-type mouse. Cell bodies of neurons in cortex as well as their fine processes were imaged at a depth of 150-200 μm. Spines are indicated by arrowhead and zoom-in image is shown. Scale bars: 10 μm.

Therefore, we conclude that the 2A peptide strategy has a powerful potential for combining genetic manipulations with the expression of FPs in subgroups of neurons at the specific brain regions, which is absolutely necessary for functional studies using optical high resolution analysis *in vivo*, and in particular for long-term investigations.

2.2.2.6 Applications of 2A-mediated Cre deletion in genetic mouse models

For more comprehensive applications of 2A-mediated Cre deletion, we used two Cre/LoxP based mouse models, Cre-inducible diphtheria toxin receptor mouse line (*iDTR*) and N-methyl-d-aspartate (NMDA) receptor 1 (*GluN1*) conditional knockout mouse line ($NR1^{2lox/2lox}$, Niewoehner *et al*., 2007), for generating brain site-specific conditional gene knockout (**Figure 2.15**). These two applications would further clarify the widespread use of 2A-mediated Cre deletion combined with rAAV site-specific delivery in the geneticly manipulated mouse models.

2.2.2.6.1 Functional iCre expression in Cre-inducible diphtheria toxin receptor (DTR) mice (*iDTR*)

To obtain site-specific cell deletion in the mouse brain, we injected rAAV-Syn-iCre2A-KO into dorsal hippocampus of adult Cre-inducible diphtheria toxin receptor (DTR) mice (*iDTR*), in which a gene encoding DTR is under the control of Rosa26 promoter in the Rosa26 locus. The DTR expression is dependent on the Cre-mediated removal of a transcriptional STOP cassette (**Figure 2.15a**, Buch *et al*., 2005). Due to the toxicity effects, after the expression of Cre recombinase, the application of diphtheria toxin (DT) in the mouse results in efficient cell ablation at the iCre expressing sites.

Two weeks after virus infection in hippocampus, DT was applied for 3 times with two days interval. And two weeks after DT application, mice were sacrificed for brain analysis. Immunostaining with NeuN antibody showed complete ablation of dorsal hippocampus (**Figure 2.15b**). However, red fluorescence of KO could not be detected within any healthy neurons, the KO positive cell debris was observed mainly in the infected dorsal hippocampus (**Figure 2.15b**) indicating the ablated KO positive cells. This demonstrated the efficient removal of the STOP cassette by iCre2A fusion and DT induced cell death via DTR. This experiment further proves that upon 2A peptide-

mediated cleavage, the functionality of iCre2A fusion is as serviceable as the "wild-type" Cre. The application of rAAV-Syn-iCre2A-KO in *iDTR* mice offers many potential options for site-specific cell ablation in the CNS in studying and manipulating different brain circuits.

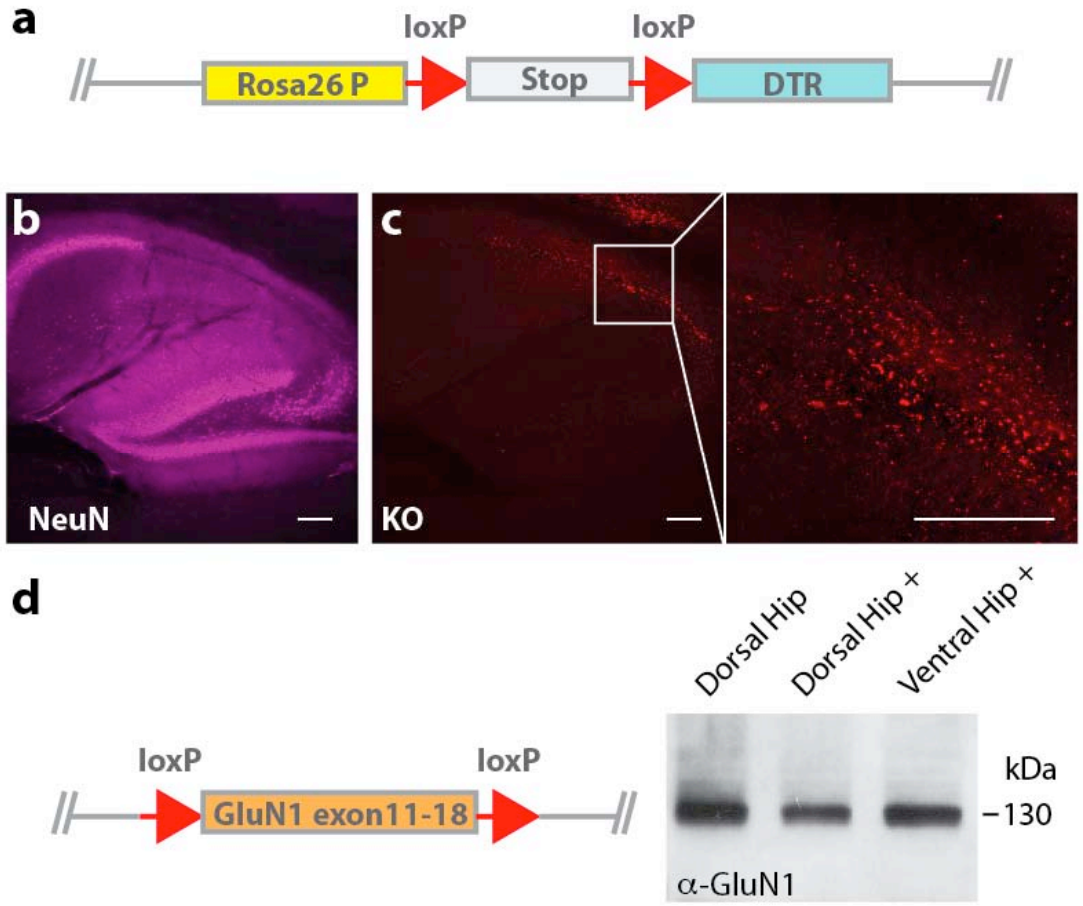

Figure 2.15 Functional applications of Cre expression in genetically manipulated mouse models. (a) Scheme of targeted Rosa26 locus of the iDTR mouse line. (b) NeuN staining of a brain section from a Cre-inducible DTR mouse 4 weeks after injection (2 weeks after DT application) of rAAV-Syn-iCre2A-KO into hippocampus. Targeted dorsal hippocampus appears completely ablated. (c) The KO red fluorescence only can be detected in cell debris at the injection site, not in any healthy cells illustrated with higher magnification in boxed region. Scale bar: 200 μm. (d) Left: Scheme of targeted *GluN1* gene. Right: Western blots of extracts from infected brain regions. In comparison with uninfected ventral hippocampus from the same brain and sample from an uninfected animal, the amount of GluN1 subunit showed dramatic reduction demonstrating the successful GluN1 (130 kDa) removal in dorsal hippocampus. Hip: Hippocampus; + = virus injected animal.

2.2.2.6.2 Removal of GluN1 in *NR1*$^{2lox/2lox}$ mice upon 2A-meidated Cre expression

For the participation in all NMDA receptor subtypes, the GluN1 subunit is the essential component of the NMDA receptor in forming functional receptor channels. The GluN1 knockout mice die 8-15 h after birth, indicating its necessity in mouse postnatal development (Tsien *et al.*, 1996). By using Cre/LoxP system, the

conditional *GluN1* knockout mice were generated (Tsien *et al*., 1996; Niewoehner *et al*., 2007). Instead of traditional method by breeding $NR1^{2lox/2lox}$ with other Cre mouse lines to obtain site-specific GluN1 deletion in the mouse brain, we applied 2A-mediated Cre expression via virus *in vivo* delivery method, and the rAAV-Syn-iCre2A-Venus was injected into the dorsal hippocampus of a adult $NR1^{2lox/2lox}$ mouse. Three weeks after virus delivery, the infected hippocampal region was demonstrated with Venus fluorescence (data not shown), and the amount of GluN1 subunit showed dramatic reduction in dorsal hippocampus in comparison with its none infected ventral hippocampal region and the one from none injected $NR1^{2lox/2lox}$ mouse (**Figure 2.15c**). This evidence confirms the successful delivery of Cre recombinase and the efficient GluN1 removal only at the injection site without affecting other brain regions, in this case the ventral hippocampus. Hence, in combination with genetic mouse models, the 2A-mediated Cre expression has big advantages in generating site-specific conditional gene knockout animals in different brain regions for further behavioral and functional studies.

2.2.3 Functional co-expression of tTA/rtTA with FPs via 2A-mediated cleavage

2.2.3.1 Doxycycline regulated gene delivery by Co-expression of tTA/rtTA with FPs in hippocampal primary neurons

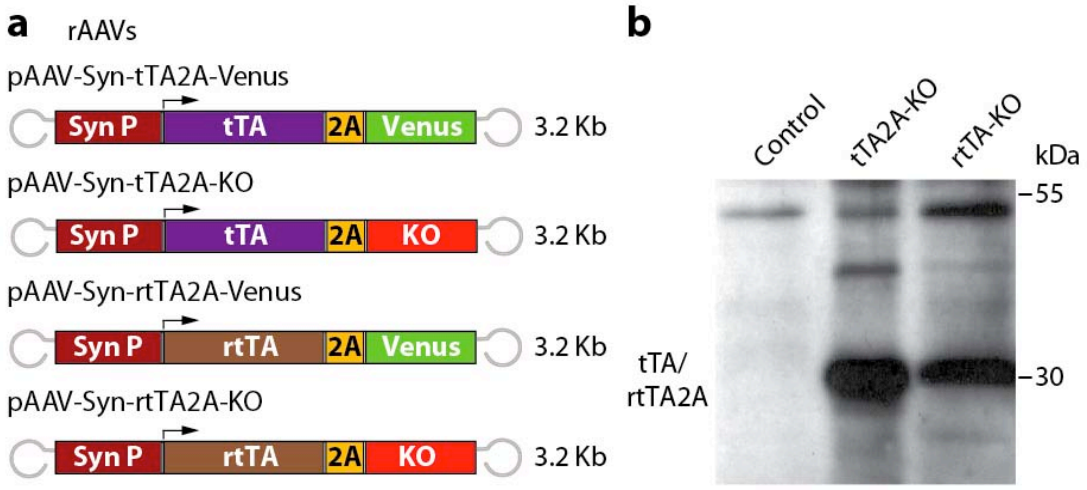

Figure 2.16 Application of 2A strategy to tTA/rtTA with other FPs. (a) Diagram of rAAV constructs of tTA/rtTA2A fusion with different FPs. Lengths of sequences between ITRs are noted. (**b**) Western blots of protein extracts from rAAV-Syn-tTA/rtTA2A-KO infected primary hippocampal neurons. The 30.5 kDa tTA/rtTA2A fusion protein was detected and 55.4 kDa full-length protein was not visible. Control: non-infected neurons.

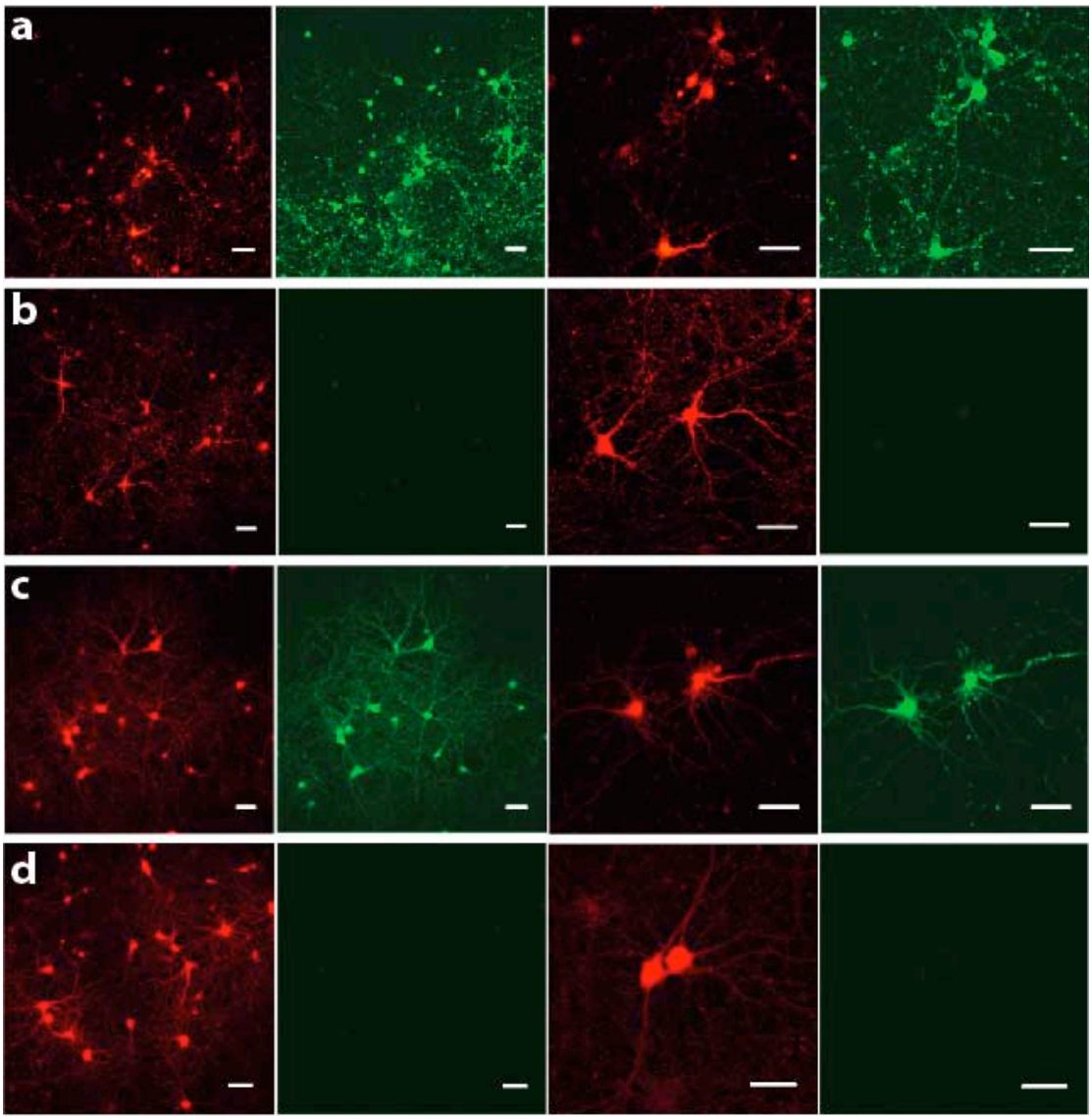

Figure 2.17 Infection of rAAVs in primary hippocampal neurons with tTA/rtTA2A fusion constructs and Dox administration. (a, b) Ten days after co-infection with rAAV-syn-tTA2A-KO and rAAV-Ptetbi-iCre-Venus in cultured neurons, without Dox treatment (a), neurons showed co-expression of both red and green fluorescence, while with Dox treatment (10 ng/ml) (b), the responder Venus fluorescence was turned off. (c, d) Primary hippocampal neurons co-infected with rAAV-syn-rtTA2A-KO and rAAV-Ptetbi-iCre-Venus showed co-expression of both KO and Venus with Dox treatment (10 ng/ml) (c), but no responder activation without Dox induction (d). Scale bar: 20 μm.

To expand our approach and to demonstrate that the auto-proteolytic activity of the 2A peptide was in dependent of the fused protein domains, we extended the 2A strategy to other activators used for conditional gene expressionl, and other FPs. We generated constructs contains between N-terminal tTA/rtTA and C-terminal Venus/KO linked by the 2A peptide (**Figure 2.16a**).

When rAAV-Syn-tTA/rtTA2A-KO expressed in primary hippocampal neurons, tTA/rtTA2A was released, which detected by Western blot analysis (**Figure 2.16b**),

suggesting that the cleavage within the 2A peptide was independent of the flanking polypeptide sequence. To provide proof of principle that tTA/rtTA2A and FPs were co-expressed and regulated by Dox, we co-infected cultured neurons with rAAV-Syn-tTA/rtTA2A-KO and the tTA/rtTA responder virus rAAV-Ptetbi-iCre-Venus (**Figure 2.3a, 2.12a**). Without Dox administration, in rAAV-Syn-tTA2A-KO and responder rAAV co-infected neurons, 10 days after infection, the co-expression of both KO and responder Venus fluorescence could be clearly detected (**Figure 2.17a**), while in the presence of Dox in the culture medium (10 ng/ml), the responder fluorescence Venus was turned off and was not visible in the culture (**Figure 2.17b**). For the Dox regulated rtTA induction, with 10 ng/ml Dox concentration, the responder Venus fluorescence was induced and was co-localized with KO (**Figure 2.17c**). Without Dox in the medium, only KO was observed (**Figure 2.17d**), indicating the off stage of the responder genes. This further confirmed the co-expression of multiple genes by 2A-mediated cleavage in the cultured neurons, and the responder genes of tTA/rtTA can be regulated simultaneously upon Dox application.

2.2.3.2 Co-infection of rAAV-tTA/rtTA-2A-fusion and responder rAAVs in wild-type mouse brain

After verifying the feasibility of FP coupled tTA/rtTA induction in cultured neurons, which can be regulated by Dox, we co-injected rAAV-Syn-tTA/rtTA2A-KO together with the responder rAAV-Ptetbi-iCre-Venus into the cortex and hippocampus of wild-type C57Bl/6 mice, following without (tTA) and with (rtTA) Dox treatments. We observed full activation of the tTA/rtTA responder genes in infected neurons, as assessed by Venus fluorescence. The FPs Venus and KO co-localized in most neurons at the injection sites, suggesting a high rate of neurons co-infected with both viruses (**Figure 2.18, 2.19**). Even when we consider the constraints of co-infection and promoter leakiness of the responder virus (Zhu *et al*., 2007), our data provide strong evidence that 2A peptide bridges can be employed universally for different activators and FPs for *in vivo* applications and that 2A cleavage is independent of the the flanking polypeptide sequences. Thus, we conclude that the simultaneous visualization of tTA/rtTA with 2A peptide lined FPs and their responder genes provides strong proof of high expression level of both activators and responders via rAAV *in vivo* gene delivery approach, and the synchronization of both activator and

responder genes can be clearly revealed. The application of this feasible combination of multiple systems provides the available possibilities to resolve the issue for the brain region specific targeting. Furthermore, together with the mouse transgenic model, it has the potential power for manipulating different brain circuits and brain functions.

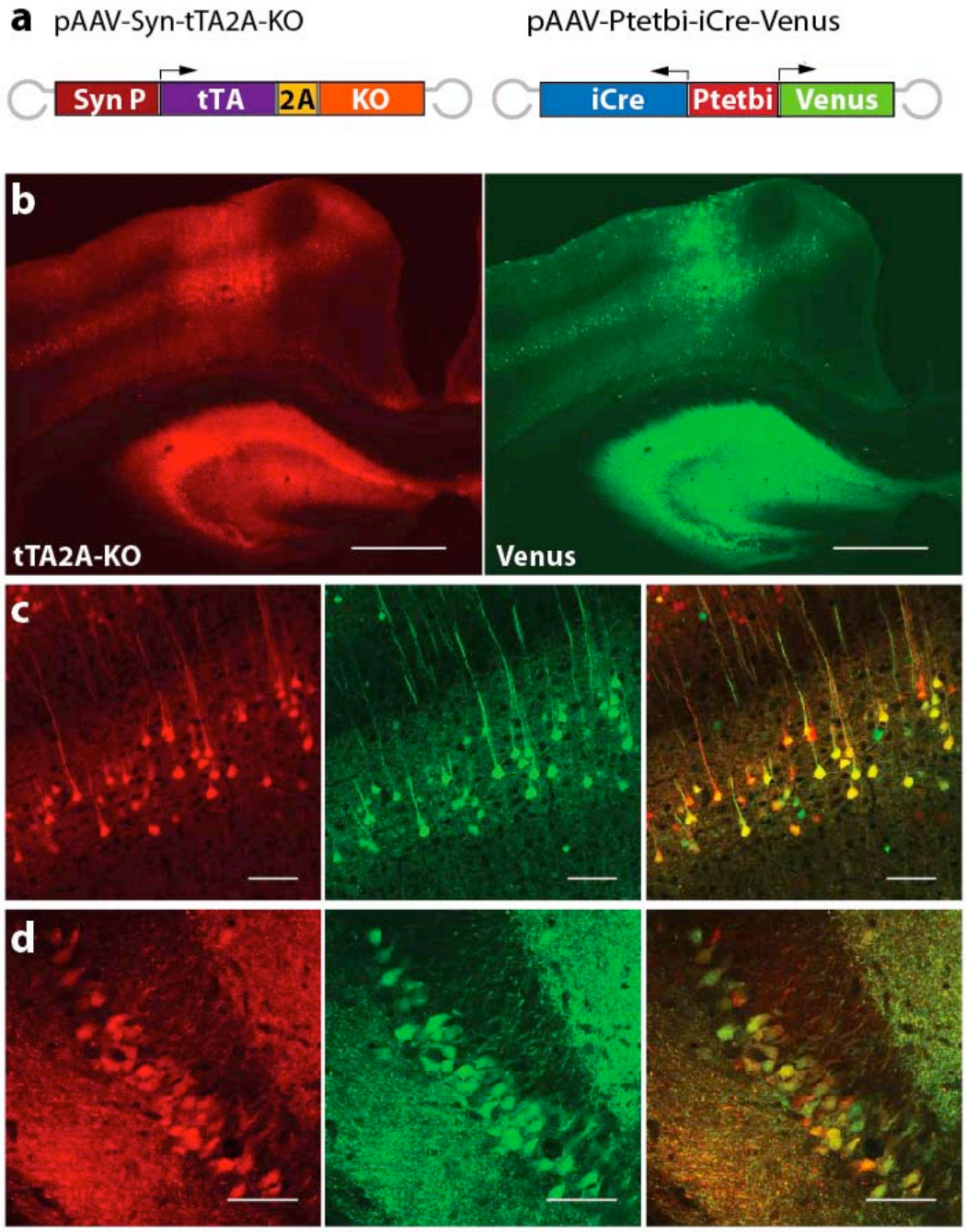

Figure 2.18. ***In vivo*** **tTA expression and its responder activation via 2A peptide cleavage.** (a) Diagram of the rAAV constructs for the dual virus activator-responder approach. (b) Confocal images of a brain section from a mouse co-injected with rAAV-Syn-itTA2A-KO and its responder virus rAAV-Ptetbi-iCre-Venus. Neurons expressing tTA were labeled with red fluorescent KO. The responder Venus expression driven by tTA was lightly detected. Scale bars: 500 μm. (c, d) At higher magnification co-expression of KO and Venus was observed in many of infected cortical (c) and hippocampal (d) neurons. Scale bars: 50 μm.

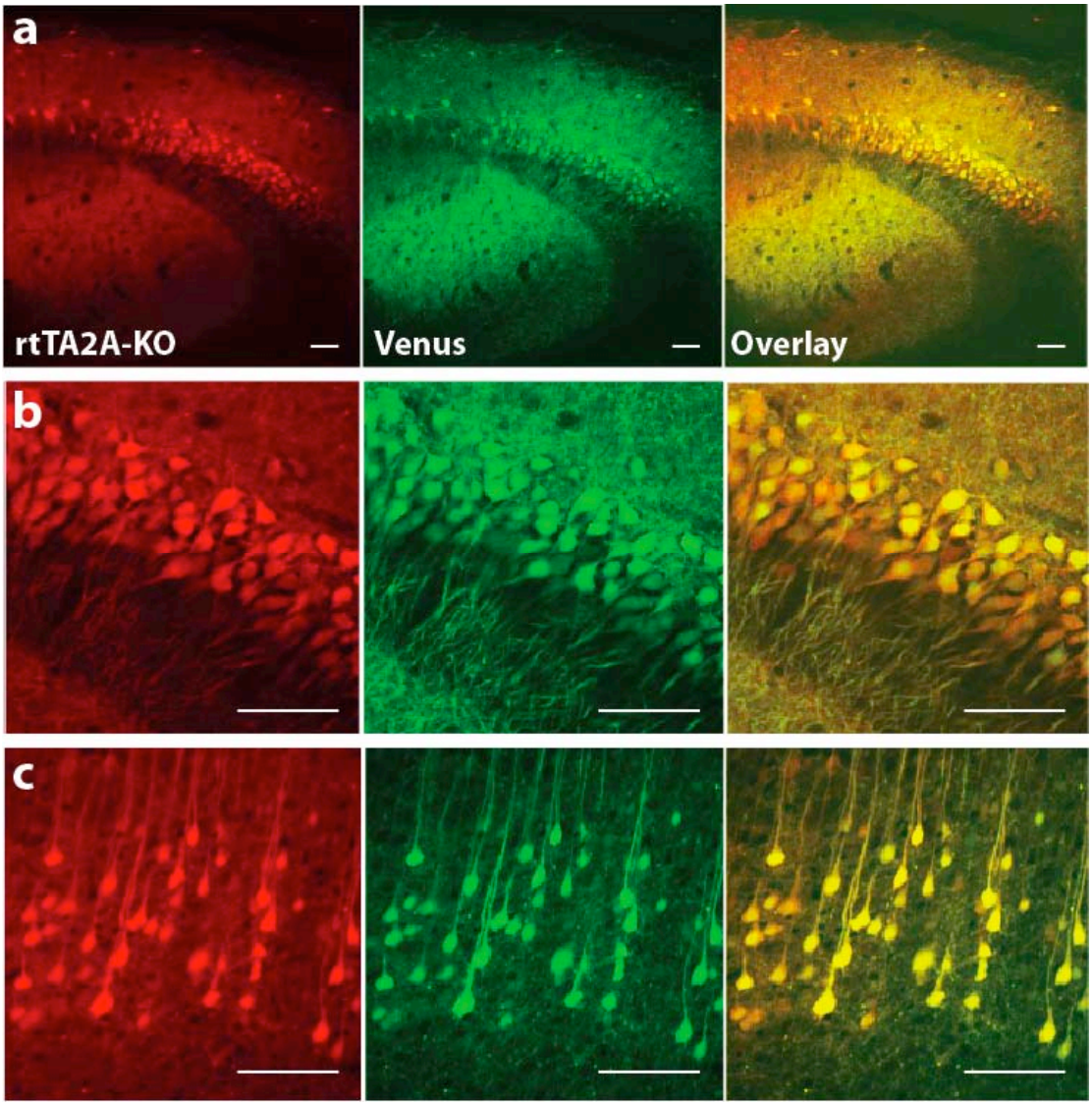

Figure 2.19. ***In vivo*** **rtTA expression and its responder activation via 2A peptide cleavage.** (a) Confocal images of a hippocampus section from a mouse co-injected with rAAV-Syn-rtTA2A-KO and the responder virus rAAV-Ptetbi-iCre-Venus. Dox treatment was administered directly after injection via drinking water. Neurons expressing rtTA were labeled with red fluorescent KO. Venus expression driven by rtTA was easily detected. (b, c) With high-magnification images, the co-expression of KO and Venus was revealed in nearly all the infected hippocampal (b) and cortical neurons (c). Scale bars: 50 μm.

2.2.3.3 Application of rAAV-tTA2A-KO in G3 responder mouse line

To verify the silencing issue in tTA responder mouse lines suggested previously (Zhu *et al*., 2007), we injected rAAV-Syn-tTA2A-KO into the cortex and the hippocampus of G3 trangenic mice expressing the conditional tTA reporters, lacZ and hGFP (Krestel *et al*., 2001). Two weeks after injection, we observed robust KO expression in many infected cortical and hippocampal neurons, as well as in dentate gyrus granule cells (**Figure 2.20 left**). However, little hGFP fluorescence could be detected

only in very few cells at the injection sites (data not shown), and the responder gene activation upon tTA was very poor (**Figure 2.20 right**). Although the tTA expression reaches a very high level, which now can be illustrated by KO fluorescence, the responder genes seem to be still silenced. This finding is consistent with the previous suggestion that despite the presence of high levels of virus delivered tTA, the responder genes are not able to be postnatally activated, indicating the incapable response of the silenced Ptetbi bi-directional promoter.

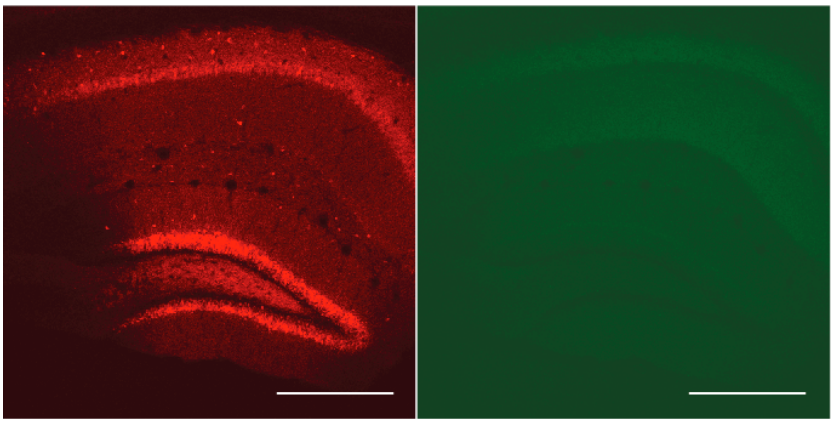

Figure 2.20 Confocal image of a brain section from a rAAV-Syn-tTA2A-KO injected G3 responder mouse. Although the expression of tTA could be illustrated by KO fluorescence, there was almost no GFP signal could be detected upon tTA activation in the infected brain regions. Scale bars: 500 μm.

Overall, we conclude that the 2A peptide bridge is a very versatile tool for co-expression of multiple heterologous proteins in neurons in vitro and in vivo, which will greatly facilitate molecular and functional analysis in cellular and system neuroscience.

2.2.4 The Cre Complementation system

2.2.4.1 Generation of split-Cre proteins

As applied in previous experiments, Cre/LoxP recombination is the most reqquently used method for conditional gene regulation in mice. Although the desired site-specific expression of Cre recombinase can be now achieved by rAAV delivery approach as described above, the cell-type-specific Cre expression *in vivo* remains an issue in many experimental approaches. The currently used promoters for Cre expression are often active in a wide range of cell types, and therefore are not suitable

for cell-type-specific Cre expression in which the Cre recombinase will be only active in subsets of cells. To overcome this limitation, the inactive "split-Cre" fragments were designed. The Cre activity is only expressed when two types of Cre fragments, which are driven by two different promoters, co-express in same cells.

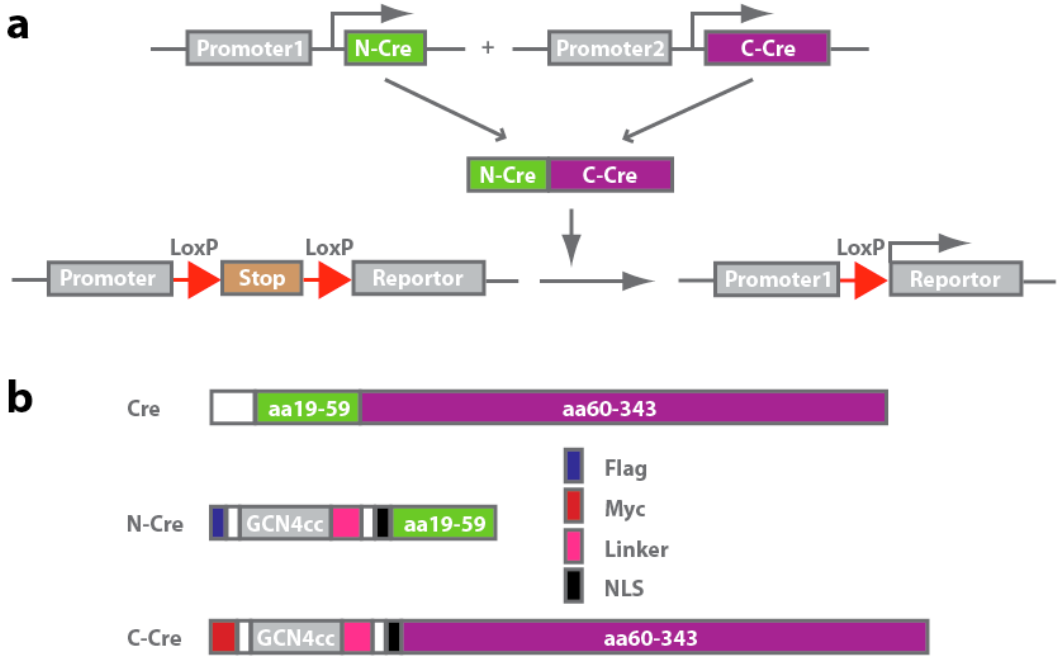

Figure 2.21 Principle of Cre complementation system and design of split-Cre proteins. (a) N-Cre and C-Cre expression are placed under the control of two different promoters (promoter 1 and 2, respectively). Only if both promoters are active, functional complementation takes place and LoxP flanked sequences are recombined, thereby activating reporter genes. (b) N-Cre and C-Cre-proteins were constructed by fusing amino acids 19-59 (N-Cre) or amino acids 60-343 (C-Cre) from Cre recombinase DNA sequence to the constitutively active coiled-coil interaction domain of the yeast transcription factor GCN4 (GCN4cc). Immunotags (Flag, Myc), a linker sequence as well as a nuclear localization sequence (NLS) were also added.

The design and primary cloning of the Cre complementation system (split-Cre) were done by the Department of Neurogenetics at the Max Planck Institute of Experimental Medicine in Goettingen. To establish this system, the coding sequence of Cre recombinase was split into two fragments coding for amino acids (aa) 19-59 and 60-343 representing the N- and C-terminal parts of Cre, respectively. These fragments have been shown to allow functional complementation (Jullien *et al*., 2003; Jullien *et al*., 2007). To further increase the complemented Cre activity by forcing split-Cre interaction, both Cre fragments were fused to the constitutively dimerizing coiled-coil leucine zipper domain of the yeast trascriptional activator GCN4 (Hope and Struhl, 1987). In addition, immunotags, a semi-flexible linker (Jullien *et al*., 2003) and a nuclear localization sequence were added to both protein fragments. The resulting split-Cre fusion proteins were named N-Cre and C-Cre, respectively (**Figure 2.21**).

2.2.4.2 Plasmid constructs of split-Cre proteins

The N-terminal and C-terminal Cre sequences were separately cloned into a recombinant AAV (rAAV) vector pAAV6P-SEWB (Shevtsova *et al*., 2005). The split-Cre protein expression was driven by cholecystokinin (CCK) 3.0 kb, glutamate decarboxylase 67 (GAD67) 3.0 kb, glial fibrillary acidic protein (GFAP) 2.2 kb and proteolipidprotein (PLP) 4.0 kb promoter, respectively (**Figure 2.22**). All 8 plasmids were used to generate rAAVs.

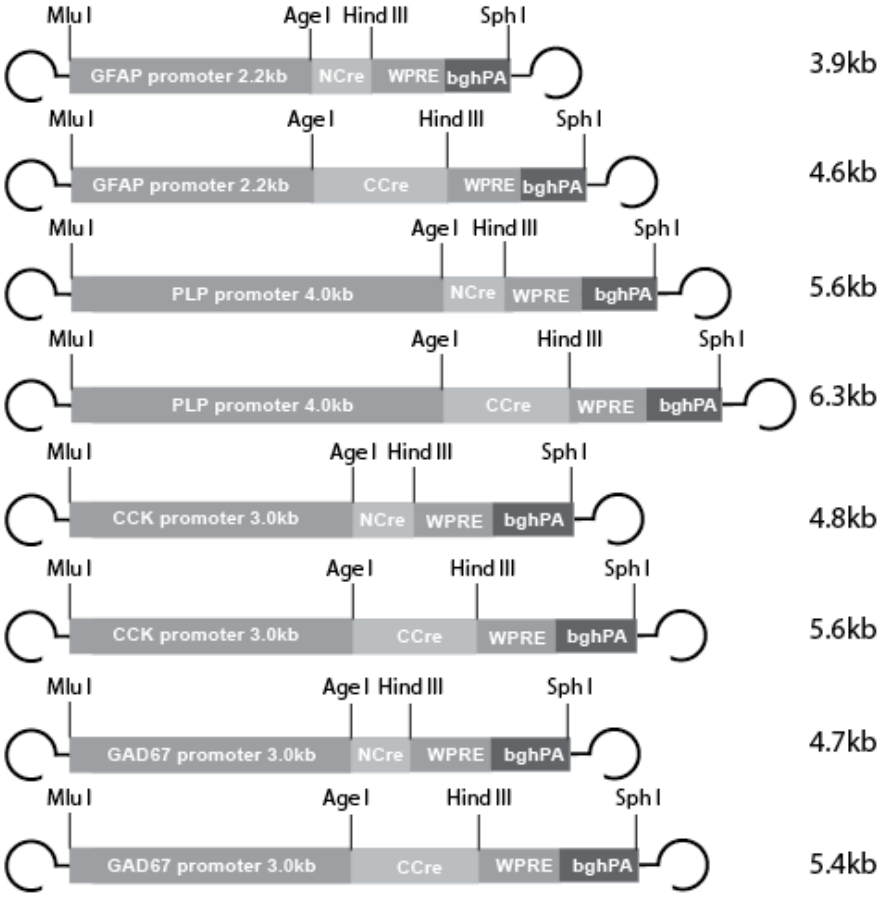

Figure 2.22 Constructs of split-Cre proteins in rAAV vector. N-Cre and C-Cre sequences were placed under the control of GFAP-, PLP-, CCK-, GAD67-promoter, respectively, with indicated lengths between ITRs.

2.2.4.3 Cre complementation *in vivo* via Co-expression of CCK-N-Cre and CCK-C-Cre, PLP-N-Cre and PLP-C-Cre

First, to test the virus mediated Cre delivery, rAAV-CCK-N-Cre and rAAV-CCK-C-Cre, rAAV-PLP-N-Cre and rAAV-PLP-C-Cre were separately co-injected into cortex

and hippocampus of two adult wild-type mice. Three weeks later, the mice were analyzed by immunostaining. Rabbit anti-Cre antibody was used for Diaminobenzidine-tetrahydrochloride (DAB) staining to visualize the Cre expression. Positive cells were found in both cortex and hippocampus at the injected region (**Figure 2.23**). Although the Cre antibody is only against the C-Cre protein, this could still show the successful virus mediated C-Cre transduction in the injection areas.

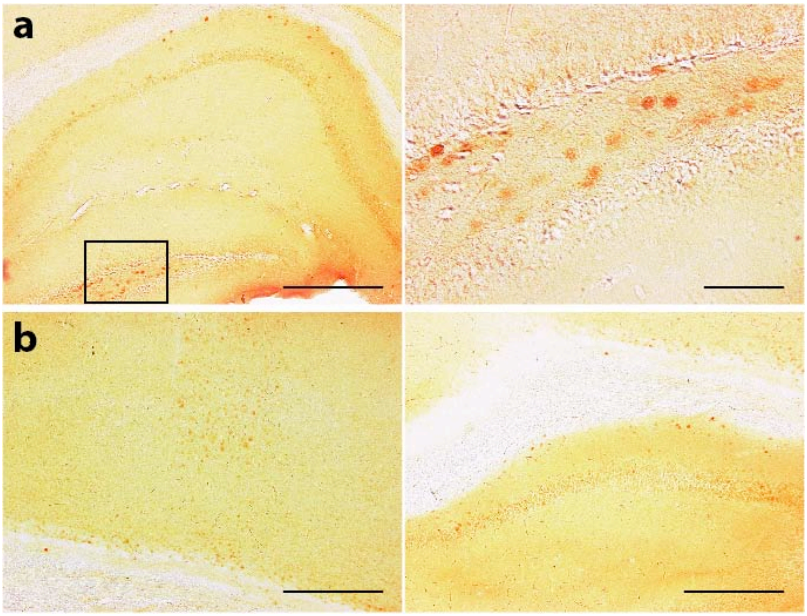

Figure 2.23 Anti-Cre immunostaining of co-injected Cre complementation viruses three weeks post injection. Brain sections showed positive Cre signal restricted to the nuclei in the injected areas. (a) Hippocampal section from rAAV-CCK-N-Cre and rAAV-CCK-C-Cre co-injected wild-type mouse. Most positive cells are located in the region of the dentate gyrus (boxed region). (b) Cortical section of rAAV-PLP-N-Cre and rAAV-PLP-C-Cre co-injected wild-type mouse. Cre signals are found both in the cortex (left) and hippocampus (right). Scale bar: 500 μm.

2.2.4.4 Co-expression of PLP-N-Cre and GFAP-C-Cre or CCK-N-Cre and GAD67-C-Cre in P0 injected Rosa26R mouse

Since the Cre antibody that we used above to detect the Cre expression is only aginst the C-Cre proteins, although Cre immunostaining was positive after virus delivery, the enzymatic activity of complete Cre recombinase still remained unclear. Therefore, we co-injected rAAV-PLP-N-Cre and rAAV-GFAP-C-Cre or rAAV-CCK-N-Cre or rAAV-GFAP-C-Cre into the cortex, the striatum/subventricular zone (SVZ) and the hippocampus of Rosa26R mice at the age P0. Four weeks after injection, we detected positive blue cells revealed by lacZ staining at the injected regions indicating the success of Cre mediated removal (**Figure 2.29, 2.30**). Therefore, the mixture of viruses expressing N-Cre and C-Cre proteins driven by two different promoters is

able to serve as functional Cre recombinase when both promoters are active in same cells. The positive blue cells could potentially defined as subpopulations of glia cells (**Figure 2.29**) or local interneurons (**Figure 2.30**), which have both promoter gene expressions, respectively.

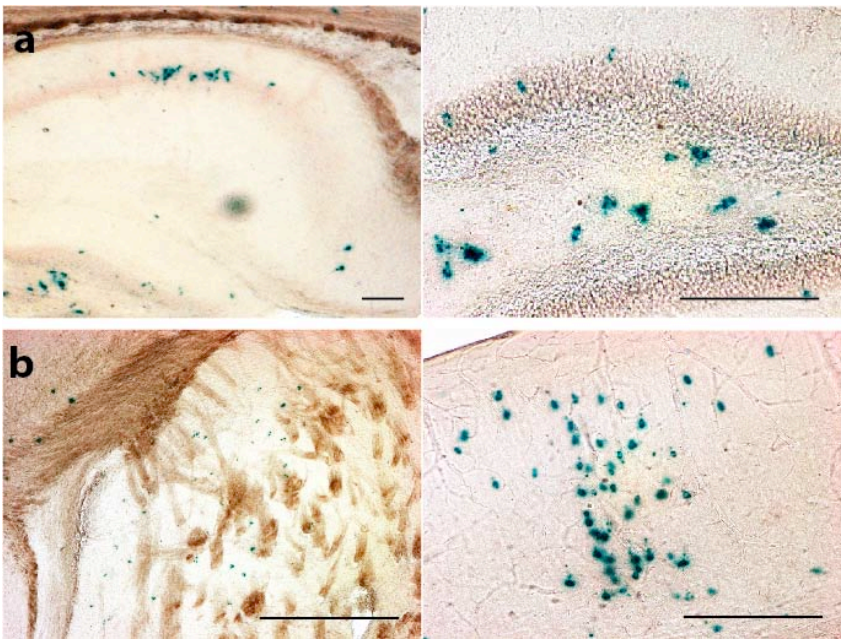

Figure 2.24 Brain sections of P0 injected Rosa26R mice with rAAV-PLP-N-Cre and rAAV-GFAP-C-Cre at the age P28. Viruses were co-injected into hippocampus, striatum and cortex. Positive blue cells were detected in all these injection sites. (a) Positive cells in hippocampus (left), in dentate gyrus (right). (b) LacZ labeling in striatum (left) and cortex (right). Scale bar: 200 μm.

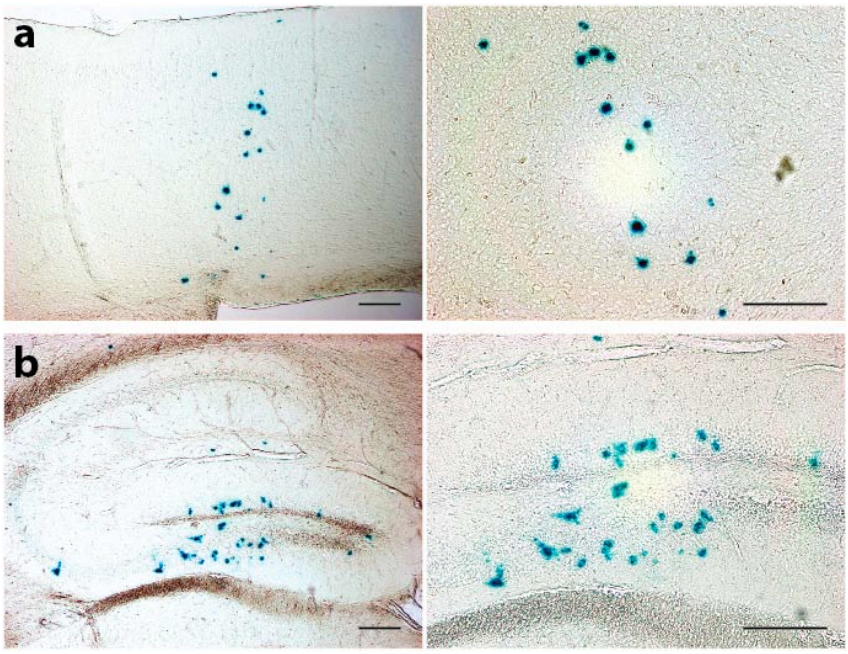

Figure 2.25 Brain sections of P0 injected Rosa26R mice with rAAV-CCK-N-Cre and rAAV-GAD67-C-Cre at the age P28. LacZ staining showed positive blue cells in cortex (a) and dentate gyrus of hippocampus (b), indicating full activity of Cre recombinase in the brain. Scale bar: 200 μm.

2.2.4.5 Co-expression of PLP-N-Cre and GFAP-C-Cre or CCK-N-Cre and GAD67-C-Cre in adultly injected Rosa26R mouse

The positive lacZ staining demonstrated the full enzymatic activity of complemented Cre recombinase, but the signal could not illustrate the exact cell type. The next question we asked is the promoter specificity. We co-injected rAAV-PLP-N-Cre and rAAV-GFAP-C-Cre or rAAV-CCK-N-Cre and rAAV-GAD67-C-Cre into the cortex and the hippocampus of 10-week old adult Rosa26R reporter mice, respectively. Two weeks after infection, brain sections from PLP-N-Cre and GFAP-C-Cre expressed animal were stained with rat-anti GFAP and rabbit-anti Cre primary antibodies visualizing with FITC and Cy3 coupled secondary antibodies, respectively. We obtained nearly 100% co-localization of both antibodies at the injection sites. The FITC fluorescence was mainly detected in the peripheral of the glial cells while Cre signals are only localized in the nuclei (**Figure 2.26**). This finding clearly indicates the promoter specificity, and the injected rAAV-GFAP-C-Cre is very precisely labeling all infected GFAP positive glia cells at the local delivery region.

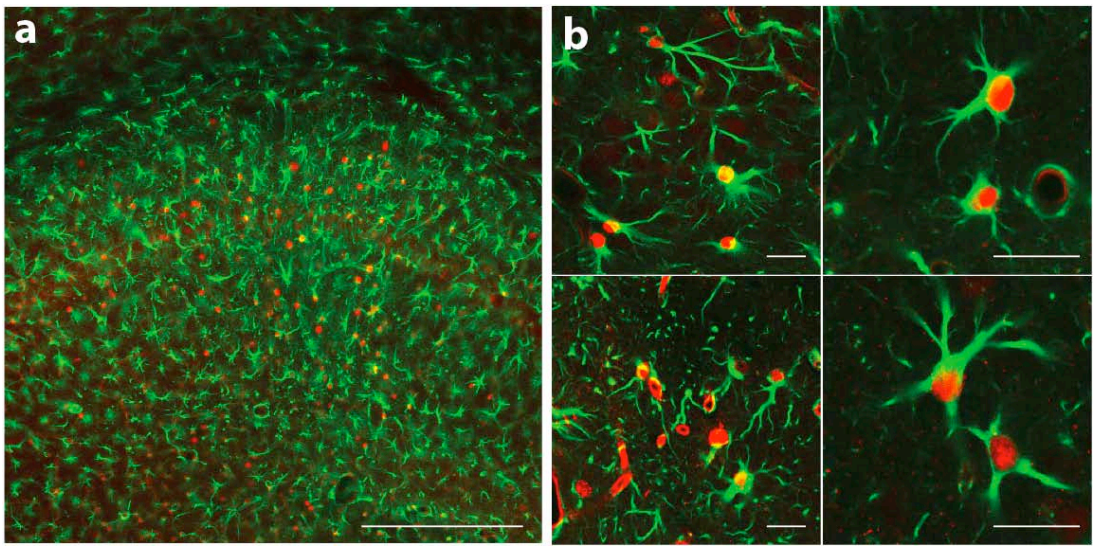

Figure 2.26 Co-localization of injected Rosa26R brain with GFAP and Cre antibodies. Adult Rosa26R reporter mouse was co-injected with rAAV-PLP-N-Cre and rAAV-GFAP-C-Cre. Brain sections were stained with GFAP (green) and Cre (red) antibodies. (a) Almost all Cre positive cells showed also GFAP positive signal in injected hippocampus. Scale bar: 500 μm. (b) Detailed imaged of co-localized glia cells. Scale bar: 20 μm.

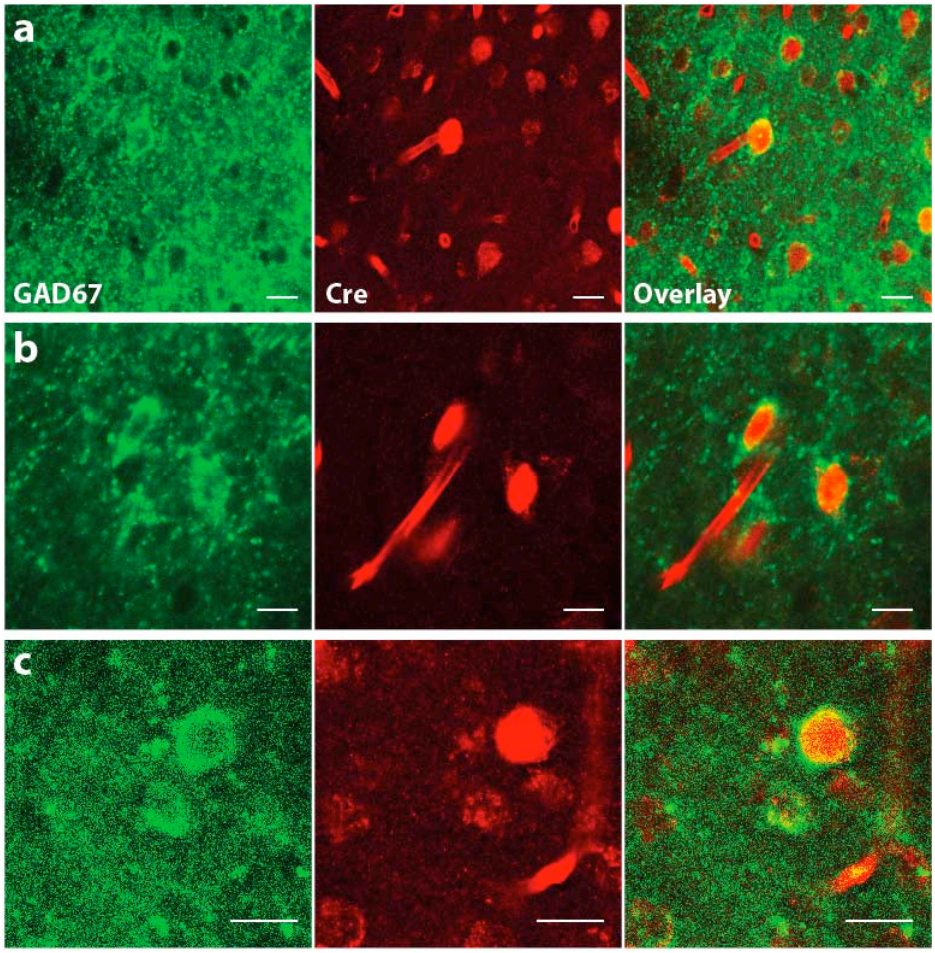

Figure 2.26 Co-localization GAD67 and C-Cre protein. Adult Rosa26R reporter mouse was co-injected with rAAV-CCK-N-Cre and rAAV-GAD67-C-Cre. Brain sections were stained with mouse anti-GAD67 (green) and rabbit anti-Cre (red) antibodies. (a) Overview of co-localized GAD67 and Cre signals. Most Cre positive cells are co-localized with Cre positive cells in injected cortical regions. (b, c) Detailed imaged of co-localized local interneurons. Scale bar: 10 μm.

Using the same strategy, we co-injected rAAV-CCK-N-Cre and rAAV-GAD67-C-Cre for investigating the local interneuron promoter specificity. Three weeks after virus infection, brain sections were stained with mouse-anti GAD67 and rabbit-anti Cre primary antibodies together with FITC and Cy3 coupled secondary antibodies, respectively. Although the GAD67 antibody staining is having a very strong background, double positive cells are still detectable in the injected regions (**Figure 2.27**).

Surprisingly, to further analyze the Cre enzymatic activity in the adult injections, we only observed very few LacZ positive blue cells in the injected regions (data not shown) for both glia cell and interneuron types. This can be explained by a weak expression of the complemented Cre recombinase in individual cells. The LoxP cassette in the Rosa26 locus was not able to be modified by such a low Cre

concentration after only two to three weeks expression period. In our P0 injected animals, the Cre activity was clearly demonstrated by the lacZ staining, but not in the injection of adult animals. At the age P0, two different promoters could be presented in a subset of glia progenitors that are active for both promoters. It might be that after development, the progenitor cells differentiate to only single promoter positive glia cells. Thus, if the injection was done at P0, the Cre-mediated LoxP cassette removal can be still active at the very early stage, and these double promoter positive gila progenitors can be revealed by the positive blue signals even in the adult age. But if the virus infection is done in adults, there might be hardly any possibility for observing double promoter positive cells in the injected brain regions. However, these two speculations do not conflict with the Cre complementation method per se, since the Cre complementation relies on the good expression of N-Cre and C-Cre in the same cell.

3. Discussion

3.1 Gene transfer technology

Cell-type specific manipulation of gene expression is a powerful tool for the analysis of gene function and for the generation of animal models. The most common approach to achieve this goal is the use of cell-type-specific promoters driving the reporter gene expression. However, in transgenic approaches, the activity of short promoter regions is in many cases strongly influenced by chromosomal sequences next to the integration site of the transgene. This position effect variegation (PEV) has a strong impact on the expression level and the activity of the promoter fragment (Palmiter *et al*., 1991).

There was the expectation that the modification via homologous recombination of bacterial artificial chromosome (BAC) covering a large sequence of construct (100 000 – 300 000 kb in size), should be able to mask the transgene from the chromosomal environment. In this case, one would expect that all transgenic animals carrying the very same BAC show the same reproducible and stable expression pattern. In the recent study, a mitral/tufted cell specific mouse line was generated using BAC transgenic technology. The EGFP expression was driven by the *Gjα9* promoter, which was within the BAC sequence. Although EGFP is not a functional protein, it could help for visualizing cells. Most of our BAC transgenic mouse lines had very specific mitral/tufted cell expression, and the expression level was high enough for *in vivo* imaging.

Among all the founders, the tissue specificity was very similar. Most founders had expression only in the olfactory bulb, not in other brain regions. All founders, however, showed differences in the expression level and the cell specificity of Venus fluorescence. It remains still unclear whether partial, instable or multiple integrations of the BAC itself were responsible for the observed differences in the expression level and the expression pattern of Venus or whether the BACs in general also suffer from position variegation effects.

3.2 The rAAV gene delivery approach

Regarding the limitations of transgenic technology, such as the long time of generating transgenics, the rAAV has emerged as an efficient gene delivery system for the nervous system. By stereotactic injection, the rAAVs could target cells in the mouse brain at the desired positions. After infection, we observed expression of the transduced gene for up to eight months. But more importantly, we could show that the rAAV approach is not only very fast, but could be applied also for functional studies of neuronal circuits in the brain. And another advantage is that due to the application for gene therapy, the production and purification methods are very well standardized, therefore, the helper dependent rAAVs are relatively reliable to produce and purify.

The low capacity for transduced genes is the main disadvantage of the rAAV gene delivery approach. As AAV, rAAV has a packaging capacity of about 4.7 kb DNA. We actually observed in our studies that the optimal packaging length is around 3 - 4 kb of DNA between both ITRs. For this length, the rAAV with high infectious titers can be easily produced; for bigger constructs (more than 4 kb insertion size) the infectious titer of the produced viruses is lower.

In each case, it has to be considered that during any cloning or reproduction of DNA procedures of rAAV constructs, the ITRs can get damaged (inverted repeats are very unstable when propagated in normal *E. coli.* strains.). Since the ITRs are obligatory for virus packaging, *E coli.* strains which are recombination defective should be used to prevent the loss of ITR sequences. We found that none of either the Sure cell (Stratagen, La Jolla, California, USA) nor the DH10B (Invitrogen, Karlsruhe, Germany) strains were safe for keeping both ITRs in the vector. Therefore, after every cloning step, the rAAV vectors have to be checked again for the presence of both ITRs in the viral sequence by restriction digests.

3.3 The Tet-inducible tTA/rtTA system and its responders

This study demonstrates that both genetic components of the Dox regulated gene expression system can be delivered by the rAAV-mediated gene transfer to specific brain regions. Co-infection of both tTA/rtTA activator and responder viruses in hippocampal neuron cultures and in the mouse brain showed very robust expression patterns. However, as already observed by Zhu *et al*., 2007, in our study the endogenous tTA-responder transgenes could not be activated in the brain by simple injection of rAAV-Syn-tTA2A-KO into different brain regions. We observed no tTA-resonder expression in any of these regions with strong tTA2A-KO expression, as indicated by the expression of KO and absence of tTA responsive hGFP. This confirmed our previous finding that upon strong tTA expression by rAAV delivery, due to unknown epigenetic silencing mechanisms, the responder expression cannot be activated when the tTA responder is inserted into the genome of the host. If the tTA-responder is present in an episomal state, as is the case of rAAV transduced tTA responder virus, tTA2A-KO can activate the episomal Ptet controlled genes.

In principle, the combination of rAAV gene delivery approach and the tTA/rtTA-inducible system provides two big advantages for the site-specific gene expression. First, the expression of rAAV delivered gene(s) can be regulated with Dox. Second, the coding capacity of the rAAV delivered gene cassette is increased by twofold, because the tissue specific promoter and tTA/rtTA can be delivered with one virus, and the gene(s) of interest in a second one. Due to the high co-infection rate, the tTA/rtTA system can be applied with high efficiencies.

3.4 The 2A peptide-mediated cleavage and multiple gene co-expression

3.4.1 Comparison of 2A-mediated multiple gene expression with other methods

Our results clearly demonstrate that the self-processing 2A peptide can be used for simultaneous expression of at least two proteins in the same neurons. This goal cannot be achieved by the use of the IRES element (Douin *et al*., 2004), the tTA dependent bi-directional promoter (Baron *et al*., 1995) or two sequential promoters (Callen *et al*.,

2004). In the case of the bi-cistronic mRNAs, the IRES-mediated translation of the second gene is severalfold lower than the translation initiation of the first ORF (Douin *et al*., 2004). And for the bi-directional promoter Ptet-bi, the strengths of the left and right promoters are not expected to be equal, and the translation efficiencies and mRNA stabilities of the left and right gene products can be very different. As we showed in our study, the unequal expression of both genes leads to an unpredictable, unbalanced expression of the left and right Ptet-bi controlled genes. And in the case of tandem promoters in a viral construct, multiple promoters can cause promoter occlusion by transcriptional interference (Callen *et al*., 2004).

Considering the difficulties to achieve reliable co-expression of heterologous proteins using current approaches, such as IRES elements, bi-directional or dual promoters, co-transfection of several plasmids, or co-infection with multiple viruses, it is surprising that the use of the 2A peptide has not received more attention. One particular advantage of the 2A system is the use of only one promoter, which can be cell-type-specific. A second one is its small size, and therefore, the potential to design constructs with several 2A elements for the expression of multiple proteins.

3.4.2 Quantitative analysis

In our study, we investigated if the 2A peptide approach can be used in neurons *in vivo* for reliable and quantitative co-expression. The co-expression, including a visible reporter at sufficient levels (e.g., for live imaging), is particularly important for gene transfer experiments, or when using conditional genetic systems. We show that genetic switches, such as iCre and tTA/rtTA, are reliably co-expressed with different fluorescent reporters and that the 2A "fusion proteins" display full biological activity.

After the gene transfer, the exact quantification of the expression of the delivered gene or the transgene by measuring the intensity of reporter fluorescence within and across experiments crucially depends on a fixed transgene/reporter expression ratio. Our data suggest that the self-processing at the 2A peptide bridge in postmitotic neurons appears to

be the method of choice to achieve this in a variety of in vitro and in vivo systems using minimally sized genetic elements. And the 2A peptide bridge represents an efficient, quantitative and very versatile tool for co-expression of multiple heterologous proteins in neurons *in vitro* and *in vivo*, which will greatly facilitate molecular and functional analysis in cellular and systems neuroscience.

In addition, the usage of the 2A peptide sequence increases the coding capacity for gene delivery by rAAV approach. In this study, the 2A peptide has been successfully used to co-express the marker fluorescent proteins (FPs) with functional proteins, such as iCre and tTA/rtTA. This co-expression offers an opportunity for visualizing the cells that express the functionality of active tTA or Cre *in vivo*, while in tTA and Cre FP fusions, the tTA or the Cre enzymatic activity is drastically reduced (personal communication). Since it is assumed that the cleavage yields a 1:1 ratio, the expression level of the Cre and tTA can be also jugged by the expression level of the FPs.

3.4.3 Delivery of more than two genes by 2A-mediated cleavage

In the presented study, only one 2A peptide sequence was used to co-express two heterologous proteins at the same time. As reported before, more than two genes can also be expressed by using more 2A peptide sequences, such as gene1-2A-gene2-2A-gene3. To date, the most complicated 2A-based construct is the assembly of the four transmembrane proteins of the CD3 complex in to a CD3δ2A-CD3γ2A-CD3ε2A-CD3ζ (Szymczak *et al*., 2004) poly protein of around 700 amino acids by using different 2A peptide sequences from foot-and mouth disease virus (F2A, VKQTLNFDLLKLAGDVESNPGP), equine rhinitisA virus (E2A, QCTNYALLKLAGDVESNPGP) and *Thosea asigna* virus (T2A, EGRGSLLTCGDVEENPGP). One important issue that had to be discussed for applying the 2A peptide in this study was whether the 2A C-terminal extension on the proteins would have some negative effects on their native functions. Szymczak *et al.* demonstrated that each cleavage was highly efficient. After the cleavage between glycine and proline, the 2A C-terminal extensions did not affect the ability of the CD3δ, γ, ε

subunits to assemble and produce a functional CD3 complex in mice. In our study, we observed consistent results that neither iCre2A nor tTA2A/rtTA2A showed loss-of-function or reduction of efficiency. Thus, the 2A-mediated cleavage could be a very suitable choice for the expression of multiple proteins.

In our other studies, we showed that the 2A peptide bridge approach can be also successfully applied to secreted (Noggin and BMP2) and membrane proteins (Channelrhodopsin2, Chr2 and Halorhodopsin, NhHP), and that even two membrane proteins together with a FP (ChR2, NpHP and Venus) can be expressed in a single protein fusion linked by two 2A peptide sequences (unpublished data). We, therefore, conclude that the 2A peptide-mediated cleavage is a very versatile tool for co-expression of multiple heterologous proteins in neurons *in vivo*, which will provide more possibilities for the site-specific gene expression.

3.5 The Cre complementation system: a powerful new tool for mouse genetics

The protein complementation assay (PCA) is a method to directly detect protein-protein interactions. The original goal of PAC is the identification of compounds that are selective for a target within the biochemical pathway that underlies a physiological process or pathology of interest, in particular to identify interaction of small molecules (Michnick *et al*., 2007). In our study, we showed that the PAC approach can be also applied for the Cre recombinase. With the successful Cre complementation, we introduced a new dimension for controlled DNA recombination in the field of the CNS research. Combined with rAAV gene delivery system, very distinct cell types can be targeted by the intersection of two promoter activities. By splitting the coding sequence of the Cre DNA recombinase into two gene fragments, and by the generation of Cre fusion proteins with strong protein-protein interaction domains, we were able to establish functional complementation of Cre activity in the mouse brain. A comparison of the Cre-mediated recombination achieved by split-Cre with that of full length Cre, revealed similar reporter gene expression patterns in Rosa26R mouse line (**Figure 2.24**, **2.25** and **Figure 2.8**, **2.14a**, respectively). Since the number of mouse lines with floxed genes is

drastically increasing, the Cre complementation provides a unique platform, which permits a well defined and restricted gene deletion in neuronal subpopulations characterized by the overlapping activity of two promoters.

As the N-Cre and C-Cre interaction domain, the GCN4-coiled coil domain has been used. It forms very stable homo-dimers (Hope and Struhl, 1987), and enables the functional complementation of dihydrofolate reductase in vitro and in *E. coli* (Pelletier *et al*., 1998) as well as for Tobacco Etch virus protease in vitro (Wehr *et al*., 2006). However, we cannot entirely exclude the possibility that our constructs interfere with cellular physiology by binding to endogenous proteins. We did not observe any obvious abnormality of the injected mice. Therefore, we assume that expression of N-Cre and C-Cre using the present promoters does not interfere with mouse physiology. And this hypothesis still needs to be substantiated by electrophysiology profiles of N-Cre and C-Cre expressing neurons as it was achieved in experiments using the 2A peptide.

3.6 Combination of rAAV gene delivery and genetically targeted mouse models

In our study, three genetically targeted mouse lines based on the Cre/LoxP system were investigated together with the rAAV *in vivo* delivery of Cre recombinase into lines Rosa26R, iDTR and $NR1^{2lox/2lox}$. The removal of the LoxP cassette can be very well activated by the virus delivery of high level of Cre recombinase at the desired brain regions. In our study, virus-mediated iCre expression in Rosa26R mice (injected with only rAAV-Syn-iCre2A-Venus, or co-injected of rAAV-Syn-tTA together with rAAV-Ptetbi-iCre-Venus) resulted in strong blue signals in infected hippocampi and cortices. Similarly the iCre expression in iDTR mice (injected with rAAV-Syn-iCre2A-KO) showed complete ablation of dorsal hippocampi. Both examples indicate a successful removal of LoxP-flanked transcriptional stop cassettes in the Rosa locus. However, by applying the virus-mediated Cre complementation system in the Rosa26R mouse line, we did not detect robust LacZ expression. It is possible that due to the requirement of certain Cre expression levels for the accessibility of the Rosa locus, the relatively low expression of complemented Cre was not able to induce high reporter expression, which resulted

only low expression of LacZ in P0 injected Rosa26R mice, and even almost no LacZ signal with the adult-injected Rosa26R mice.

For the conditional knockout models, the combination of 2A-mediated Cre expression via rAAV gene delivery is very useful and a flexible tool for site-specific gene deletion. With the visualization of Cre recombinase by FPs, the conditional gene knockout also can be localized to individual neurons for further electrophysiologic applications. By Western blot analysis, the *NR1*$^{2lox/2lox}$ mice injected with rAAV-Syn-iCre2A-Venus showed dramatic reduction of the *GluN1* subunit in the injected hippocampal region 3 weeks after injection. Behavioral and electrophysiologic experiments based on this virus-induced conditional *GluN1* knockout can further be performed to study channel functions and properties in selected brain regions.

3.7 Future perspectives

This study combined a variety of newly developed biological tools, and took the individual advantages to further achieve the tissue-specific gene expression and manipulation in the mouse brain. The application of local rAAV gene delivery provides a wide range of research perspectives for studying the function of local brain circuits. In particular, in combination with genetically modified mouse strains, the local gene expression or deletion can be easily accessed at the desired brain regions. Moreover, the Dox regulated tTA/rtTA system together with 2A-mediated cleavage can elevate the flexibility of the gene regulation. Taken together, many further behavioral and functional experiments can be designed with this combination to obtain site-specific and cell-type-specific gene manipulation in the mouse brain.

4. Materials and Methods

4.1 Standard molecular methods

For the applied standard molecular biological methods refer to: Molecular Cloning: a Laboratory Manual (3rd Edition; Sambrook J, Russell DW; Cold Spring Harbor Laboratory Press, 2001), Current Protocols in Molecular Biology (Ausubel FM, Brent R, Kingston RE, Moore DD, Seidman JG, Smith JA, Struhl K; Wiley Interscience, 1989), Manipulating the Mouse Embryo (Hogan B, Beddington R, Costantini F, Lacy E; Cold Spring Harbor Laboratory Press, 1994).

4.2 List of mouse lines

G9GFP (BAC line, generated), C57Bl/6 Charles River (Germany) or RCC/BRL (Basel, Switzerland), Rosa26R (Soriano P, 1999), iDTR (Buch T *et al*., 2005), $NR1^{2lox/2lox}$ (Niewoehner *et al*., 2007), G3 ((Krestel *et al*., 2001).

4.3 Generation of a BAC transgenic mouse line

4.3.1 Bacterial artificial chromosome (BAC) recombineering by homologous recombination

Bacterial artificial chromosome (BAC) recombineering was done as described (Copeland *et al*., 2001; Liu *et al*., 2003) by Genesat project at the Rockefeller University (http://www.gensat.org/index.html). The modification of *Gjα9*-EGFP BAC was described before (Gong *et al*., 2002).

4.3.2 Southern blot

Southern blot analysis was applied to confirm the correct BAC modification. NEBlot Phototope Kit and Phototope-Star Detection Kit (New England Biolabs, Catalog number N7550S, N7020S, Frankfurt am Main, Germany) were used for this non-radioactive southern blot method. Biotinylated probes were synthesized and used for

hybridization to the target nucleic acid immobilized on a membrane. The target nucleic acid was detected by an enzyme catalyzed light-emitting reaction.

Probes were synthesized first by PCR reaction (primer p-GFP5sep and p-VPGFP1), an approximately 500 bp long template DNA was generated. About 5 ng to 1 μg template DNA were denatured at 99 °C for 5 minutes and incubated at 37 °C for the calculated reaction time with 10 μl of 5x labeling mix (contains biotinylated random octamers), 5 μl of dNTP mix (contains dNTP and biotin-dATP) and 1 μl of Klenow fragment (3'→5' exo-). Synthesized probes were precipitated and resuspended in 20 μl of 1x TE buffer for further use.

Sample DNA (5 μg) was separated on a 1.5% agarose gel at 30 V for 12 - 16 hours. DNA was visualized by a brief incubation in ethidium bromide. Then it was denatured in 1.5 M NaCl/0.5 M NaOH for 30 minutes and neutralized in 1.5 M NaCl/1.5 M Trishydroxyaminomethan (Trizma. Sigma, Steinheim, Germany), pH7.4. Subsequently, DNA was transferred overnight onto a nitrocellulose membrane (Porablot. Macherey-Nagel, Düren, Germany) through a concentration gradient from 20xSSC to 5xSSC. Membranes were washed in 5xSSC, air-dried and UV-cross linked twice. Then the membrane was place in a hybridization bag and prehybridized for 1 hour at 68 °C in prehybridization solution. Approximately 20 ng/ml of denatured probes were hybridized with the membrane 6 hours up to overnight at 68 °C. After hybridization, the membrane was removed from the bag and washed twice in 2xSSC, 0.1% SDS at room temperature for 5 minutes each time and washed twice in 0.1xSSC, 0.1% SDS at 68 °C for 15 minutes each. The membrane was then placed into blocking solution for 5 minutes at room temperature. Using 0.05 ml of diluted streptavidin per cm^2 of membrane, it was incubated for 5 minutes at room temperature. The membrane was again washed twice after streptavidin incubation with wash solution I, and incubated 5 minutes with 0.05 ml of diluted phosphatase per cm^2 of membrane and washed once with blocking solution and twice with wash solution II. CDP-Star reagent was used for detection.

4.3.3 Bacterial artificial chromosome (BAC) DNA purification

The Bacterial artificial chromosome (BAC) DNA (50 μg) was digested with NotI in reaction buffer together with 2.5mM spermidine (Sigma, Steinheim, Germany). Digested BAC DNA was loaded on a sucrose gradient. After 20 hours centrifugation at 35 kg, fractions were taken (150 μl each) and from every 4th fraction 10 μl were loaded on a 1% agarose gel. Positive fractions were determined after gel electrophoresis. Separated linearized BAC DNA was collected from all positive fractions and purified with Microcon Centrifugal Filter (Millipore Schwalbach, Germany).

4.3.4 Pronuclear injection of purified BAC DNA and mouse tail genotyping

Pronuclear injection was done by Biotechnologielabor (BTL), Die Interfakultäre Biomedizinische Forschungseinrichtung (IBF), Heidelberg. Purified BAC DNA was injected at a concentration of 1 μg/ml into pronuclei of C57Bl/6 mice zygotes. Transgene F0 generation was identified by mouse tail genotyping using 3 PCR primers (p-Gja9-geno5S: GGTTGGGACGCACATAGATTGCTTC, p-Gja9-geno-wt3AS: CGGGTAATCCCTTAATGCAGGCAAC, p-EGFP-147-3AS: GCAGATGAACTTCAGGGTCAGCTTGC) amplifying a 362bp DNA fragment for transgenic mice and a 440bp fragment for wild type mice. Transgenic mouse lines were maintained in the IBF.

4.3.5 Immunohistochemistry of mouse brain sections

Mice were anesthetized with Isofluran and either decapitated directly or perfused intracardiacly with warm 1xPBS (137 mM NaCl, 2.7 mM KCl, 4.3 mM $Na_2HPO_4/2H_2O$, 1.4 mM KH_2PO_4) and 4% paraformaldehyde (PFA) in PBS prior to decapitation. Brains were removed and fixed in ice-cold 4% PFA for 2 hours, embedded in 2.5% Agarose/1xPBS and sliced on a vibratome (VT1000S, Leica, Wetzlar, Germany) into 70-100 μm sections. Fluorescent sections were partially analyzed directly under the microscopy after mounting with Aqua Poly/Mount (Polysciences, Inc., Warrington, PA, USA) and cover slips. Sections for 3,3-Diaminobenzidine-tetrahydrochloride (DAB) staining were treated with 0.5% H_2O_2/ 1xPBS for 15 minutes at room temperature to reduce endogenous peroxidase activity.

Blocking step was done in 4% normal goat serum/ 1% bovine serum albumin (BSA)/ 0.3% Triton X-100 (Sigma, Steinheim, Germany). Sections were incubated overnight at room temperature in primary antibody diluted in 1xPBS/ 1% BSA/ 1% normal goat serum/ 0.3 % Triton X-100: anti-GFP 1:10,000 (polyclonal, Abcam, Cambridge, UK); anti-Cre 1:3000 (rabbit polyclonal, Covance, California, USA). The second day sections were washed twice in 1xPBS/0.3% BSA/ 0.1% Triton X-100 (D2 buffer) followed by secondary antibody incubation diluted 1:600 staining (peroxidase-labeled anti-mouse, anti-rabbit or anti-goat secondary antibody. Vector Laboratories, Burlingame, CA, USA) for 1 hour at room temperature. After two times wash with D2 buffer and 1 time with 1xPBS, signals were detected using 0.04% 3,3-Diaminobenzidine-tetrahydrochloride (DAB, Fluka, Fuchs, Switzerland) in 20mM Tris-HCl pH 7.6/ 0.025% H_2O_2. Three washes in 1xPBS were used to stop the color reaction. Sections were mounted on glass slides with Aqua Poly/Mount and cover slips. Immunofluorescent staining was done with the same procedures as DAB staining, but without H_2O_2 treatment at the beginning and with primary antibodies: anti-Cre 1:3000 (rabbit polyclonal. Covance, California, USA); anti-NeuN 1:1000 (mouse monoclonal. Chemicon, California USA), anti-GFAP 1:1000 (rat monoclonal. ZYMED, San Francisco, California, USA) and anti-GAD67 (monoclonal. Chemicon, California USA), and Cy3 or Cy5 coupled secondary antibody (1:200 dilution, Jackson ImmunoResearch, West Grove, PA, USA). Samples were mounted on glass slides with Aqua Poly/Mount (Polyscience, Inc., Eppelheim, Germnay) and cover slips.

4.3.6 The X-gal staining for vibratome sections

Vibratome sections were incubated in X-gal solution (5mM $K_4Fe(CN)_6$, 5mM$K_3Fe(CN)_6$, 2 mM $MgCl_2$, 2 mg/ml X-Gal in Dimethylformamid /1xPBS. Sigma, Steinheim, Germany) at room temperature 5 to 60 minutes. Sections were washed in 1xPBS and once 10 mM Tris-HCl pH7.5, and mounted on glass slides with Aqua Poly/Mount (Polyscience, Inc., Eppelheim, Germnay) and cover slips.

4.3.7 Fluorescent light imaging and confocal imaging

Light and fluorescent images were acquired on a Zeiss Axioplan2 (Carl Zeiss, Jena,

Germany) with a camera system AxioCam HRC (Carl Zeiss, Jena, Germany), 2.5x to 40x dry or 63x oil-immersion objectives, software (Axiovision version 4.6.3), a compact light source (Leistungselectronic Jena GmbH, Jena, Germany), 488nm filter and 568nm filter. Confocal images were acquired either on a Zeiss LSM5 PASCAL coon-focal laser scanning microscope with 63x oil-immersion objective, equipped with an Argon laser (457, 476, 488, 514 nm) and a Helium Neon laser (543nm) (Carl Zeiss, Jena, Germany) or a Leica TCS SP2 confocal microscope (Leica, Wetzlar, Germany) with 10x to 63x glycerin-immersion objectives, equipped with an Argon UV laser (352, 364 nm), an Argon laser (457, 476, 488, 514 nm), and two Helium Neon lasers (543 and 633 nm, respectively). Image analysis was done with imageJ (v10.2), Leica Confocal Software (LCS) or Imaris (Bitplane, Zürich, Switzerland).

4.4 Recombinant adeno-associated virus (rAAV) delivery system

4.4.1 List of plasmids

pAAV-Syn-tTA	Zhu *et al*., 2007
pAAV-CMV-tTA	Zhu *et al*., 2007
pAAV-Ptetbi-iCre-Venus	Zhu *et al*., 2007
pAAV-Syn-rtTA	Hasan MT
pAAV-Ptetbi-iCre-tdTomato	Hasan MT
pAAV-CMV-iCre2A-GFP	Generated
pAAV-Syn-iCre2A-GFP	Generated
pAAV-Syn-iCre2A-Venus	Generated
pAAV-Syn-iCre2A-KO	Generated
pAAV-Syn-tTA2A-Venus	Generated
pAAV-Syn-tTA2A-KO	Generated
pAAV-Syn-rtTA2A-Venus	Generated
pAAV-Syn-rtTA2A-KO	Generated
pHD-iCre	Shimshek *et al*., 2002
pHD-AP	Shimshek *et al*., 2002
PHD-iCre2A-Venus	Generated
pAAV-CCK-N-Cre	Zhu P
pAAV-CCK-C-Cre	Zhu P

pAAV-GAD67-N-Cre	Generated
pAAV-GAD67-C-Cre	Generated
pAAV-GFAP-N-Cre	Zhu P
pAAV-GFAP-C-Cre	Zhu P
pAAV-Plp-N-Cre)	Zhu P
p-AAV-Plp-C-Cre	Zhu P

4.4.2 Construction of rAAV 2A containing plasmids

The *Thosea asigna* virus 2A peptide coding sequence together with 5'-CTC and 3'-GCACCGGGATCCACC flanking sequences was synthesized and subcloned between BamHI and AgeI sites of plasmid pAAV-6P-SEWB (Shevtsova *et al*., 2005). The iCre gene sequence (Shimshek *et al*., 2002) was cloned between the Synapsin promoter and the 2A peptide sequence to generate pAAV-Syn-iCre2A-EGFP. The pAAV-CMV-iCre2A-EGFP was constructed by substitution of the promoter for Synapsin by the CMV promoter from pAAV-CMV-tTA (Zhu *et al*., 2005). The Venus sequence was inserted as PCR product by 5'-blunt end 3'-BsrGI ligation into pAAV-Syn-iCre2A-EGFP vector in place of EGFP. The tTA and KO (Karasawa, S. *et al*., 2004) sequences were generated by PCR to replace iCre and Venus sequences in pAAV-Syn-iCre2A-Venus, respectively. For construction of plasmid pHD-iCre2A-Venus, the iCre2A-Venus fragment was isolated from plasmid pAAV-Syn-iCre2A-Venus with EcoRI and BsrGI and subcloned between BglII and XhoI in plasmid pHD-iCre (Shimshek *et al*., 2002) by 5'- and 3'- blunt ligation to replace iCre sequence. All plasmids were sequenced after cloning.

4.4.3 Construction of rAAV Cre-complementation plasmids

For Cre-complementation experiment, the N-terminal and C-terminal sequences were separately constructed into recombinant AAV (rAAV) backbone flanked by AAV2 ITRs by 5'-AgeI and 3'HindIII, and driven by CCK 3.0 kb, GAD67 3.0 kb, GFAP 2.2 kb and PLP 4.0 kb promoter, respectively, inserted as 5'-BspMI-blunt, XbaI-blunt and 3'-SalI into p-AAV6P-SEWB (Shevtsova *et al*., 2005). All plasmids were sequenced after cloning.

4.4.4 Preparation and purification of rAAVs

A cross-packaging of AAV serotype 1 and serotype 2 were performed by triple-transfection of rAAV vector plasmids and both p-DP1 and p-DP2 plasmids that express the AAV2 rep and cap genes as well as the adenovirus E4, VA, E2a helper regions into HEK 293 cells (Zhu *et al*., 2007; Grimm *et al*., 2003). Virus was harvested by three times freezing and thawing as described before (During *et al*., 2003). Virus purification was performed by Iodixanal gradient as introduced (Zolotukhin *et al*., 1999). Infectious titers of rAAVs from all fluorescent expressing constructs were determined by infection of hippocampal primary cultures (5×10^4 cell per well in 24-well plates). At 4 days *in vitro*, neurons were infected with 0.1 µl virus. After two weeks, fluorescent cells were counted to calculate the infectious titer (1.0×10^7-10^8 particles/ml for all rAAVs). The rAAVs were stored at -70°C.

4.4.5 CV1 cell Transfection and Staining Assays

Experiment design was described as before (Shimshek *et al*., 2002). HEK293 cells were transfected as previously described (Shimshek *et al*., 2002) with pAAV-CMV-iCre2A-EGFP. Other plasmids (pHD-iCre2A-Venus and pHD-iCre) were separately co-transfected with control plasmid (600 ng/well) pHD-AP into CV1/lacZ indicator cells in 24-well plate. The β-gal and alkaline phosphatase activities were detected by X-Gal solution and Fast Red staining solution (Roche, Mannheim, Germany). Cre activity is indicated by the ratio of blue to red cells.

4.4.6 Hippocampal primary cultures and rAAV infection

Dissociated hippocampal neurons of E18 rats were plated at a density of 5×10^4 cells per well in 24-well plates coated with poly-L-lysine (Sigma, Steinheim, Germany, Brewere *et al*., 1993). Neurons were infected with rAAVs after 4 days *in vitro*, and evaluated by Western blots or immunohistochemistry 10 days post infection.

4.4.7 Stereotactic injections

All procedures were performed according to the guidelines of the local animal use and care committees. Five to six-week old mice (C57Bl/6, Rosa26R, iDTR or $NR1^{2lox/2lox}$)

were deeply anesthetized (Ketamine/Xylazine mix or isofluorane), and the head was shaved and disinfected. Animals were fixed in a sterotactic frame (Kopf Instruments, California, USA), and the skin overlying the skull was cut. Small holes were drilled in the skull at coordinates AP –2.1 mm, Lat ± 1.6 mm relative to bregma to target the hippocampus. Virus was injected at depths of 350 μm, 1100 μm and 1600 μm, delivering ~300 nl at each step via glass pipettes (tip diameter 10-20 μm). The skin was sutured, and the wound disinfected. Analgesic (Metacam, Boehringer Ingelheim, Germany) was administered before and after surgery.

4.4.8 Mouse P0 injections

The rAAV particles were injected into newborn Rosa26R mice, cryo-anaesthesized on ice for 5 minutes. Using a UMP2 micro injection pump (World Precision Instruments, Sarasota, FL, USA) with a hamilton 710 syringe, 1 μl virus was injected bilaterally into the brain ventricles and hippocampus, 2 mm rostral and 0.7 mm lateral from lambda at a depth of 1.8 mm measured from the skin, and 1mm rostral and 1mm lateral from lambda at a depth of 1.5 mm measured from the skin, respectively. The animals were recovered on a heating pat after injection and grew up with their mother in the home cage. Four to six weeks later, injected animals were sacrificed for immunohistochemistry analysis.

4.4.9 Protein extraction and Western blot analysis

For protein analysis, HEK293 cells were harvested 48h after transfection. Primary hippocampal cultures were harvested with lysis buffer (50 mM Tris-HCl, pH7.6; 5 mM $MgCl_2$; 130 mM NaCl; 10 mM KCl; 1% Triton X-100; 5% Glycerin) 10 days after virus infection. Brain tissues (cortex and hippocampus) was collected two weeks after virus infection and homogenized in ice-cold buffer (25 mM Hepes, pH 7.4) containing a protease inhibitor cocktail (CompleteTM; Roche, Mannheim, Germany). From rAAV infected neuron cultures, 10 μg of total cell lysate and 20 μl of culture medium were separated by SDS-Page gel. Samples were run on SDS-polyacrylamid gels (10% separating and 4% stacking gels) and transferred to nitrocellulose membranes. Western blots were probed with polyclonal rabbit anti-Cre (1:8000, Covance, California, USA), monoclonal mouse anti-GFP (1:10000, Clontech,

California, USA), polyclonal rabbit anti-tTA (1:10,000, provided by Prof. Dr. Wolfgang Hillen, Institute of Biology, Friedrich-Alexander University, Erlangen, Germany), and monoclonal rat anti-Noggin (1:1000, R&D Systems, Wiesbaden, Germany) antibodies. Horseradish peroxidase-linked anti-rabbit, anti-mouse or anti-rat were used as secondary antibodies (1:15000, Vector Laboratories, Peterborough, UK). Blots were visualized by enhanced chemiluminescence (ECL kit, Amersham Pharmacia Biotech, Freiburg, Germany). Quantification of Western blots was done by ImageJ (NIH, Washington D.C., USA).

4.4.10 *In vivo* two-photon imaging.

Two-photon imaging was performed three weeks after virus injection into somatosensory cortex using a custom-built two-photon microscope (Hasan *et al*., 2004). Mice were anesthesized with urethane (1.5 mg/g) and body temperature was maintained at 37°C. A custom-built headplate with an imaging window (4 × 3 mm) was glued to the top of the skull using cyano-acrylate (Uhu, Bühl/Baden, Germany) and attached to a fixed metal bar. The microscope objective was positioned so that the optical axis was perpendicular to the surface of the cortex. Two-photon image sequences were collected in regions of interest with a MicroMax, 512 × 512 back-illuminated CCD camera (Roper Scientific, Duluth, GA, USA).

4.4.11 Diphtheria toxin administration

Two weeks after virus injection, diphtheria toxin (DT) (Sigma, Stinheim, Germany) was i.p. injected 3 times, each two days, at dose 25 ng/g mouse body weight. Mice were analyzed 2 weeks after last DT injection.

5. References

Abremski K and Hoess R. Bacteriophage P1 site-specific recombination. Purification and properties of the Cre recombinase protein. *J. Biol. Chem.* **259,** 1509-1514 (1984).

Alisky JM, Hughes SM, Sauter SL, Jolly D, Dubensky TW Jr, Staber PD, Chiorini JA, and Davidson BL. Transduction of murine cerebellar neurons with recombinant FIV and AAV5 vectors. *Neuroreport* **11,** 2669–2673 (2000).

Al-Ubaidi MR, White TW, Ripps H, Poras I, Avner P, Gomes D, Bruzzone R. Functional properties, developmental regulation, and chromosomal localization of murine connexin 36, a gap junctional protein expressed preferentially in retina and brain. *J Neurosci Res* **59,** 813-826 (2000).

Andersen P, Morris R, Amaral D, Bliss T and O'Keefe J. The hippocampus book. *Oxford University Press, New York.* (2007).

Atchison RW, Casto BC, Hammon WM. Electron microscopy of adenovirus-associated virus (AAV) in cell cultures. *Virology* **29,** 353–357 (1966).

Ausubel FM, Brent R, Kingston RE, Moore DD, Seidman JG, Smith JA, Struhl K. Current Protocols in Molecular Biology. *Wiley Interscience*. (1989).

Baron U, Freundlieb S, Gossen M, Bujard H. Co-regulation of two gene activities by tetracycline via a bidirectional promoter. *Nucleic Acids Res* **23**, 3605-3606 (1995).

Baron U, Gossen M, Bujard H. Tetracycline-controlled transcription in eukaryotes: novel transactivators with graded transactivation potential. *Nucleic Acids Res* **25,** 2723-2729 (1997).

Berns KI, Giraud C. Biology of adeno-associated virus. *Curr Top Microbiol Immunol*

218, 1–23 (1996).

Berns KI. *Parvoviridae*: The viruses and their replication. In *Fields Virology*, 3rd edn, pp. 2173–2197. Edited by Fields BN, Knipe DM and Howley PM. Philadelphia: Lippincott–Raven (1996).

Beyer EC, Paul DL and Goodenough DA. Connexin family of gap junction proteins. *J. Membr. Biol.*, **116,** 187–194 (1990).

Blacklow NR. Adeno-associated viruses of human. In *Parvoviruses and Human Disease* (Pattison JR Ed.), pp. 165-174. CRC Press: Boca Raton, FL (1988).

Blouin V, Brument N, Toublance E, Raimbaud I, Moullier P, and Salvetti A. Improving rAAV production and purification: Towards the definition of a scaleable process. *J. Gene Med.* **6(Suppl. 1),** S223–S228 (2004).

Bockamp E, Sprengel R, Eshkind L, Lehmann T, Braun JM, Emmrich F, and Hengstler, JG. Conditional transgenic mouse models: from the basics to genome-wide sets of knockouts and current studies of tissue regeneration. *Regen. Med.* **3,** 217-235 (2008).

Brewere, G.J., Torricelli, J.R., Evege, E.K., Price, P.J. Optimized survival of hippocampal neurons in B27-supplemented neurobasal, a new serum-free medium combination. *J. Neurosci. Res.* **35**, 567-576 (1993).

Bruzzone R, Ressot C. Connexins, gap junctions and cell– cell signalling in the nervous system. *Eur J Neurosci* **9,** 1– 6 (1997).

Buch T, Heppner LF, Tertilt C, Heinen TJA, Kremer M, Wunderlich FT, Jung S and Waisman A. A Cre-inducible diphtheria toxin receptor mediates cell lineage ablation after toxin administration. *Nature Methods* **2**, 419-426 (2005).

Buck L, Axel R. A novel multigene family may encode odorant receptors: a molecular basis for odor recognition. *Cell* **65,** 175-187 (1991).

Burger C, Gorbatyuk OS, Velardo MJ, Peden CS, Williams P, Zolotukhin S, Reier PJ, Mandel RJ, and Muzyczka N. Recombinant AAV viral vectors pseudotyped with viral capsids from serotypes 1, 2, and 5 display differential efficiency and cell tropism after delivery to different regions of the central nervous system. *Mol. Ther.* **10,** 302–317 (2004).

Buller RM, Rose JA. Characterization of adenovirus-associated virus-induced polypeptides in KB cells. *J Virol* **25,** 331–338 (1978).

Callen BP, Shearwin KE, Egan JB. Transcriptional interference between convergent promoters caused by elongation over the promoter. *Mol Cell.* **14,** 647-656 (2004).

Chess A, Simon I, Cedar H, Axel R. Allelic inactivation regulates olfactory receptor gene expression. *Cell* **78,** 823-834 (1994).

Chiorini JA, Yang L, Liu Y, Safer B and Kotin RM. Cloning of adeno-associated virus type 4 (AAV4) and generation of recombinant AAV4 particles. *J Virol* **71,** 6823–6833 (1997).

Chiorini JA, Kim F, Yang L and Kotin RM. Cloning and characterization of adeno-associated virus type 5. *J Virol* **73,** 1309–1319 (1999).

Christie J, Bark C, Hormuzdi SG, Helbig I, Monyer H and Westbrook GL. Connexin36 mediates spike synchrony in olfactory bulb glomeruli. *Neuron* **46**, 761-772 (2005).

Condorelli DF, Parenti R, Spinella F, Salinaro T, Belluardo N, Cardile V, Circirata F. Cloning of a new gap junction gene (Cx36) highly expressed in mammalian neurons. *Eur J Neurosci* **19,** 1202-1208 (1998).

Conway JE, Zolotukhin S, Muzyczka N, Hayward GS and Byrne BJ. Recombinant adeno-associ ated virus type 2 repli cat ion and packaging is entirely supported by a herpes simpl ex virus type 1 ampl icon expressing Rep and Cap. *J Virol* **71,** 8780–8790 (1997).

Copeland NG, Jenkins NA, Court DL. Recombineering: a powerful new tool for mouse functional genomics. *Nat Rev Genet.* **2,** 769-779 (2001).

Davidoff AM, Ng CY, Sleep S, Gray J, Azam S, Zhao Y, Mcintosh JH, Karimipoor M, and Nathwani AC. Purification of recombinant adeno-associated virus type 8 vectors by ion exchange chromatography generates clinical grade vector stock. *J. Virol. Methods* **121,** 209–215 (2004).

Davidson BL, Stain CS, Heth JA, Martins I, Kotin RM, Derksen TA, Zabner J, Ghodsi A, and Chiorini JA. Recombinant adeno-associated virus type 2, 4, and 5 vectors: Transduction of variant cell types and regions in the mammalian central nervous system. *Proc. Natl. Acad. Sci. U.S.A.* **97,** 3428–3432 (2000).

de Felipe P, Luke GA, Hughes LE, Gani D, Halpin C, Ryan MD. E unum pluribus: multiple proteins from a self-processing polyprotein. *Trends Biotechnol* **24,** 68-75 (2006).

Di Pasquale G, Davidson BL, Stein CS, Martins IS, Scudiero D, Monks A and Chiorini JA. Identification of PDGFR as a receptor for AAV-5 transduction. *Nat. Med.* **9,** 1306–1312 (2003).

Donnlly ML, Luke G, Mehrotra A, Li X, Hughes LE, Gani D and Ryan MD. Analysis of the aphthovirus 2A/2B polyprotein 'cleavage' mechanism indicates not a proteolytic reaction, but a novel translational effect: a putative ribosomal 'skip'. *J. Gen. Virol.* **82,** 1013-1025 (2001).

Donnelly ML, Hughes LE, Luke G, Mendoza H, ten Dam E, Gani D, Ryan MD. The 'cleavage' activities of foot-and-mouth disease virus 2A site-directed mutants and naturally occurring '2A-like' sequences. *J Gen Virol* **82,** 1027-1041 (2001).

Douar AM, Poulard K, Stockholm D, Danos O. Intracellular trafficking of adeno-associated virus vectors: routing to the late endosomal compartment and proteasome degradation. *J Virol* **75,** 1824–1833 (2001).

Douin V, Bornes S, Creancier L, Rochaix P, Favre G, Prats A and Couderc B. Use and comparison of different internal ribosomal entry sites (IRES) in tricistronic retroviral vectors. *BMC Biotechnol*. **4,** 16 (2004).

Feigenspan A, Teubner B, Willecke K, Weiler R. Expression of neuronal connexin36 in AII amacrine cells of mammalian retina. *J Neurosci* **21,** 230-239 (2001).

Flotte TR and BJ Carter. Adeno-associated virus vectors for gene therapy. *Gene Ther* **2,** 357–362 (1995).

Furler S, Paterna JC, Weibel M, Büeler H. Recombinant AAV vectors containing the foot and mouth disease virus 2A sequence confer efficient bicistronic gene expression in cultured cells and rat substantia nigra neurons. *Gene Therapy* **11,** 864-873 (2001).

Gao GP, Alvira MR, Wang L, Calcedo R, Johnston J and Wilson JM. Novel adeno-associated viruses from rhesus monkeys as vectors for human gene therapy. *Proc Natl Acad Sci USA* **99,** 11854–11859 (2002).

Gao G, Vandenberghe LH, Alvira MR, Lu Y, Calcedo R, Zhou X and Wilson JM. Clades of Adeno-associated viruses are widely disseminated in human tissues. *J Virol* **78,** 6381–6388 (2004).

Gao, G, Vandenberghe, LH and Wilson, JM. New recombinant serotypes of AAV vectors. *Curr Gene Ther* **5,** 285–297 (2005).

Gong S, Yang XW, Li C, Heintz N. Highly efficient modification of bacterial artificial chromosomes (BACs) using novel shuttle vectors containing the R6Kgamma origin of replication. *Genome Res.* **12,**1992–1998 (2002).

Gordon JW, Scangos GA, Plotkin DJ, Barbosa JA and Ruddle FH. Genetic transformation of mouse embryos by microinjection of purified DNA. *Proc Natl Acad Sci USA* **77,** 7380–7384 (1980).

Gordon, JW and Ruddle FH. Integration and stable germ line transformation of genes injected into mouse pronuclei. *Science* **214,** 1244-1246 (1981).

Gossen M, Bujard H. Tight control of gene expression in mammalian cells by tetracycline-responsive promoters. *Proc Natl Acad Sci U.S.A.* **89,** 5547–5551 (1992).

Gossen M, Bonin AL, Bujard H. Control of gene activity in higher eukaryotic cells by prokaryotic regulatory elements. *Trends Biochem Sci* **18,** 471–475 (1993).

Gossen M, Freundlieb S, Bender G, Muller G, Hillen W, Bujard H. Transcriptional activation by tetracyclines in mammalian cells. *Science* **268,** 1766-1769 (1995).

Grimm D, Kern A, Rittner K and Kleinschmidt JA. Novel tools for production and purification of recombinant adenoassociated virus vectors. *Hum Gene Ther* **9,** 2745–2760 (1998).

Grimm D, Kay MA and Kleinschmidt JA. Helper virus-free, optically controllable, and two-plasmid-based production of adeno-associated virus vectors of serotypes 1 to 6. *Mol Ther* **7,** 839–850 (2003).

Guldenagel M, Sohl G, Plum A, Traub O, Teubner B, Weiler R, Willecke K. Expression of connexin genes in mouse retina. *J Comp Neurol* **425,** 193-201 (2000).

Haberly LB and Price JL. The axonal projection patterns of the mitral and tufted cells of the olfactory bulb in the rat. *Brain Res* **129,** 152–157 (1977).

Hansen J, Qing K, Kwon H, Mah C and Srivastava A. Impaired intracellular trafficking of adeno-associated virus type 2 vectors limits efficient transduction of murine fibroblasts. *J Virol* **74,** 992–996 (2000).

Hasan MT, Friedrich RW, Euler T, Larkum ME, Giese G, Both M, Duebel J, Waters J, Bujard H, Griesbeck O, Tsien RY, Nagai T, Miyawaki A, Denk W. Functional fluorescent Ca^{2+} indicator proteins in transgenic mice under TET control. *PloS Biol.* **2**, e163 (2004).

Hecht B, Muller G, Hillen W. Noninducible Tet repressor mutations map from the operator binding motif to the C terminus. *J Bacteriol* **175,** 1206-1210 (1993).

Hennecke M, Kwissa M, Metzger K, Oumard A, Kröger A, Schirmbeck R, Reimann J and Hauser H. Composition and arrangement of genes define the strength of IRES-driven translation in bicistronic mRNAs. *Nucleic Acids Res*. **29,** 3327-3334 (2001).

Hermonat PL and N Muzyczka. Use of adeno-associated virus as a mammal ian DNA cl oning vector: transducti on of neomycin resi st ance into mammal ian ti ssue culture cell s. *Proc Natl Acad Sci U.S.A*. **81,** 6466–6470 (1984).

Hogan B, Beddington R, Costantini F, Lacy E. Manipulating the Mouse Embryo. *Cold Spring Harbor Laboratory Press*. (1994).

Hoggan MD, Blacklow NR, Rowe WP. Studies of small DNA viruses found in various adenovirus preparations: physical, biological, and immunological characteristics. *Proc*

Natl Acad Sci U.S.A. **55,** 1467–1474 (1966).

Hope IA and Strhl K. GCN4, a eukaryotic transcriptional activator protein, binds as a dimmer to target DNA. *EMBO J.* **6,** 2781-2784 (1987).

Jerecic J, Single F, Kruth U, Krestel H, Kolhekar R, Storck T, Kask K, Higuchi M, Sprengel R, and Seeburg PH. Studies on conditional gene expression in the brain. *Ann N Y Acad Sci* **868,** 27-37 (1999).

Jullien N, Sampieri F, Enjalbert A, Herman JP. Regulation of Cre recombinase by ligand-induced complementation of inactive fragments. *Nucleic Acids Res.* **31,** e131 (2003).

Jullien N, Goddard I, Selmi-Ruby S, Fina JL, Cremer H, Herman JP. Conditional transgenesis using Dimerizable Cre (DiCre). *PLoS One.* **2,** e 1355 (2007).

Kaludov N, Handelman B, and Chiorini JA. Scalable purification of adeno-associated virus type 2, 4, or 5 using ion-exchange chromatography. *Hum. Gene Ther.* **13,** 1235–1243 (2002).

Karasawa S, Araki T, Nagai T, Mizuno H and Miyawaki A. Cyan-emitting and orange-emitting fluorescent proteins as a donor/acceptor pair for fluorescence resonance energy transfer. *Biochem. J.* **381**, 307-312 (2004).

Kim J. Improvement and establishment of the tTA dependent inducible system in the mouse brain. Max-Planck-Institute for Medical Research, Molecular Neurobiology. University of Heidelberg, Heidelberg, p.80 (2001).

Kistner A, Gossen M, Zimmermann F, Jerecic J, Ullmer C, Lübbert H, Bujard H. Doxycycline-mediated quantitative and tissue-specific control of gene expression in transgenic mice. *Proc Natl Acad Sci U.S.A.* **93,** 10933-10938 (1996).

Krestel HE, Mayford M, Seeburg PH, Sprengel R. A GFP-equipped bidirectional expression module well suited for monitoring tetracycline-regulated gene expression in mouse. *Nucleic Acids Res* **29**, E39 (2001).

Laughlin CA, Tratschin JD, Coon H, Carter BJ. Cloning of infectious adeno-associated virus genomes in bacterial plasmids. *Gene* **23,** 65–73 (1983).

Lewandoski M. Conditional control of gene expression in the mouse. *Nat. Rev. Genet.* **2,** 743-755 (2001).

Linden RM, Berns KI. Molecular biology of adeno-associated viruses. *Contrib Microbiol* **4,** 68–84 (2000).

Liu P, Jenkins NA, and Copeland NG. A highly efficient recombineering-based method for generating conditional knockout mutations. *Genome Res.* **13,** 476–484 (2003).

Luo L, Callaway EM, and Svoboda K. Genetic dissection of neural circuits. *Neuron* **57,** 634-660 (2008).

Lusby E, Fife KH, Berns KI. Nucleotide sequence of the inverted terminal repetition in adeno-associated virus DNA. *J Virol* **34,** 402–409 (1980).

Maccaferri G and Lacaille JC. Interneuron diversity series: Hippocampal interneuron classifications--making things as simple as possible, not simpler. *Trends Neurosci.* **27,** 564-571 (2003).

Markram H, Toledo-Rodriguez M, Wang Y, Gupta A, Silberberg G and Wu C. Interneurons of the neocortical inhibitory system. *Nat. Rev. Neurosci.* **5,** 793-807 (2004).

McGee Sanftner LH, Rendahl KG, Quiroz D, Coyne M, Ladner M, Manning WC, Flannery JG. Recombinant AAV-mediated delivery of a tet-inducible reporter gene to the

rat retina. *Mol Ther* **3,** 688-696 (2001).

Mendelson E, Trempe JP, Carter BJ. Identification of the transacting Rep proteins of adeno-associated virus by antibodies to a synthetic oligopeptide. *J Virol* **60,** 823–832 (1986).

Mombaerts P, Wang F, Dulac C, Chao SK, Nemes A, Mendelsohn M, Edmondson J, Axel R. Visualizing an olfactory sensory map. *Cell.* **87**, 675-686 (1996).

Monyer H and Markram H. Interneuron diversity series: Molecular and genetic tools to study GABAergic interneuron diversity and function. *Trends Neurosci.* **27,** 90-97 (2004).

Mori K, Kishi K, and Ojima H. Distribution of dendrites of mitral, displaced mitral, tufted, and granule cells in the rabbit olfactory bulb. *J Comp Neurol* **219,** 339 –355 (1983).

Mori, S, Wang, L, Takeuchi, T and Kanda, T. Two novel adeno-associated viruses from cynomolgus monkey: pseudotyping characterization of capsid protein. *Virology* **330,** 375–383 (2004).

Muramatsu S, Mizukami H, Young NS and Brown KE. Nucleotide sequencing and generation of an infectious clone of adeno-associated virus 3. *Virology* **221,** 208–217 (1996).

Muzyczka N. Use of adeno-associated virus as a general transduction vector for mammalian cells. *Curr Top Microbiol Immunol* **158,** 97–129 (1992).

Muzyczka N, and Berns KI. Parvoviridae: The viruses and their replication. In *Fields Virology*. Edited by Knipe DM and Howley PM (Lippincott, Williams & Wilkins, New York) pp. 2327–2360 (2001).

Nagga A, Gertsenstein M, Vintersten K, Behringer R. Manipulating the Mouse Embryos, a Laboratory Manual. 2nd ed. *Cold Spring Harbor Laboratory Press, New York* (2002).

Nielsen LB, McCormick SPA, Pierotti V, Tam C, Gunn M, Shizuya H and Yong SG. Human apolipoprotein B transgenic mice generated with 207- and 145-kilobase pair bacterial artificial chromosomes. Evidence that a distant 5´- element confers appropriate transgene expression in the intestine. *J. Biol. Chem*. **272,** 29752–29758 (1997).

Niewoehner B, Single FN, Hvalby Ø, Jensen V, Meyer zum Alten Borgloh S, Seeburg PH, Rawlins JNP, Sprengel R and Bannerman DM. Impaired spatial working memory but spared spatial reference memory following functional loss of NMDA receptors in the dentate gyrus. *Eur J Neurosci.* **25,** 837-846 (2007).

O'Brien J, Al-Ubaidi MR, Ripps H. Connexin35, a gap junctional protein expressed preferentially in the skate retina. *Mol Biol Cell* **7,** 233-243 (1996).

Orona E, Rainer EC, and Scott JW. Dendritic and axonal organization of mitral and tufted cells in the rat olfactory bulb. *J Comp Neurol* **226,** 346 –356 (1984).

Palmiter RD, Sandgren EP, Avarbock MR, Allen DD, Brinster RL. Heterologous introns can enhance expression of transgenes in mice. *Proc Natl Acad Sci U.S.A.* **88,** 478–482 (1991).

Parenti R, Gulisamo M, Zappala M, Cicirata F. Expression of connexin 36 mRNA in adult rodent brain. *NeuroReport* **11,** 1497-1502 (2000).

Passini MA, Watson DJ, Vite CH, Landsburg DJ, Feigenbaum AL, and Wolfe JH. Intraventricular brain injection of adeno-associated virus type 1 (AAV1) in neonatal mice results in complementary patterns of neuronal transduction to AAV2 and total long-term correction of storage lesions in the Brains of β-glucuronidase-deficient mice. *J. Virol.* **77,** 7034–7040 (2003).

Pawelzik H, Hughes DI and Thomson AM. Physiological and morphological diversity of immunocytochemically defined parvalbumin- and cholecystokinin-positive interneurones in CA1 of the adult rat hippocampus. *J. Comp Neurol.* **443,** 346-367 (2002).

Pelletier JN, Campbell-Valois FX and Michnick SW. Oligomerization domain-directed reassembly of active dihydrofolate reductase from rationally designed fragments. *Proc. Natl. Acad. Sci. U.S.A.* **95,** 12131-12146 (1998).

Pinching AJ and Powell TP. The neuron types of the glomerular layer of the olfactory bulb. *J Cell Sci* **9,** 305–345 (1971).

Pinkert CA, and Polites HG. Transgenic animal production focusing on the mouse model. In *Transgenic Animal Technology*, Edited by Pinkert CA. Academic Press, Inc., San Diego (1994).

Qing K, Mah C, Hansen J, Zhou S, Dwarki V, and Srivastava A. Human fibroblast growth factor receptor 1 is a co-receptor for infection by adeno-associated virus 2. *Nat. Med.* **5,** 71–77 (1999).

Rash JE, Staines WA, Yasumura T, Pater D, Furman, Stelmack GL, Nagy JI. Immunogold evidence that neuronal gap junctions in adult rat brain and spinal cord contain connexin-36 but not connexin-32 or connexin-43. *Proc Natl Acad Sci U.S..A* **97,** 7573-7578 (2000).

Rozental R, Srinivas M, Gökhan S, Urban M, Dermietzel R, Kessler JA, Spray DC, Mehler MF. Temporal expression of neuronal connexins during hippocampal ontogeny. *Brain Res Brain Res Rev* **32,** 57-71 (2000).

Russell DW and Kay MA. Adeno-associated virus vectors and hemalology. *Blood* **94,** 864–874 (1999).

Rutledge, EA, Halbert, CL and Russell, DW. Infectious clones and vectors derived from adeno-associated virus (AAV) serotypes other than AAV type 2. *J Virol* **72,** 309–319 (1998).

Ryan MD, King AM, Thomas GP. Cleavage of foot-and-mouth disease virus polyprotein is mediated by residues located within a 19 amino acid sequence. *J Gen Virol* **72,** 2727-2732 (1991).

Sambrook J, Russell DW. Molecular Cloning: a Laboratory Manual (3rd Edition). *Cold Spring Harbor Laboratory Press* (2001).

Samulski RJ, Berns KI, Tan M, Muzyczka N. Cloning of adeno-associated virus into pBR322: rescue of intact virus from the recombinant plasmid in human cells. *Proc Natl Acad Sci* **79,** 2077–2081 (1982).

Samulski RJ, Srivastava A, Berns KI and Muzyczka N. Rescue of adeno-associated virus from recombinant plasmids: gene correction within the terminal repeats of AAV. *Cell* **33,** 135–143 (1983).

Satou M. Synaptic organization, local neuronal circuitry, and functional segregation of the teleost olfactory bulb. *Prog Neurobiol.* **34,** 115-142 (1990).

Sauer B. Manipulation of transgenes by site-specific recombination: use of Cre recombinase. *Methods Enzymol* **225,** 890-900 (1993).

Schmidt M, Voutetakis A, Afione S, Zheng C, Mandikian D and Chiorini JA. Adeno-associated virus type 12 (AAV12): a novel AAV serotype with sialic acid- and heparan sulfate proteoglycan-independent transduction activity. *J Virol* **82,** 1399–1406 (2008).

Schoenfeld TA and Macrides F. Topographic organization of connections between the

main olfactory bulb and pars externa of the anterior olfactory nucleus in the hamster. *J Comp Neurol* **227,** 121–135 (1984).

Schoenfeld TA, Marchand JE, and Macrides F. Topographic organization of tufted cell axonal projections in the hamster main olfactory bulb: an intrabulbar associational system. *J Comp Neurol* **235,** 503–518 (1985).

Schultz BR and Chamberlain JS. Recombinant adeno-associated virus transduction and integration. *Molecular Therapy* **16,** 1189–1199 (2008).

Scott JW, McBride RL, and Schneider SP. The organization of projections from the olfactory bulb to the piriform cortex and olfactory tubercle in the rat. *J Comp Neurol* **194,** 519 –534 (1980).

Shepherd GM, Chen WR, Greer CA. Olfactor y bulb. In *The synaptic organization of the brain.* Edited by Shpherd GM. New York: Oxford University Press. p 165–216 (2004).

Shevtsova Z, Malik JM, Michel U, Bähr M, Kügler S. Promoters and serotypes: targeting of adeno-associated virus vectors for gene transfer in the rat central nervous system *in vitro* and *in vivo*. *Exp Physiol* **90**, 53-59 (2005).

Shimshek DR, Kim J, Hübner MR, Spergel DJ, Buchholz F, Casanova E, Stewart AF, Seeburg PH and Sprengel R. Codon-improved Cre recombinase (iCre) expression in the mouse. *Genesis* **32**, 19-26 (2002).

Shipley MT, Ennis M. Functional organization of olfactory system. *J Neurobiol.* **30,** 123-176 (1996).

Skeen LC and Hall WC. Efferent projections of the main and the accessory olfactory bulb in the tree shrew (*Tupaia glis*). *J Comp Neurol* **172**, 1–35 (1977).

Smith RH, Ding C, and Kotin RM. Serum-free production and column purification of adeno-associated virus type 5. *J. Virol. Methods* **114,** 115–124 (2003).

Söhl G, Degen J, Teubner B, Willecke K. The murine gap junction gene connexin 36 is highly expressed in mouse retina and regulated during development. *FEBS Lett* **428,** 27-31 (1998).

Somogyi P, Hodgson AJ, Smith AD, Nunzi MG, Gorio A and Wu JY. Different populations of GABAergic neurons in the visual cortex and hippocampus of cat contain somatostatin- or cholecystokinin- immunoreactive material. *J. Neurosci.* **4,** 2590-2603 (1984).

Soriano P. Generalized lacZ expression with the ROSA26 Cre reporter strain. *Nat. Genet.* **21**, 70-71 (1999).

Sprengel R and Hasan MT. Tetracycline-controlled genetic switches. *Handb. Exp. Pharmacol.* **178,** 49-72 (2007).

Spengel R and Single FN. Mice with genetically modified NMDA and AMPA receptors. *Ann N Y Acad Sci.* **868,** 494-501 (1999).

Summerford C, and Samulski RJ. Membrane-associated heparan sulfate proteoglycan is a receptor for adeno-associated virus type 2 virions. *J. Virol.* **72,** 1438–1445 (1998).

Summerford C, Bartlett JS, and Samulski RJ. $\alpha_V\beta_5$integrin: A co-receptor for adeno-associated virus type 2 infection. *Nat. Med.* **5,** 78–82 (1999).

Sun JY, Anand-Jawa V, Chatterjee S and Wang KK. Immune responses to adeno-associated virus and its recombinant vectors. *Gene Therapy* **10,** 964-976 (2003).

Szymczak, AL, Workman CJ, Wang Y, Vignali KM, Dilioglou S, Vanin EF. Correction

of multi-gene deficiency *in vivo* using a single 'self-cleaving' 2A peptide-based retroviral vector. *Nat. Biotechnol.* **22,** 589-594 (2004).

Taymans JM, Vandenberghe LH, Haute CV, Thiry I, Deroose CM, Mortelmans L, Wilson JM, Debyser Z, Baekelandt V. Comparative analysis of adeno-associated viral vector serotypes 1, 2, 5, 7, and 8 in mouse brain. *Human Gene Therapy* **18,** 195–206 (2007).

Teubner B, Degen J, Söhl G, Güldenagel M, Bukauskas FF, Trexler EB, Verselis VK, De Zeeuw CI, Lee CG, Kozak CA, Petrasch-Parwez E, Dermietzel R, Willecke K. Functional expression of the murine connexin 36 gene coding for a neuron-specific gap junctional protein. *J Membr Biol* **176,** 249-262 (2000).

Trempe JP, Carter BJ. Alternate mRNA splicing is required for synthesis of adeno-associated virus VP1 capsid protein. *J Virol* **62,** 3356–3363 (1988).

Tsien JZ, Huerta PT and Tonegawa S. The essential role of hippocamal CA1 NMDA receptor-dependent synaptic plasticity in spatial memory. *Cell*. **87,** 1327-1338 (1996).

Vite CH, Passini MA, Haskins ME and Wolfe JH. Adeno-associated virus vector-mediated transduction in the cat brain. *Gene Ther.* **10,** 1874–1881 (2003).

Wachowiak M, Denk W, Friedrich RW. Functional organization of sensory input to the olfactory ulb glomerulus analyzed by two-photon calcium imaging. *Proc Natl Acad Sci USA*. 101, 9097-9102 (2004).

Walters RW, Yi SM, Keshavjee, S, Brown KE, WELSH MJ, CHIORINI JA, and ZABNER J. Binding of adeno-associated virus type 5 to 2,3-linked sialic acid is required for gene transfer. *J. Biol. Chem.* **276,** 20610–20616 (2001).

Wehr MC, Laage R, Bolz U, Fischer TM, Grunewald S, Scheek S, Bach A, Nave KA, and Rossner MJ. Monitoring regulated protein-protein interactions using split TEV. *Nat. Methods* **3,** 985-993 (2006).

Willecke K, Hennemann H, Dahl E, Jungbluth S and Heynkes R. The diversity of connexin genes encoding gap junctional proteins. *Eur. J. Cell Biol.* **56**, 1–7 (1991).

Xiao W, Chirmule N, Berta SC, McCullough B, Gao G and Wilson JM. Gene therapy vectors based on adeno-associated virus type 1. *J Virol* **73,** 3994–4003 (1999).

Xiao W, Warrington KH, Hearing P, Hughes J and Muzyczka N. Adenovirus-facilitated nuclear translocation of adeno-associated virus type 2. *J Virol* **76,** 11505–11517 (2002).

Yamaguchi A, Udagawa T, Sawai T. Transport of divalent cations with tetracycline as mediated by the transposon Tn10-encoded tetracycline resistance protein. *J Biol Chem* **265,** 4809-4813 (1990).

Yan Z Zak R, Zhang Y, Ding W, Godwin S, Munson K, Peluso R and Engelhardt. Distinct classes of proteasome-modulating agents cooperatively augment recombinant adeno-associated virus type 2 and type 5-mediated transduction from the apical surfaces of human airway epithelia. *J Virol* **78,** 2863–2874 (2004).

Yang GS, Schmidt M, Yan Z, Lindbloom JD, Harding TC, Donahue BA, Engelhardt JF, Kotin R and Davidson BL. Virus-mediated transduction of murine retina with adeno-associated virus: Effects of viral capsid and genome size. *J. Virol.* **76,** 7651–7660 (2002).

Yang XW, Model P and Heintz N. Homologous recombination based modification in Escherichia coli and germline transmission in transgenic mice of a bacterial artificial chromosome. *Nat. Biotechnol*. **15,** 859–865 (1997).

Zhang X, Firestein S. The olfactory receptor gene superfamily of the mouse. *Nat Neurosci* **5,** 124-133 (2002).

Zhao H, Ivic L, Otaki JM, Hashimoto M, Mikoshiba K, Firestein S. Functional expression of a mammalian odorant receptor. *Science* **279,** 237-242 (1998).

Zhou X and Muzyczka N. In vitro packaging of adeno-associated virus DNA. *J Virol* **72,** 3241–3247 (1998).

Zhu P, Aller MI, Baron U, Cambridges S, Bausen M, Herb J, Sawinski J, Cetin A, Osten P, Nelson ML., Kügler S, Seeburg PH, Sprengel R, Hasan MT. Silencing and un-silencing of tetracycline-controlled genes in neurons. *PLoS ONE* **2,** e533 (2007).

Zolotukhin S, Potter M, Zolotukhin I, Sakai Y, Loiler S, Fraites TJ, Chiodo VA, Phillipsberg T, Muzyczka N, Hauswirth WW, Flotte TR, Byrne BJ and Snyder RO. Production and purification of serotype 1, 2, and 5 recombinant adeno-associated viral vectors. *Methods* **28,** 158–167 (2002).

6. Abbreviations

α alpha

α- anti

β beta

μ micro

BAC bacterial artificial chromosome

bp base pair

BSA bovine serum albumin

CCK cholecystokinin

Cre Cre-Recombinase

CMV cytomegalovirus

CNS central nervous system

Cx connexin

DAB diaminobenzidine-hydrochloride

DNA desoxyribonucleic acid

DG dentate gyrus

EC entorhinal cortex

EDTA ethylenediaminetetraacetic acid

EPL external plexiform layer

FP fluorescent protein

g gram

GABA γ-aminobutyric acid

GAD67 glutamate decarboxylase 67

GCL granule cell layer

GFAP glial fibrillary acidic protein

GFP green fluorescent protein

Gjα9 gap junction α9

GL glomerular layer

IPL internal plexiform layer

IRES internal ribosomal entry sites

ITR inverted terminal repeat

kb kilobase pair

kDa Kilodalton

M Mol

MCL mitral cell layer

nls nuclear localization signal

NMDA N-methyl-D-aspartate

OB olfactory bulb

ONL olfactory nerve layer

OSN olfactory sensory neurons

P postnatal day

PA Polyadenylation signal

PCR polymerase chain reaction

PBS Phosphate based buffer solution

PFA Paraformaldehyde

pH potential Hydroxyl

rAAV Recombinant adeno-associated virus

rtTA reverse tetracycline-controlled transactivator

SDS Sodium dodecyl sulfate

SSC Sodiumchloride-Sodiumcitrate-Solution

tTA tetracycline-controlled transactivator

X-gal 5-Brom-4-Chlor-3-Indolyl-b-D-Galactopyranoside

7. Publications

Hirrlinger J, Scheller A, Hirrlinger PG, Kellert B, Tang W, Wehr MC, Goebbels S, Reichenbach A, Sprengel R, Rossner MJ and Kirchhoff F. Split-Cre complementation indicates coincident activity of different genes *in vivo*. *PLoS ONE* **4**, e4286 (2009).

Tang W, Ehrlich I, Wolff S, Michalski A, Mazahir H, Luethi A, and Sprengel R. Faithful expression of multiple proteins via 2A-peptide self-processing: A versatile and reliable method for manipulating brain circuits. (2009, submitted).